Exploring the role of DYRK1A in RNA polymerase III transcription: DYRK1A as a potential regulator of TFIIIC

Rianne Angelica Cort

TESI DOCTORAL UPF / 2019

THESIS SUPERVISORS

Dra. Susana de la Luna & Dra. Chiara Di Vona

Gene Regulation, Stem Cells and Cancer Programme

Centre for Genomic Regulation

DEPARTMENT OF EXPERIMENTAL AND HEALTH SCIENCE

To my family for always being there,

“If you are always trying to be normal you will never know how amazing you can be.” - Maya Angelou

Table of contents

Materials and Methods

Results

Abstract

The kinase DYRK1A (dual-specificity tyrosine-regulated kinase 1A) is a member of a conserved protein kinase family, encoded by a dosage sensitive gene; in fact, both haploinsufficiency and overexpression when in trisomy lead to pathological phenotypes in humans. Previous work from our group indicated that DYRK1A plays a role in the regulation of RNA polymerase II transcription by acting as a gene-specific CTD kinase at the promoter regions of target genes enriched in the palindromic motif TCTCGCGAGA. Additionally, a pool of DYRK1A was found to be associated with intergenic regions enriched in transfer RNAs (tRNA) genes, which are transcribed by RNA polymerase III in eukaryotes. In this Thesis work, the possible role of DYRK1A in regulating RNA polymerase III transcription has been explored. Results from chromatin immunoprecipitation coupled with high-throughput sequencing show that DYRK1A is recruited to RNA polymerase III-bound tRNA genes in multiple human cell lines. The RNA polymerase III-associated loci lack the specific DYRK1A palindromic motif, suggesting an alternative mode of DYRK1A recruitment to these loci compared to the RNA polymerase II-associated regions. The results also show that DYRK1A co-localises with the RNA polymerase III basal transcription factor TFIIIC only at tRNA genes and not at other TFIIIC genomic loci. DYRK1A interacts physically with TFIIIC, and furthermore, it phosphorylates several subunits of the TFIIIC complex *in vitro*. This functional association may regulate the recruitment of TFIIIC to tRNA genes since the inhibition of DYRK1A results in loss of TFIIIC at these loci. Thus, this work identifies DYRK1A as a TFIIIC novel kinase, the first described in mammals, and allows to propose DYRK1A as a potential novel regulator of RNA polymerase III transcription by acting on TFIIIC.

Resumen

La proteína quinasa DYRK1A (dual-specificity tyrosine-regulated kinase 1A) pertenece a una familia de proteína quinasas evolutivamente conservada y está codificada por un gen altamente sensible a la dosis. En particular, tanto la perdida de un alelo como su ganancia en trisomía están asociadas a patologías en humanos. Trabajo previo de nuestro grupo ha demostrado que DYRK1A es un regulador de la transcripción dependiente de la RNA polimerasa II al fosforilar la CTD de la subunidad catalítica de la polimerasa, directamente en regiones promotoras caracterizadas por la presencia del motivo palindrómico TCTCGCGAGA. Adicionalmente, DYRK1A se encontró asociada a regiones intergénicas que contenían genes codificantes para RNAs de transferencia (tDNAs). Los tDNAs son transcritos por la RNA polimerasa III en eucariotas. En esta Tesis se ha explorado la posibilidad de que DYRK1A pudiera regular la transcripción dependiente de RNA polimerasa III. Resultados de experimentos de inmunoprecipitación de cromatina asociados a secuenciación de alto rendimiento muestran que DYRK1A se recluta a tDNAs que tienen unida la RNA polimerasa III, en distintas líneas celulares humanas. Estas regiones genómicas carecen del motivo palindrómico, lo que sugiere la posibilidad de un modo de reclutamiento para DYRK1A distinto del utilizado para regiones asociadas a la RNA polimerasa II. Los resultados también muestran que DYRK1A co-localiza con el factor de transcripción basal para la RNA polimerasa III TFIIIC únicamente en tDNAs y no en otras regiones genómicas unidas por TFIIIC. DYRK1A interacciona físicamente con TFIIIC, y fosforila varias subunidades del complejo TFIIIC *in vitro*. Esta asociación funcional podría regular el reclutamiento de TFIIIC a tDNAs, ya que la inhibición de DYRK1A conlleva la perdida de TFIIIC en estos *loci*. En conjunto, este trabajo identifica a DYRK1A como una nueva quinasa del complejo TFIIIC, la primera descrita en mamíferos, y permite proponer a DYRK1A como un nuevo regulador de la transcripción dependiente de la RNA polimerasa III actuando sobre TFIIIC.

Introduction

1. Dual-specificity tyrosine-regulated kinase 1A (DYRK1A)

1.1. The DYRK subfamily of proteins

Protein kinases are one of the largest superfamily of proteins, and are classified according to the homology of the catalytic domain (Manning et al., 2002). Dual-specificity tyrosine-regulated kinases (DYRKs) belong to the CMGC family of proteins, which is also comprised of the Cyclin-dependent kinases (CDKs), Mitogen-activated protein kinases (MAPKs), CDK-like kinases (CDKLs), Serine-arginine-rich protein kinases (SRPKs), Cdc2-like kinases (CLKs) and RCK family (Figure I.1A). The DYRK family is composed of three subfamilies that include the DYRK subfamily, Homeodomain-interacting kinases (HIPKs), and pre-messenger RNA processing protein 4 kinases (PRP4Ks) (Figure I.1B). Henceforth, DYRKs will refer to the DYRK subfamily.

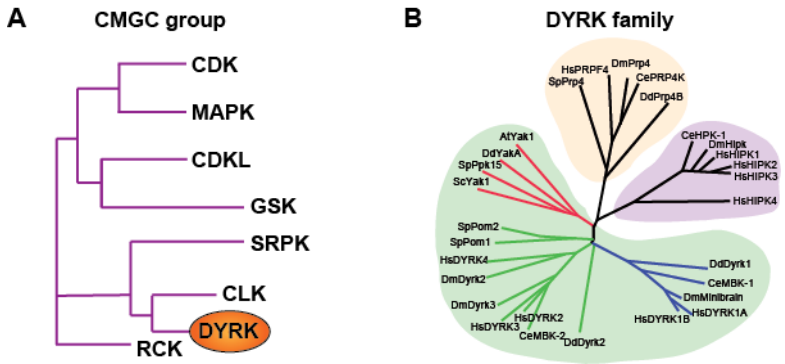

Figure I.1: Phylogenetic organisation of the DYRK family of kinases. (A) Schematic representation of the phylogenetic relatedness among the families belonging to the CMGC group (see text for the complete name of the families). **(B)** Unrooted evolutionary tree depicting the DYRK subfamily members, PRP4K (in orange), HIPK (in violet) and DYRK (in green). At: *Arabidopsis thaliana*; Ce: *Caenorhabditis elegans*; Dd: *Dictyostelium discoideum*; Dm: *Drosophila melanogaster*; Hs: *Homo sapiens*; Sc: *Saccharomyces cerevisiae*; Sp: *Schizosaccharomyces pombe*. Adapted from Aranda et al., 2011.

Within the DYRK subfamily, three classes are found based on phylogenetic analysis. One of the classes, represented by Yak1 from *Saccharomyces cerevisiae*, does not contain any representatives in the animal kingdom (Figure I.1B). In humans, there are five members of

DYRKs: DYRK1A and DYRK1B are in class I, and DYRK2, DYRK3 and DYRK4 are in class II (reviewed in Aranda et al., 2011) (Figure I.1B). Among the five members, the catalytic domain and the DYRK homology (DH)-box are highly conserved but they also contain class-specific domains (reviewed in Becker and Joost, 1999) (Figure I.2). Thus, the class II proteins are characterised by a N-terminal conserved domain called N-terminal auto-phosphorylation accessory (NAPA) region, which is required for the catalytic activation of the kinases (Kinstrie et al., 2010). This work will focus on the member DYRK1A, thus more details on the protein are provided in the upcoming sections.

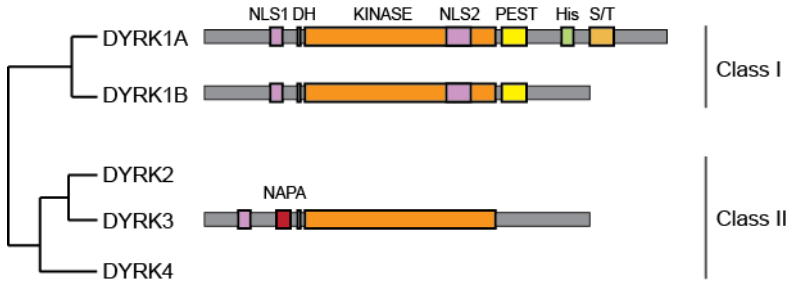

Figure I.2: Classification and protein structure of the mammalian DYRK subfamily. Schematic representation of mammalian DYRK subfamily members indicating the protein domains: a common central kinase domain (KINASE) and the DYRK-homology box (DH). Class I presents two nuclear localization signals (NLS1 and NLS2) and a PEST region (PEST); DYRK1A has a stretch of 13 histidine residues (His) and a region enriched in serine and threonine residues (S/T). The non-catalytic NAPA domain, distinctive of class II DYRKs, is shown. The two classes in which DYRK members are divided are indicated on the right. Adapted from Aranda et al., 2011.

1.2. DYRK1A protein kinase

The human *DYRK1A* gene is located on chromosome 21 and it was first discovered by deducing its sequence homology from the *D. melanogaster minibrain (mnb)* gene (Guimera et al., 1996). Since then, orthologues in many other species have been identified (Becker and Sippl, 2011).

1.2.1. Mechanism of activation

DYRK1A is known as a dual-specific kinase due to its ability to phosphorylate both Tyr and Ser/Thr residues. Though, the phosphorylation of Tyr residues is restricted to auto-phosphorylation,

which is essential for the activation of the kinase. During its protein synthesis, DYRK1A is auto-phosphorylated at residue Tyr321 within the activation loop, which generates a constitutively active kinase (Himpel et al., 2001; Kentrup et al., 1996; Lochhead et al., 2005). A proposed intermediate form of DYRK1A during translation with a different substrate specificity compared to the mature form explains why Tyr-phosphorylation is only possible at that specific time (Lochhead et al., 2005). However, some authors have argued that DYRK1A retains the ability to target Tyr residues in substrates as well, and that Tyr321 phosphorylation occurs in the mature form (Walte et al., 2013). Furthermore, it has been shown that de-phosphorylation of Tyr321 does not completely inactivate the kinase *in vitro*, indicating that phosphorylation of Tyr321 might not be required for the maintenance of the full kinase activity (Adayev et al., 2007; Becker and Sippl, 2011). The consensus sequence for DYRK1A phosphorylation is RPX(S/T)P (Himpel et al., 2000), indicating that DYRK1A is a proline-directed kinase; however, DYRK1A allows small hydrophobic residues (serine, alanine, valine) in the P+1 position (Soundararajan et al., 2013).

1.2.2. Modulators of DYRK1A catalytic activity

Due to the DYRK1A activation mechanism, the kinase appears to be constitutively active; however, there should exist regulatory mechanisms of the enzymatic activity. For instance, it would be reasonable to assume that de-phosphorylation of DYRK1A active loop would inactivate the kinase as it is the case for the other CMGC kinases. However, as of yet no phosphatase has been described. Despite this, several proteins have been shown to modulate the enzymatic activity of DYRK1A:

- DYRK1A is substrate of the activity of the protease Calpain I (Jin et al., 2015), which generates a truncated from in situations of overactivation of the protease (Jin et al., 2015; Souchet et al., 2019). Interestingly, while global kinase activity of DYRK1A is not affected, the truncated form shows an increased ability to phosphorylate the DYRK1A substrates Tau and signal transducer and activator of transcription-3 (STAT3) (Jin et al., 2015; Souchet et al., 2019), suggesting an alteration in substrate preference.

- The scaffold proteins 14-3-3 enhance the intrinsic catalytic activity of DYRK1A by binding two DYRK1A sites: one at the non-catalytic N-terminus (14-3-3ε) and other at Ser520 residue when autophosphorylated (14-3-3β) (Alvarez et al., 2007; Kim et al., 2004).
- The interaction with Sprouty-related-EVH1 domain-containing protein 1/2 (SPRED1/2) hinder DYRK1A accessibility to its substrates (Li et al., 2010).
- The large tumour suppressor kinase 2 (LATS2) phosphorylates DYRK1A and promotes DYRK1A-dependent phosphorylation of Lin52, a component of dimerization partner, retinoblastoma (pRb)-like, E2F and multi-vulval class B (DREAM) complex involved in cell cycle regulation (Tschop and Dyson, 2011).

1.2.3. DYRK1A expression

DYRK1A is ubiquitously expressed with varied expression across different tissues (see for instance, the expression pattern in human tissues in the GTEX portal: gtexportal.org/home/gene/DYRK1A). At least three alternative promoters (pM, pA and pB) have been described for *DYRK1A*, resulting in distinct transcripts (Maenz et al., 2008) (Figure I.3A), although if they show tissue/developmental specificity has not been explored. The expression of *DYRK1A* could be modulated by several transcription factors, including: E2F1, RE1 silencing transcription factor (REST), Nuclear factor of activated T-cells (NFAT) during osteoblast differentiation and T-box transcription factor 5 (TBX5) during breast carcinogenesis (Kim et al., 2016; Lee et al., 2009; Lu et al., 2011; Maenz et al., 2008) (Figure I.3A). An alternative splicing event of an acceptor site of exon 4 results in two different isoforms with a difference of 9 aa in the non-catalytic N-terminus (Guimera et al., 1999) (Figure I.3B). However, there is no reported difference in expression nor function. Moreover, *DYRK1A* expression has been shown to be controlled post-transcriptionally by the microRNAs miR-199b and miR-1246 (da Costa Martins et al., 2010; Zhang et al., 2011). Finally, our lab has observed that *DYRK1A* expression appears to be cell cycle dependent in HeLa cells, with an

increase in protein and mRNA levels in the S phase and reaching its maximum levels during G2/M (Di Vona, de la Luna, unpublished results).

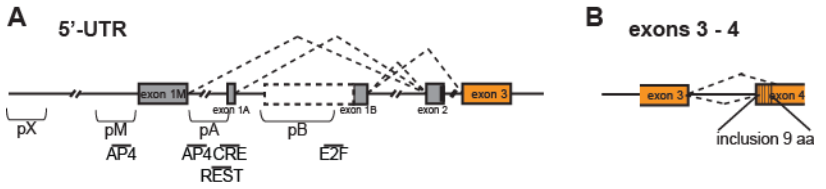

Figure I.3: Regulation of *DYRK1A* expression. (A, B) Promoter usage (**A**) and alternative spliced events (**B**) in *DYRK1A*. The location of the binding sites for the known regulatory transcription factors is shown. The existence of an upstream promoter (pX) is inferred from the presence of chromatin marks based on ENCODE data. The use of promoter pB, together with skipping of exon 2, could generate a 29-aa shorter isoform. Image adapted from Aranda et al., 2011.

1.2.4. DYRK1A protein stability

The PEST domain, which has been linked to rapid degradation (Rogers et al., 1986), in the non-catalytic C-terminus region of DYRK1A suggests that the DYRK1A protein has a short half-life. Evidence has shown that DYRK1A is targeted by the proteasome pathway and that the catalytic activity of DYRK1A appears to be important for its stability (Alvarez, 2004). Further supporting this, auto-phosphorylation of Ser97 has been shown to be important to increase the stability of the protein (Kii et al., 2016). In addition, the phosphorylation of DYRK1A at several sites by Nemo-like kinase has been proposed to mediate the degradation via the proteasome pathway (Arato, 2010). Only a few factors have been shown to regulate the DYRK1A turnover, including the E3 ubiquitin ligases SCF^{TrCP} and MDM2 and the chaperone heat shock protein 90 (HSP90) (Liu et al., 2016; Sonamoto et al., 2015; Xu et al., 2019). In addition, the scaffold protein DDB1 and CUL4 associated factor 7 (DCAF7), a DYRK1A-interactor evolutionary conserved, appears to be important for DYRK1A stability as protein levels of DYRK1A are reduced in DCAF7-knockout cells (Yousefelahiyeh et al., 2018). Of note, this dependence has not been observed by other groups (Glenewinkel et al., 2016; Roewenstrunk et al., 2019).

1.2.5. DYRK1A subcellular localisation

DYRK1A has been shown to have a variable subcellular distribution depending on the cellular context, which is in accordance with the kinase having targets in both the cytoplasm and the nucleus. For instance, its localisation appears to be prevalent in the cytoplasm in various cell lines (Di Vona et al., 2015; Luna et al., 2019; Rozen et al., 2018), and in glial cells in chick embryos (Hammerle et al., 2003). However, it is also present in the nuclei in various cells of the central nervous system (CNS) such as the granular cell layer of the cerebellum, hippocampal neurons and in the embryonic neocortex neurons (Marti et al., 2003; Sitz et al., 2004; Yabut et al., 2010). In addition, DYRK1A has been observed in specific cytosolic structures, such as synaptic membranes, cytoskeleton and vesicle containing fractions (Aranda et al., 2008; Murakami et al., 2009; Wegiel et al., 2004), as well as in nuclear speckles and at genomic regions (Alvarez et al., 2003; Di Vona et al., 2015; Jang et al., 2014; Salichs et al., 2009). Finally, the ability of DYRK1A to promote the formation of phase-separated liquid droplets via the C-terminal His-track has also been reported (Lu et al., 2018).

Not much is known about the regulation of the nuclear-cytoplasmic transport of DYRK1A. Two nuclear localisation signals (NLSs) have been shown to be essential to direct the kinase to the nucleus (Alvarez et al., 2003) (Figure I.2). In addition, the His-tract localised in the C-terminal region of the protein is involved in directing DYRK1A to nuclear speckles (Alvarez et al., 2003; Salichs et al., 2009). Finally, unpublished results from the group suggest the existence of active nuclear export via a dedicated nuclear export signal. Interestingly, DYRK1A accumulates exclusively in the nucleus in several cell lines when it is exogenously expressed (Alvarez et al., 2003; Becker et al., 1998; Rozen et al., 2018; Sitz et al., 2004), indicating the existence of a saturating mechanism regulating its subcellular accumulation. Furthermore, the overexpression of DCAF7 and the adenovirus oncoprotein E1A forces the accumulation of DYRK1A in the cytoplasm (Glenewinkel et al., 2016), indicating that some

factors may be involved in DYRK1A subcellular accumulation. Finally, different phosphorylated forms of DYRK1A are differentially distributed across subcellular compartments in human and mouse brain samples (Kaczmarski et al., 2014; Kida et al., 2011), suggesting that post-translational modifications might be involved in the process.

1.3. DYRK1A in disease

DYRK1A is a dosage sensitive gene as both extra-dosage as well as haploinsufficiency are associated to developmental defects and human pathologies (reviewed in Arbones et al., 2019). As previously mentioned, the human *DYRK1A* gene is located on chromosome 21, and in individuals with trisomy of this chromosome *DYRK1A* is upregulated 1.5-fold (Dowjat et al., 2007; Guimera et al., 1996). Furthermore, Down syndrome (DS) mouse models where DYRK1A is overexpressed are capable of reproducing a wide range of DS-associated features, which are attenuated when the levels of DYRK1A are normalised either by genetic or pharmacological means; these include motor alternations, memory defects, retinal abnormalities, skeletal alterations and an increased risk of developing childhood leukaemia (Ahn et al., 2006; Altafaj et al., 2001; Blazek et al., 2015; Dowjat et al., 2007; Garcia-Cerro et al., 2014; Garcia-Cerro et al., 2017; Laguna et al., 2013; Lee et al., 2009; Malinge et al., 2012; Martinez de Lagran et al., 2004; Ortiz-Abalia et al., 2008).

DYRK1A has been included in a list among the intolerant to loss-of-function genes (Lek et al., 2016). In accordance, *Dyrk1a*$^{-/-}$ mice are embryonic lethal (death at E10.5-E13.5) (Fotaki et al., 2002). In fact, haploinsufficiency of *DYRK1A* is considered a rare clinical syndrome within the autism spectrum disorders (ASD). In the Online Mendelian Inheritance in Man (OMIM) database it is recorded as Mental Retardation, Autosomal Dominant 7 (MRD7; OMIM: 614104), as well as in the Orphanet (ORPHA: 464306). The clinical traits associated with the syndrome include developmental delay, microcephaly, seizures, feeding problems, speech impairment and a characteristic facial gestalt (van Bon

et al., 2016). The pathological phenotype is conserved as a mouse model heterozygous for *Dyrk1a* presents low neonatal viability, developmental delay, small body size, microcephaly, seizures and behavioural traits of ASD (Arranz et al., 2019; Fotaki et al., 2002). In addition, a mouse model recreating one of the *DYRK1A* frameshift mutations suffers cognitive impairments (Raveau et al., 2018). The list of mutations includes small insertion/deletions causing frame-shift, nonsense mutations and missense mutations, which as revealed by an extensive biochemical characterisation from our group cause total impairment of DYRK1A kinase activity (Arranz et al., 2019).

In addition, DYRK1A is linked to the development of neurodegenerative diseases as it phosphorylates key factors in various diseases, such as Amyloid precursor protein (APP), Tau, α-Synuclein and Huntingtin interacting protein 1 (HIP1) (Kang et al., 2005; Kim et al., 2006; Ryoo et al., 2008; Ryoo et al., 2007). Furthermore, dysregulation of DYRK1A could potentially lead to heart defects due to alterations in the pRb-E2F and NFAT pathways (da Costa Martins et al., 2010; Hille et al., 2016; Kuhn et al., 2009; Raaf et al., 2010). Moreover, inhibition of DYRK1A could be a potential therapeutic target to ameliorate diabetes by stimulating pancreatic β-cells proliferation via NFAT signalling (Belgardt and Lammert, 2016; Kumar et al., 2018; Wang et al., 2019b).

Finally, recent work has pointed to DYRK1A as having a role in cancer, playing either a positive or a negative role depending on the tumour type (Liu et al., 2014; Luna et al., 2019; Pozo et al., 2013; Radhakrishnan et al., 2016). In addition, work from our group and others suggest that DYRK1A could act as a driver in specific cancers (Boni, 2019; Campbell et al., 2016).

1.4. DYRK1A inhibitors

Considering the potential use of an inhibitor of DYRK1A as a therapeutic tool, the interest is high in developing an inhibitor specific for DYRK1A.

However, there are no inhibitors that are strictly specific to DYRK1A to date. Here will be a brief overview of some of the current inhibitors in use (for recent and more extensive reviews Jarhad et al., 2018; Nguyen et al., 2017).

Harmine, a β-carboline alkaloid, is a natural ATP competitor that is able to target the Tyr321 auto-phosphorylation during the maturation process, thereby inhibiting the activity of DYRK1A (Bain et al., 2007; Gockler et al., 2009). Despite the success of harmine attenuating some features attributed to DYRK1A overexpression in mouse models and cellular systems (Bellmaine et al., 2017; Kuhn et al., 2009; Laguna et al., 2013; Luna et al., 2019; Pozo et al., 2013; Rozen et al., 2018; Wang et al., 2019b), its capability of inhibiting monoamine oxidase enzymes poses a difficulty in entering clinical studies.

The natural compound epigallocatechin gallate (EGCG), which is a polyphenol derivative found in green tea leaves, is an inhibitor with anti-tumour activities (reviewed in Yang et al., 2009). It is capable of inhibiting DYRK1A both *in vitro* and *in vivo* (De la Torre et al., 2014; Guedj et al., 2009; McElyea et al., 2016). In fact, it is currently in clinical trials as a treatment for DS individuals (de la Torre et al., 2016). Nevertheless, both harmine and EGCG have other targets aside from DYRK1A, thus there is still a need to develop a specific inhibitor.

INDY and FINDY are two compounds that are derivatives from benzothiazole and have shown promise as inhibitors by attenuating head malformations induced by DYRK1A overexpression in *Xenopus laevis* (Kii et al., 2016; Ogawa et al., 2010). However, even these inhibitors are not completely specific for DYRK1A, thus more research will be required.

1.5. DYRK1A: a pleiotropic kinase

The substrates associated with DYRK1A are both in the cytoplasm and in the nucleus reflecting the presence of DYRK1A in both compartments

(Figure I.4). The current list links DYRK1A with a variety of cellular processes as diverse as endocytosis, cytoskeletal dynamics, cell survival, proliferation, metabolism and others.

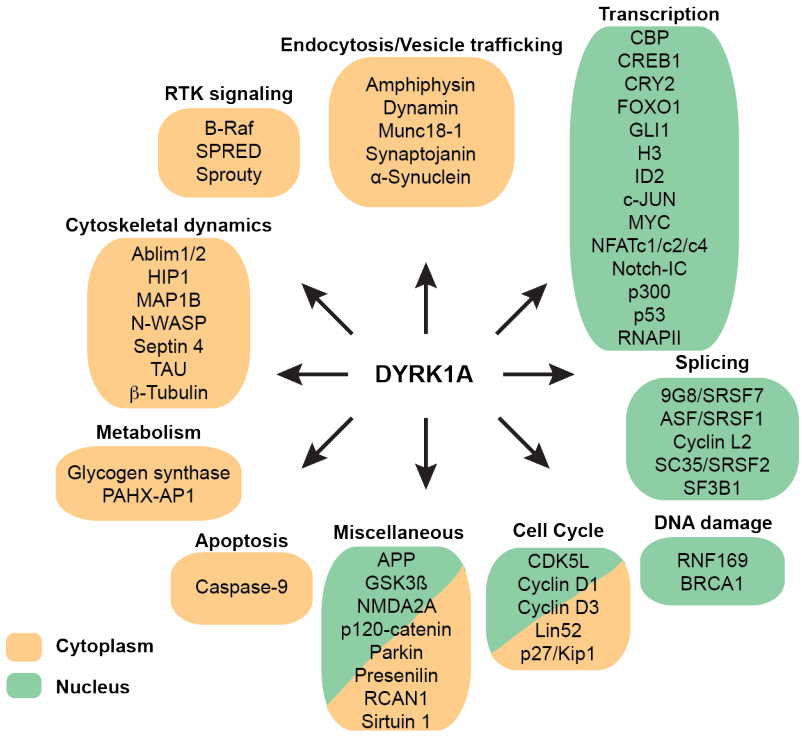

Figure I.4: Substrates for mammalian DYRK1A. DYRK1A substrates are grouped according to their associated function within the cell, indicated on top of the box. Yellow boxes indicate proteins found in the cytosol or exerting cytosolic activities; green boxes indicate proteins with nuclear activities. For complete names, see abbreviations' section.

Given the diverse nature of the substrates, DYRK1A is considered a pleiotropic kinase, and it is likely that the list of substrates and modifiers will keep on growing in the future. Thus, recent proteomics-based interaction screens performed by our lab and others unveiled multiple novel proteins involved in different signalling pathways that could interact with DYRK1A potentially expanding the role of the kinase (Guard et al., 2019; Menon et al., 2019; Roewenstrunk et al., 2019). In fact, the three screens linked DYRK1A to RNF169 and the DNA damage response, which appears as a novel pathway to which DYRK1A is related. However,

most of the substrates of DYRK1A have been described *in vitro*, thus further studies are required to determine if they are phosphorylated by DYRK1A *in vivo*. In addition to a direct role as a primary kinase, DYRK1A is a priming kinase for GSK3, facilitating the phosphorylation of Tau, microtubule-associated protein 1B (MAP1B) or cryptochrome circadian clock 2 (CRY2) (Kurabayashi et al., 2010; Scales et al., 2009; Woods et al., 2001).

1.6. DYRK1A is a direct regulator of RNA polymerase (Pol) II transcription

DYRK1A has been described to be involved in Pol II transcription (Figure I.4) through the phosphorylation of different transcription factors and chromatin regulators:

- DYRK1A may act as a negative regulator of NFATc transcription factors in specific cellular environments by phosphorylating NFATs, thereby retaining them in the cytoplasm (Arron et al., 2006; Lee et al., 2009).
- DYRK1A acts as a transcriptional activator of GLI1-dependent gene transcription by retaining GLI1 in the nucleus, therefore enhancing its transcriptional activity (Ehe et al., 2017; Mao et al., 2002).
- DYRK1A phosphorylates p53 at Ser15 leading to the induction of p53 target genes (Park et al., 2010).
- DYRK1A positively regulates androgen and glucocorticoid receptor-mediated transcriptional activation via its interaction with the chromatin remodelling factor ARIP4 (Sitz et al., 2004).
- DYRK1A phosphorylates histone H3 *in vivo* at T45 and S57, causing an alteration of the binding of the heterochromatin protein 1 (HP1), thus antagonizing its repressor function on cytokine-respondent genes (Jang et al., 2014).

Work from our group has shown that DYRK1A is recruited to a subset of proximal promoter regions of Pol II-transcribed genes, enriched in a palindromic sequence (TCTCGCGAGA, henceforth known as DYRK1A-motif), based on chromatin immunoprecipitation coupled with high-

throughput sequencing (ChIP-seq) studies. Furthermore, the study showed that DYRK1A phosphorylates the carboxy-terminal domain (CTD) of the Pol II catalytic subunit at Ser3 and Ser5 both *in vitro* and *in vivo*. This was the proposed mechanism on how DYRK1A would regulate the transcriptional activation of the targets (Di Vona et al., 2015) (Figure I.5A). Among these targets, a subset of ribosomal protein genes is found (Barba, 2018).

In recent years, several studies have expanded the role of DYRK1A in transcription. Lu and colleagues showed that the His-rich domain (HRD) of cyclin T1 of positive transcription elongation factor b (P-TEFb) is important for inducing phase-separated liquid droplets that trap the CTD and promote hyperphosphorylation of the CTD (Lu et al., 2018). Interestingly, this study suggested a likewise mechanism for DYRK1A through its histidine-tract in the c-terminus. Moreover, a recent study indicated that DYRK1A, through its interaction with DCAF7, is tethered to key myogenic gene loci where it promotes their transcription (Yu et al., 2019). Furthermore, DYRK1A has been found to interact and co-localise with the histone acetyltransferases (HATs) CBP and p300 at enhancer sites in multiple cell lines, and to be able to modulate the activity of CBP/p300 as depletion of DYRK1A resulted in reduced levels of H3K27 acetylation at these sites (Li et al., 2018).

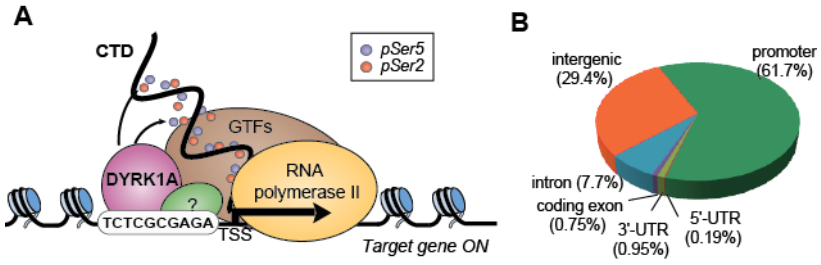

Figure I.5: DYRK1A is recruited to proximal promoter regions. (A) Scheme showing the working model proposed for DYRK1A-dependent transcription activation of gene targets. See text for details. GTFs are depicted as well as unknown putative DYRK1A binding partners in this context. **(B)** Pie chart representing the distribution of DYRK1A genomic loci over the distinct genomic features in T98G cells as appeared in Di Vona et al., 2015.

The analysis of the DYRK1A-associated loci suggested that DYRK1A could be linked to Pol III transcription since one of the categories correspond to intergenic regions, which was enriched in tRNA genes (Di Vona, 2013) (Figure I.5B). These results were the foundation of this Thesis project, which has focused on exploring this putative link. The next section is dedicated to an overview on Pol III transcription and what it is currently known about its regulation.

2. RNA polymerase (Pol) III transcription and regulation

2.1. Pol III promoter elements and transcription factors

The multi-subunit Pol III complex synthesises exclusively small noncoding RNAs that are important in a multitude of processes such as translation (tRNAs, 5S rRNA), mRNA splicing (U6 small nuclear RNAs [snRNAs]) and Pol II transcriptional regulation (7SK) others (reviewed in Dieci et al., 2007) (Figure I.6). In mammals, the Pol III-transcribed genes are classified into three different types based on the presence and position of *cis*-regulatory elements within their promoters, and on the requirement of specific basal or accessory transcription factors (reviewed in Schramm and Hernandez, 2002) (Figure I.6).

Pol III is a 17-subunit enzyme that acts together with general transcription factors IIIA, IIIB and IIIC (TFIIIA, TFIIIB and TFIIIC) in various combinations. TFIIIA is a single protein that is specific for the transcription of the 5S rRNA genes. TFIIIB is composed of three proteins TATA-binding protein (TBP), which is common to all eukaryotic Pols, B double prime 1 (BDP1) and TFIIB-related factor 1 (BRF1). TFIIIB is always present in the Pol III complex. In mammals, BRF1 is replaced by another isoform, BRF2, on type 3 promoters (Schramm et al., 2000; Teichmann et al., 2000; Willis, 2002). Lastly, TFIIIC is a large six-subunit complex that is associated with all type 1 and type 2 promoters (Figure I.6).

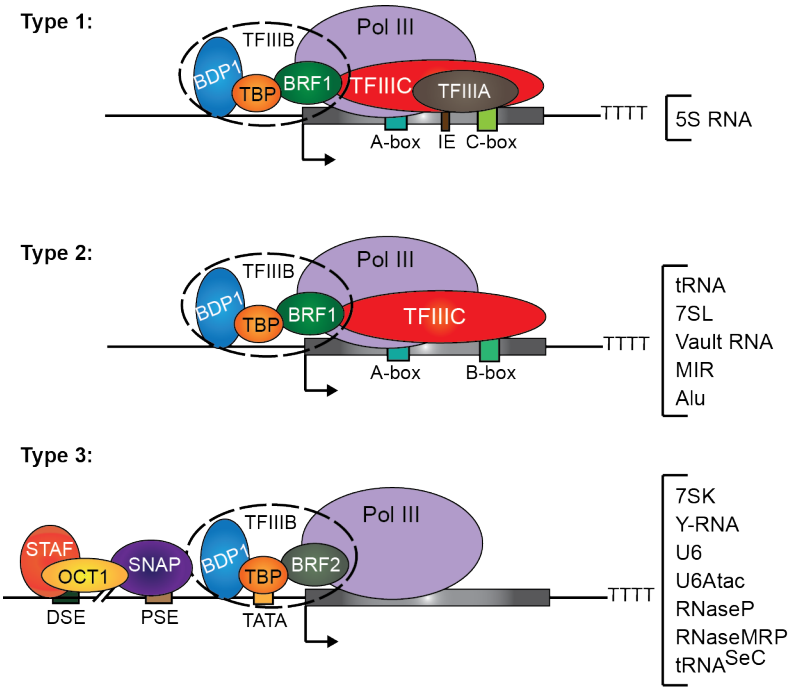

Figure I.6: Mammalian Pol III-associated machinery. Scheme depicting the classification of the Pol III-associated promoters and the genes transcribed by each promoter type. Image adapted from Oler et al., 2010. For more details see the text.

2.1.1. Type 1 promoters and associated genes

The ribosomal 5S RNAs are the only genes transcribed by a type 1 promoter. 5S rRNAs are an essential component of the large ribosomal subunit of the ribosome. The type 1 promoters are internal promoters within the primary sequence of the gene that comprise of the A-box, the intermediate element (IE) and the C-box (Bogenhagen et al., 1980; Sakonju et al., 1980). The transcription factor TFIIIA, unique to type 1 promoters, is responsible for recognising the promoter elements thus allowing the recruitment of the multi-subunit TFIIIC complex (Figure I.6).

2.1.2. Type 2 promoters and associated genes

The tRNA genes represent the majority of the type 2 genes. tRNAs are the decoders of the genetic code, and therefore, an essential piece in the process of protein synthesis. There are 20 different tRNA isotypes, that is tRNAs carrying one specific amino acid; in addition, the isotypes are

further classified into different tRNA isoacceptor families, which are different tRNA species carrying the same amino acid but with a different anticodon sequence. Lastly, the tRNA isoacceptors families can be further subdivided into multiple tRNA isodecoders, which are distinct tRNA species carrying the same amino acids and anticodons, but with a sequence variation in the tRNA body (for recent reviews, Rak et al., 2018; Schimmel, 2018) (Figure I.7). Due to this complexity in the repertoire of tRNAs, the number of tRNA genes in the genome can vary greatly in different species, and explains how in humans there are 600 predicted tRNA genes (gtrnadb.ucsc.edu; Chan and Lowe, 2016). Interestingly, unlike yeast where all tRNA genes are occupied and transcribed by Pol III, in humans only around 60% of the tRNA genes are occupied by Pol III in one cell line (Barski et al., 2010; Canella et al., 2010; Moqtaderi et al., 2010; Oler et al., 2010), which reflects on-going transcription (Orioli et al., 2016).

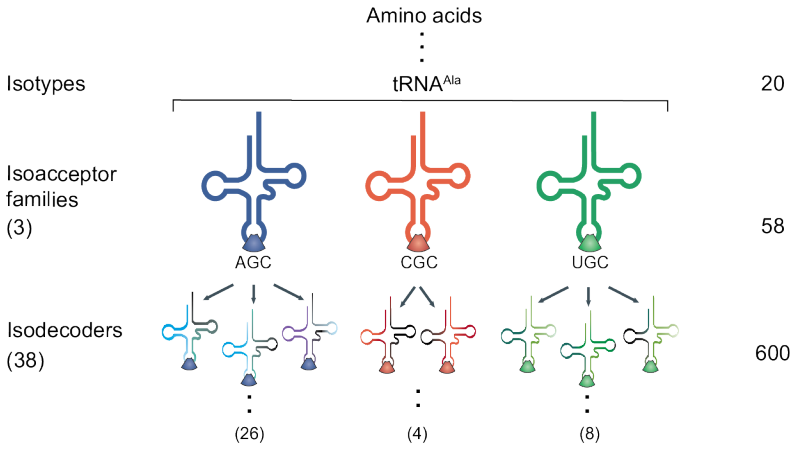

Figure I.7: The complexity of the tRNA world. Scheme showing the subdivision of the tRNA isotypes, each tRNA coding for one amino acid, using $tRNA^{Ala}$ as an example. There are three isoacceptor families for $tRNA^{Ala}$, which are further subdivided into 38 isodecoders. The numbers to the right show the total numbers for all the tRNAs in the human genome. Figure adapted from Schimmel, 2018.

The internal A-box and B-box promoters lie within the gene, and are directly recognised by TFIIIC (Lassar et al., 1983) (Figure I.6). These sequences are well conserved among various species as they encode

parts of the D- and T-loops of the tRNAs, respectively (Figure I.8). The structure of tRNAs are highly stable with a cloverleaf-like secondary structure, that is further folded into the final L-shaped tertiary structure before the aminoacylation step, loading of amino acid, and translation. Following transcription, which will be further explained in sections below, the pre-tRNAs (initial transcripts) undergo several processing steps to generate the mature tRNA that include trimming of the 5' leader and 3' trailer, splicing of any potential introns, modifications and the addition of the CCA-tail (Figure I.8) (recent review in Rak et al., 2018). The extensive RNA modifications, with an average of 11 to 13 nucleotides modified (recent review in Sokolowski et al., 2018), add another layer complexity to the pool of tRNAs as they can have important effects on tRNA folding and stability, amino acid loading, and the codon-anticodon base pairing of tRNAs.

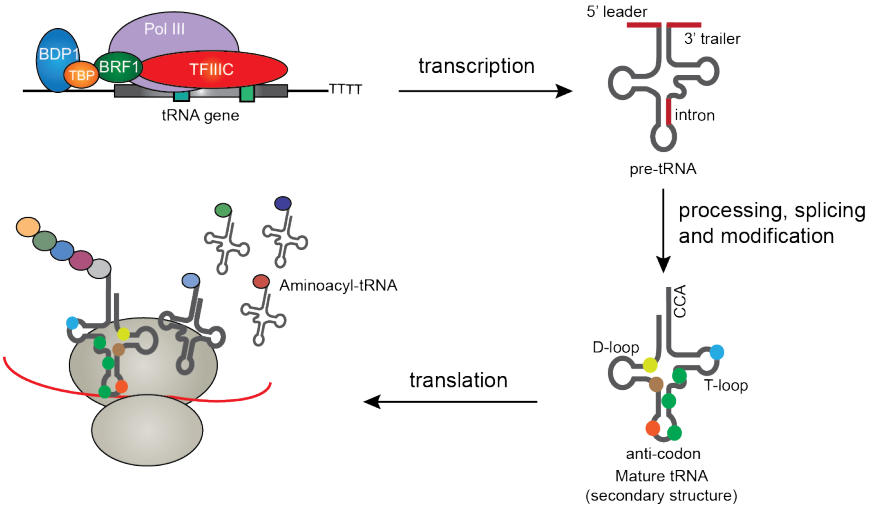

Figure I.8: The biogenesis of tRNAs. After transcription, the initial transcripts (pre-tRNAs) undergo trimming of the 3´trailer and 5' leader, splicing of introns (where applicable), CCA addition at 3´end and post-transcriptional modifications on various nucleotides (represented by coloured circles on the tRNA body). Finally, the mature tRNAs are loaded with their cognate amino acid (aminoacyl-tRNAs) and are available for translation. Note that for simplicity tRNAs are always depicted in their secondary structure.

2.1.3. Type 3 promoters and associated genes

Lastly, type 3 promoters are responsible for the synthesis of various RNAs involved in different processes. These include: the spliceosomal U6 snRNA genes, RMRP and RPPH1 RNAs (required for maturation of rRNAs and tRNAs, respectively), 7SK RNA (involved in regulation of the Pol II transcription elongation factor PTEF-b), the vault RNA component of vault particles (implicated in intracellular transport and drug resistance), and finally the Y RNAs (implicated in DNA replication) (Figure I.6). Whereas type 1 and 2 promoters have internal promoters, the type 3 promoters are characterised by external promoter elements, such as a TATA box found in Pol II promoters. In addition, these promoters contain upstream proximal and distal sequence elements (PSEs and DSEs), which are targeted by the type 3 specific factors OCT1 and snRNA activating protein complex ($SNAP_c$), respectively (Figure I.6).

This Thesis work will focus on the regulation of the type 2 promoters and their associated genes, specifically tRNAs, and thus the next sections will provide a brief overview on what is known about the mechanism and the regulation of their transcription in mammals.

2.2. Pol III transcription on type 2 promoters

The majority of what is currently known about the mechanism of Pol III transcription on type 2 promoters is based on data from yeast. Aside from the Pol III enzyme the transcription factors TFIIIB and TFIIIC are essential for the process of transcription. In the sections below, a brief overview of the different steps involved in Pol III transcription is provided (for more detailed overviews, see recent reviews for initiation: Ramsay and Vannini, 2018; for termination and reinitiation: Arimbasseri et al., 2014; regulation of transcription factors: Graczyk et al., 2018; and for aspects related to epigenetic regulatory mechanisms, see Shukla and Bhargava, 2018) (Figure I.9).

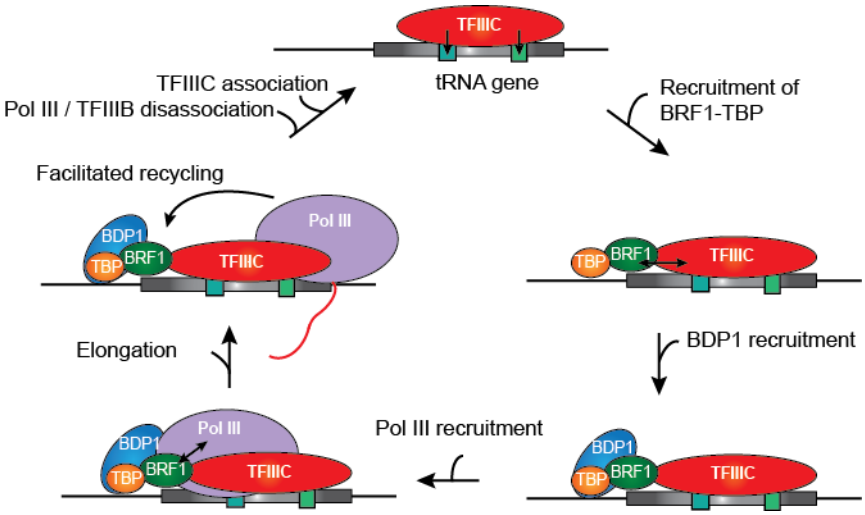

Figure I.9: A simplified model of the steps involved in the transcription of type 2 promoters: TFIIIC is recruited to the template by recognising and binding to the internal promoters. This is followed by the sequential recruitment of the TFIIIB complex by TFIIIC with BRF1/TBP recruited first followed by BDP1. Before elongation may proceed, the TFIIIB complex recruits the Pol III enzyme to form the pre-initiation complex. After termination, reinitiation occurs allowing multiple other rounds of transcription before releasing the Pol III complex from the template. The red line represents the newly synthetized Pol III transcript.

2.2.1. Pol III initiation

TFIIIC is a six-subunit complex whose composition is conserved from yeast to humans (Dumay-Odelot et al., 2007). TFIIIC recognises and binds the A- and B-box through the subunit TFIIIC-220 and TFIIIC-110 (Shen et al., 1996). The TFIIIB complex is subsequently recruited upstream to the transcription start site (TSS), possibly via protein-protein interactions with the TFIIIC-102 subunit, both in yeast (Male et al., 2015) and mammals (Hsieh et al., 1999) with BRF1/TBP recruited first followed by BDP1. Lastly, Pol III is recruited to form the pre-initiation complex via interactions with all members of the TFIIIB complex, mainly with BRF1. However, TFIIIC might mediate some interactions with Pol III as TFIIIC has been shown to interact with Pol III (Hsieh et al., 1999). Recent data from cryo-electron microscopy maps have shown that DNA melting and promoter opening is promoted by rearrangements of Pol III subunits through the binding of TFIIIB, mainly BDP1 (Abascal-Palacios et al., 2018; Vorlander et al., 2018).

2.2.2. Pol III elongation

The mechanism of the transition from initiation to elongation remains still mostly unknown. *In vitro* experiments in yeast have suggested that TFIIIC is not required for elongation (Bardeleben et al., 1994). Furthermore, genome-wide ChIP experiments revealed that TFIIIC occupancy increased on tRNA genes during transcriptional repression, suggesting that TFIIIC may act as a physical barrier (Roberts et al., 2003). TFIIIC occupancy has also been reported to be lower on tRNAs compared to TFIIIB and Pol III (Soragni and Kassavetis, 2008), indicating that it may need to be displaced for elongation to proceed. However, the mechanism of how Pol III overcomes the presence of TFIIIC within the gene body still needs to be determined. In this regard, data from yeast show that Pol III has an uneven distribution on tRNA genes with a strong peak over the A-box and another peak at the B-box suggesting a slow clearance from the initiation site (Turowski et al., 2016). Thus, a possibility could be that Pol III displaces TFIIIC from the A-box then the B-box, but not both simultaneously.

2.2.3. Pol III termination and reinitiation

Termination of transcription is mediated by three subunits of the Pol III enzyme: RPC11, RPC37 and RPC53 (human POLR3D, POLR3E and POLR3K) (Arimbasseri and Maraia, 2015; Rijal and Maraia, 2016; Turowski et al., 2016), when the machinery encounters a tract of thymidine residues on the non-template strand (Bogenhagen and Brown, 1981). The weak base-pairing promotes polymerase pausing, formation of the pre-termination complex and transcript release (Arimbasseri and Maraia, 2015). *In vitro* studies in yeast have shown that Pol III undergo reinitiation following termination allowing multiple rounds of transcription without disassembling the Pol III complex, i.e. facilitated recycling, a mechanism conserved in humans (Cabart et al., 2008; Dieci and Sentenac, 1996). Furthermore, *in vitro* studies have indicated that TFIIIB, and not TFIIIC, is required for multiple rounds of transcription unless the gene size is greater than 300 base pairs (Ferrari et al., 2004). The

efficiency of transcription reinitiation may also be linked to termination (Turowski et al., 2016). Interestingly, *in vitro* studies have shown that, as in yeast, Pol III transcription is stimulated by the DNA helicase SUB1/PC4, which interact with human TFIIIC and enhance the binding of TFIIIC to tRNA genes covering the termination signal, and promoting multiple rounds of transcription (Tavenet et al., 2009; Wang and Roeder, 1998). It has been shown *in vitro*, that SUB1 also cooperates with the HAT p300 in promoting TFIIIC binding. Furthermore, it has been shown that the two factors occupy tRNA genes *in vivo* (Mertens and Roeder, 2008). Thus, TFIIIC could be involved in reinitiation *in vivo*, possibly through interactions with SUB1/PC4.

2.3. Regulation of Pol III transcription

Given the nature of Pol III target genes and their link to protein synthesis, Pol III transcriptional activity is modulated by a wide variety of regulatory influences in mammals. For instance, in response to differentiation or stress, the activity of Pol III is decreased (Crighton et al., 2003; Ernens et al., 2006; White et al., 1989), whereas its activity increases in response to growth factors, hormones, nutrients and inflammatory signals (Graczyk et al., 2015; Michels et al., 2010; Zhong et al., 2004). Importantly, these signals can also affect the processing of tRNAs, their maturation and modification (see recent reviews Graczyk et al., 2018; Willis and Moir, 2018). Indeed, the levels of tRNAs are cell type-dependent, and respond to a wide variety of physiological processes such as differentiation or circadian rhythms (Chen et al., 2018; Dittmar et al., 2006; Gingold et al., 2014; Mange et al., 2017; Van Bortle et al., 2017), In recent years, several studies have highlighted the importance of the available pool of tRNAs in a cell and their impact on not only protein abundance, but also protein folding, as well as translation fidelity (reviewed in Rak et al., 2018; Willis and Moir, 2018), which ultimately can influence the growth of the cell and its response to extracellular cues. All these findings suggest that a tight regulation of Pol III transcription should exist.

In yeast, most of the regulation of Pol III transcription converges on the negative regulator MAF1, which is conserved from yeast to humans (reviewed in Boguta, 2013; Graczyk et al., 2018). The activity of yeast MAF1 is regulated by phosphorylation (Towpik et al., 2008), with dephosphorylated MAF1 binding to elongating Pol III and blocking subsequent transcription reinitiation (Vannini et al., 2010). In mammals, MAF1 also acts as a Pol III repressor (Johnson et al., 2007; Reina et al., 2006). It is a rapamycin-sensitive phosphoprotein (Reina et al., 2006), which is directly phosphorylated by mTORC1 (Kantidakis et al., 2010; Michels et al., 2010). As in yeast, only the hypophosphorylated form interacts with Pol III and represses Pol III transcription (Michels et al., 2010; Reina et al., 2006). Experimental evidence suggests that MAF1 might act by promoting Pol III release (Orioli et al., 2016). In addition, mTORC1 associates with TFIIIC, likely via TFIIC-63, which might recruit mTORC1 to chromatin where it phosphorylates MAF1 (Kantidakis et al., 2010).

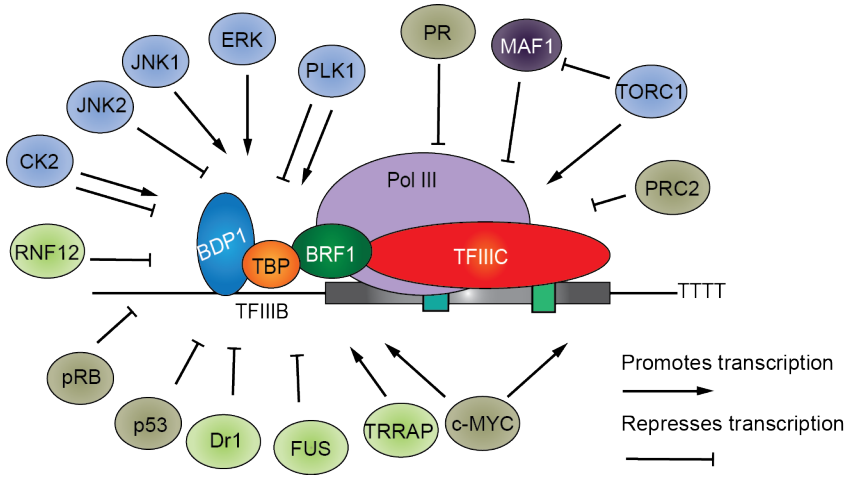

Figure I.10: The regulation of Pol III transcription. A scheme showing the various proteins involved in regulating Pol III transcription. In dark purple is the negative repressor MAF1. In light blue are the kinases, in light green are transcription factors, and in bright green are other proteins. The arrows indicate if they promote or repress transcription, and which complex is regulated. Dual arrows represent multiple roles in regulation. For more details, see the text.

In addition to MAF1, several factors have been described to be involved in regulating Pol III transcription, including transcription factors and protein kinases (summarised in Figure I.10). In general, most of the transcription factors regulate transcription by modulating the association of TFIIIB with either TFIIIC and/or with the DNA. For instance, both pRb and p53 repress Pol III transcription by impairing the association of TFIIIB with TFIIIC, while Down-regulator of transcription of 1 (DR1) also disrupts the binding of BRF1 to TBP, thus destabilising the TFIIIB complex on the DNA (Crighton et al., 2003; Kantidakis and White, 2010; Sutcliffe et al., 1999; White et al., 1994). On the other hand, c-MYC has been reported to positively regulate Pol III transcription by promoting the expression of both TFIIIB and TFIIIC subunits (Campbell and White, 2014). Furthermore, it has been shown that c-Myc promotes the recruitment of transformation/transcription domain associated protein (TRRAP), a common component of many HAT complexes that acts as a positive regulator of Pol III transcription (Kenneth et al., 2008). Other factors found to act as negative regulators of Pol III transcription include: the progesterone receptor (PR), which is present at a subset of tRNA genes and inhibits transcription via interaction with the Pol III holoenzyme in breast cancer cells (Finlay-Schultz et al., 2017); the polycomb repression complex 2 (PRC2) component EZH2, which can repress Pol III transcription via interaction with TFIIIC (Liu et al., 2015); or FUS RNA binding protein, which associates with Pol III genes *in vivo* via TBP interaction (Tan and Manley, 2010).

Aside from transcription factors, Pol III transcription could be regulated by post-translational modifications of the transcriptional machinery, including SUMOylation of TFIIIC, TFIIIB and Pol III (Hendriks et al., 2017), ubiquitination of BRF1 by RNF12 (Wang et al., 2019a), and phosphorylation. Notably, kinases have a dual role on Pol III transcription depending on the cellular context analysed. For instance, both polo-like kinase 1 (PLK1) and casein kinase 2 (CK2) repress transcription during mitosis by phosphorylating BRF1 and BDP1, respectively (Fairley et al.,

2012; Hu et al., 2004). However, during interphase they promote Pol III transcription, PLK1 by phosphorylating another site of BRF1 and CK2 by phosphorylating BRF1 (Fairley et al., 2012; Johnston et al., 2002). Extracellular signal-regulated kinases (ERKs) have been described to promote transcription by two different mechanisms: stimulating the expression of BRF1 during hypertrophic growth in cardiomyocytes (Goodfellow et al., 2006), and by phosphorylation of BRF1, which promotes its binding to TFIIIC and the recruitment of Pol III and BRF1 to tRNA genes (Felton-Edkins et al., 2003). Finally, the c-Jun N-terminal kinases (JNKs) have been shown to stimulate the expression of TFIIIB and BDP1 in the case of JNK1, but also to downregulate their expression as is the case with JNK2 (Zhong and Johnson, 2009). In the case of mTORC1, it is possible that, in addition to MAF1, it may target the Pol III machinery directly, as it is present on Pol III-transcribed genes during growth promoting conditions (Chaveroux et al., 2013; Kantidakis et al., 2010; Shor et al., 2010).

Thus, whilst a multitude of kinases have been shown to regulate TFIIIB, no kinase has so far been identified to phosphorylate TFIIIC, even though it TFIIIC is known to be phosphorylated (Shen et al., 1996). In addition, it has been reported that de-phosphorylation could be associated to TFIIIC inactivation (Clark and Dasgupta, 1990). Therefore, another layer of regulation in Pol III transcription via the regulation of TFIIIC could exist.

2.4. The role of TFIIIC outside of Pol III transcription

Besides its role as coding genes, tRNA genes act as insulators in both *S. cerevisiae* and *S. pombe* (McFarlane and Whitehall, 2009), and appear to affect local chromatin structure, which results in effects on long-range chromosome architecture (Hamdani et al., 2019). This function is conserved in mammals as a cluster of tRNA genes act as insulators in mouse and human cells (Ebersole et al., 2011; Raab et al., 2012). Interestingly, this action appears to be dependent on TFIIIC as a mutation in the B-box impairs this activity (Raab et al., 2012).

Moreover, TFIIIC is recruited to other loci on the chromatin not bound by Pol III, which are named Extra TFIIIC sites (ETCs) (Barski et al., 2010; Moqtaderi et al., 2010; Oler et al., 2010). This observation suggests that TFIIIC is involved in other processes aside from Pol III transcription. Indeed, TFIIIC could possibly act an insulator protein, such as CCCTF-binding factor (CTCF), and mediate long-range interactions. In this regard, it has been reported that TFIIIC interacts directly with the chromatin organisation factor condensin II and is responsible for its recruitment to chromatin on TFIIIC-bound regions in mouse and human cells (Yuen et al., 2017). Interestingly, a subset of these sites coincides with boundaries of topological associated domains (TADs), where condensin II was shown to be important in maintaining high levels of expression (Yuen et al., 2017). Other experimental evidence on TFIIIC-involvement in long-range interactions include the co-localisation of TFIIIC with cohesin (Carriere et al., 2012; Yuen et al., 2017), the enrichment of TFIIIC binding sites over CTCF binding sites when investigating long-range interactions (Raab et al., 2012), and the fact that tRNA genes have long-range interactions with other tRNA genes and ETC sites (Van Bortle et al., 2017). These effects have been shown to impact the expression of Pol II genes in different physiological contexts as macrophage differentiation, induction of activity in neurons or serum starvation (Crepaldi et al., 2013; Ferrari et al., 2019; Van Bortle et al., 2017).

2.5. Pol III machinery dysregulation and disease

Mutations in the components of the Pol III machinery are associated to various tissue- and disease-specific disorders. Mutations in the two catalytic subunits of the Pol III enzyme (POLR3A and POLR3B), the POL31C subunit, along with recently found mutations in the POL31K subunit, are causative of CNS hypomyelinating leukodystrophy (Bernard et al., 2011; Kraoua et al., 2019; Tetreault et al., 2011; Thiffault et al., 2015). Furthermore, mutations in the subunits BDP1 and BRF1 of the TFIIIB complex cause hearing and neurodevelopmental disorders, respectively (Borck et al., 2015; Girotto et al., 2013). In addition, mutations

in proteins involved in the extensive post-transcriptional modification of tRNAs have been associated with neurodevelopmental disorders among others (for a recent review Schaffer et al., 2019). Moreover, mutations in the body of cytoplasmic tRNAs itself have also been linked to disease (see review Lant et al., 2019).

Given the association with regulation of protein translation, links to cancer have been observed as the overexpression of TFIIIC-110 in ovarian tumours (Winter et al., 2000). In fact, enhanced Pol III transcription has been shown to be important for tumour formation in mice (Johnson et al., 2008). Breast cancer and myeloma cells show increased expression levels not only of total tRNAs but individual tRNA isoacceptors (Pavon-Eternod et al., 2009; Zhou et al., 2009). In this regard, various studies have shown that overexpression of the initiator methionine tRNA promotes tumour cell migration and metastasis in mice (Birch et al., 2016; Clarke et al., 2016). Interestingly, a study observed that the overexpression of two specific tRNAs ($tRNA^{Glu}UUC$ and $tRNA^{Arg}CCG$) lead to an increased metastatic state of breast cancer cells, by promoting the transcription of pro-metastatic transcripts enriched in the corresponding codons (Goodarzi et al., 2016).

In summary, dysregulation of Pol III transcription is important in disease progression in different physiological scenarios and therefore, a tight control of Pol III transcription should assure proper cellular homeostasis and adequate responses to the extracellular environment.

Objectives

Objectives

The DYRK1A protein kinase acts as a transcriptional activator directly at gene-specific promoters of Pol II-transcribed genes enriched in the palindromic motif TCTCGCGAGA. It has also been shown that DYRK1A is recruited to intergenic regions; these regions include tRNA genes that are transcribed by Pol III. There is an accumulation of evidence supporting the importance of the regulation of tRNAs in disease, especially in cancer and neurodevelopmental disorders. Thus, this research aims to provide not only a mechanistic context for DYRK1A-related phenotypes, but also to contribute to the current knowledge on the regulation of Pol III.

Therefore, the main objective in this Thesis work is to determine how DYRK1A is involved in the regulation of Pol III transcription by:

I. Characterising the recruitment of DYRK1A to Pol III-associated genomic regions, and in particular to tRNA genes.
II. Determining how DYRK1A functionally interacts with the Pol III machinery.

Materials and Methods

1. Plasmids

All plasmids used in this work were either purchased from companies, provided by other laboratories or generated by cloning or site-directed mutagenesis during the thesis work, as indicated. The identities of the plasmids were confirmed by DNA sequencing.

1.1. Backbone vectors

- pGEX-4-T3: expression vector for bacterial cells with an isopropyl β-D-1-thiogalactopyranoside (IPTG) inducible N-terminal glutathione S-transferase (GST) tag (Amersham Biosciences).
- pGEX-6-P1: expression vector for bacterial cells with and IPTG inducible N-terminal GST tag and a pre-Scission protease cutting site (Amersham Biosciences).

1.2. Bacterial expression plasmids for tag-fusion proteins

- pGST-DYRK1A: expression plasmid encoding human DYRK1A (754 amino acid (aa) isoform; Acc. No. NM_130436) with an N-terminal GST-tag (Alvarez et al., 2007).
- pGST-DYRK1A^{KM}: expression plasmid encoding for an N-terminally GST-tagged catalytic inactive version of DYRK1A with a point mutation in the lysine residue 179 within the ATP binding pocket (Alvarez et al., 2007).
- pHis$_6$-GST-HsGTF3C35: expression plasmid encoding human TFIIIC-35 (NM_138408) with an N-terminal GST-tag and a TEV protease cutting site. The plasmid was kindly provided by Dr. Martin Teichmann (Institut Européen de Chimie et Biologie, France) (Dumay-Odelot et al., 2007).

The plasmids listed below in Table MM.1 were generated by Gibson cloning (Gibson et al., 2009). In short, DNA fragments corresponding to the aa indicated were amplified by polymerase chain reaction (PCR) from the specified source (MM1.3) and the primers listed in Table MM.4, and

subsequently ligated into the BamHI site of the pGEX-6-P1 vector (MM1.1) to produce N-terminally tagged GST-fusion proteins. More details are provided in MM2.3. Further on in the work, mutated non-phosphorylatable versions of some of the plasmids, listed in Table MM.6, were generated by site-directed mutagenesis.

Table MM.1: The resulting plasmids generated by Gibson cloning with size of DNA fragments corresponding to the aa amplified from the indicated original cDNA source.

Plasmid	Amino acids	Accession No.	Source of cDNA
pGST-TFIIIC-220.1	1-367	NP_001511	pBKS-TF3C220
pGST-TFIIIIC-220.2	368-804	NP_001511	pBKS-TF3C220
pGST-TFIIIC-220.3	805-1164	NP_001511	pBKS-TF3C220
pGST-TFIIIC-220.4	1165-1595	NP_001511	pBKS-TF3C220
pGST-TFIIIC-220.5	1596-2109	NP_001511	pBKS-TF3C220
pGST-TFIIIC-110.1	1-714	NP_001512	pRSET-TF3C110
pGST-TFIIIC-110.2	715-911	NP_001512	HeLa genomic DNA
pGST-TFIIIC-102.1	1-528	NP_036218	pRSET-TF3C102
pGST-TFIIIC-102.2	529-886	NP_036218	pRSET-TF3C102
pGST-TFIIIC-90	1-822	NP_ 036336	pFLAG-GTF3C4
pGST-TFIIIC-63	1-519	NP_036219	pRSET-TF3C63

1.3. Sources for cDNA for cloning

- pBKS-TF3C220: plasmid containing cDNA of human *GTF3C1* (NM_001520; TFIIIC-220), provided by M. Teichmann.
- pRSET-TF3C110: plasmid containing cDNA of human *GTF3C2* (NM_001521; TFIIIC-110) until amino acid 714, provided by M. Teichmann.
- pRSET-TF3C102 plasmid containing cDNA of human *GTF3C3* (NM_012086; TFIIIC-102), provided by M. Teichmann.
- pFLAG-GTF3C4: expression plasmid encoding human *GTF3C4* (NM_012204; TFIIIC-90) open reading frame with a N-terminal Flag-tag. The plasmid was purchased from Genscript.
- pRSET-TF3C63: plasmid containing cDNA of human *GTF3C5* (isoform 2; NM_012087; TFIIIC-63). Three aa (EED) are missing from the E-run at the C-terminus. The plasmid was provided by M. Teichmann.

1.4. Plasmids for lentiviral vector preparation

- pCMV-VSV-G: lentiviral packaging vector that expresses the vesicular stomatitis virus G envelope protein (Stewart et al., 2003). Obtained from Addgene (Plasmid #8454).
- pCMV-dR8.91: second generation packaging plasmids containing *gag*, *pol*, and *rev* genes proceeding from human immunodeficiency 1 virus (Zufferey et al., 1997), kindly provided by Dr. Trono (Laboratory of Virology and Genetics, École Polytechnique Fédérale de Lausanne, Switzerland).
- pshControl: MISSION® pLKO.1-puro Non-target shRNA Control plasmid (Sigma #SHC016).
- pshDYRK1A-1: MISSION® pLKO.1-puro shRNA DYRK1A plasmid (Sigma #TRCN0000022999).

2. Techniques for Genetic Manipulation

2.1. Purification of plasmids

Plasmid DNA was extracted from bacterial mini cultures (3 ml) using the QIAGEN Plasmid Mini Kit (Qiagen) according to the manufacturer's instructions.

2.2. DNA sequencing

Plasmids were sequenced using the Sanger sequencing method at the Genomic Sequencing Service (UPF-PRBB, Barcelona). The Big Dye Terminator v3.1 Ready Reaction Cycle Sequencing Kit (Applied Biosystems) was used along with 3.2 pmol of primers. The amount of plasmid DNA was calculated using the following equation: ng DNA = 25 ng x (size in kb of the whole plasmid, insert included) in a total volume of 12 μl. The PCR conditions are listed in Table MM.2. The sequences were visualised with the free software 4peaks™ (Nucleobytes).

Table MM.2: PCR conditions for the DNA sequencing reaction

	T	Time
Denaturation	95ºC	3 min
30 cycles	94ºC	10 sec
	55ºC	30 sec
	60ºC	4 min

2.3. Gibson cloning

Gibson cloning procedure was performed to generate the GST-fusion proteins of the subunits of the TFIIIC complex. DNA fragments were PCR-amplified from their corresponding template listed in Table MM.1. The primers used (listed in Table MM.4, purchased from Sigma Aldrich) contain BamHI cutting sites that were incorporated into the flanks of the PCR products. The PCR reactions were performed with either 5 ng or 0.5 ng of template DNA, 0.4 μM of forward and reverse primers, 200 μM of deoxyribonucleotides (dNTPs), 2.5 μl of 10x reaction buffer (Expand High Fidelity PCR system, Roche) and 0.5 μl Expand Polymerase (3.5 U/μl; Expand High Fidelity PCR system, Roche) in a final volume of 25 μl. The conditions of the PCR programme are in Table MM.3.

Table MM.3: PCR conditions amplification of inserts for Gibson cloning

	T	Time
Denaturation	94ºC	2 min
30 cycles	94ºC	15 sec
	55ºC	30 sec
	72ºC	2 min
Extension	72ºC	10 min

The donor vector pGEX-6P-1 was digested with the BamHI-HF restriction enzyme (New England Biolabs) according to the manufacturer's conditions, and it was fractionated in a 1% (w/v) agarose gel (Ecogen) prepared in 1x Tris/Borate/EDTA (TBE) buffer. The linear plasmid was purified from the melted agarose with the QIAQuick Gel Extraction kit (Qiagen) following manufacturer's indications. The Gibson reactions were

performed with 150 ng of the purified vector, 1 μl of the PCR product and 10 μl of 2x Gibson reaction mixture (CRG Biomolecular Screening & Protein Technologies Unit) in a final volume of 20 μl for 1 h at 50ºC.

Table MM.4: Sequences of oligonucleotides used for PCR amplification of Gibson cloning products.

Fragment	Forward primer	Reverse primer
pGST-TFIIIC-220.1	GGGGCCCCTGGGATCCATGGACGCGCTGGAGTCG	GGAATTCCGGGGATCCCTAATCCCGCTCGAACACAATG
pGST-TFIIIC-220.2	GGGGCCCCTGGGATCCATGCTCACACAGACCTACGAC	GGAATTCCGGGGATCCCTAGTGGACCACCCGCAGGC
pGST-TFIIIC-220.3	GGGGCCCCTGGGATCCATGTTTCTGTGGTACCTCATC	GGAATTCCGGGGATCCCTATGGGCGCTTGGACAGAAATG
pGST-TFIIIC-220.5	GGGGCCCCTGGGATCCATGGTGGAGAATGAGGTCATC	GGAATTCCGGGGATCCCTAGAGGTGGATCCACTTGTTCC
pGST-TFIIIC-110.1	GGGGCCCCTGGGATCCATGGATACCTGCGGGGTCG	GGAATTCCGGGGATCCTTAGGATCCTGAAAGACTCCAAACG
pGST-TFIIIC-110.2	GGGGCCCCTGGGATCCGACTGGCTTGGGACAATAGC	GGAATTCCGGGGATCCTTAGGGAGTGGGCAGAAGGCG
pGST-TFIIIC-102.1	GGGGCCCCTGGGATCCATGTCAGGGTTCAGTCCGG	GGAATTCCGGGGATCCTTAAGCATTTGCATCCTGTGCTAAAG
pGST-TFIIIC-102.2	GGGGCCCCTGGGATCCGCACAGCAGGAACTGAAGTTATTG	GGAATTCCGGGGATCCTTATATAGAACAATAGGTATACAAAAGCG
pGST-TFIIIC-63	GGGGCCCCTGGGATCCATGGCGGCGGAGGCGGC	GGAATTCCGGGGATCCTCACACGTAGTCCAGAATCTCTG

For a better description of the fragments, see Figure R.13E, R.14B and R.15B.

For bacterial transformations, 1.5 μl of the final product was added to 20 μl of competent *Escherichia coli* XL-10 Gold bacteria (Agilent Technologies) and the heat shock method was used (0ºC/30 min, 42ºC/30 sec, 0ºC/2 min). Cells were allowed to grow in 200 μl of SOC medium (20 g/l tryptone, 5 g/l yeast extract, 10 mM NaCl, 10 mM $MgCl_2$, 10 mM $MgSO_4$, 20 mM glucose) for 1 h at 37ºC with 220 rpm agitation. The cultures were plated on Lysogeny Broth (LB) plates (10 g/l tryptone, 5 gl/l NaCl, 5 g/l yeast extract, 12 g/l agar) supplemented with ampicillin (100 μg/ml) at 37ºC overnight.

Lastly, some colonies were picked in 200 μl of LB media supplemented with ampicillin. Plasmid validation was performed by colony-PCR using 1 μl of inoculated LB, 0.4 μM of forward and reverse primers, 5 μl of 2x PCR master mix (Promega) in a final volume of 10 μl. The conditions of the PCR programme are in Table MM.5.

Table MM.5: PCR conditions for the colony screening

	T	Time
Denaturation	94ºC	1 min
30 cycles	94ºC	30 sec
	55ºC	30 sec
	72ºC	2 min
Extension	72ºC	7 min

The PCR products were fractionated in a 1% agarose gel, and the positive samples were confirmed by digestion and sequencing. The plasmid DNA was transformed into *E. coli* BL21 (DE3) pLysS B F' bacteria (Agilent Technologies) for expression of the fusion proteins.

2.4. Site-directed mutagenesis

Point mutations were introduced in plasmids using either the QuikChange® Multi Site-Directed Mutagenesis kit or the QuikChange® Lightning Multi Site-Directed Mutagenesis kit (Agilent Technologies) following the manufacturer's instructions. The primers were purchased from Sigma Aldrich (see Table MM.6). All mutants were checked by DNA sequencing covering the area of the inserted mutation.

Table MM.6: Sequences of oligonucleotides used for site-directed mutagenesis of the GST-fused TFIIIC fragments. Mutated codon is highlighted in bold.

Plasmid	Mutation	Mutagenesis primer
pGST-TFIIIC-220.2	T514A	CCCAGCCTCATCACTCC**GCC**CCAACCAAGG GTGGGTG
pGST-TFIIIC-220.5	S1735A	GCTGGAGCTGTCTGGGTAT**GCT**CCCGAAGA CCTGACTGC
pGST-TFIIIC-220.5	S1808A	GGAGCCAAGGCCAGGC**AGC**GCCCATGGCT ACCAGGC

pGST-TFIIIC-220.5	S1856A	CAGGCACCTCCTTCTCAC**GCC**CCCCGGGG CACCAAGAG
pGST-TFIIIC-220.5	S1911A	GCAGAAGCCCAGGCCCCA**GCT**CCACCCCC AGCTCTTG
pGST-TFIIIC-220.5	S1937A	AGGGTGTCGGTGAGTTCAGT**GCC**CCAGGC CAAGAGCAGCTG
pGST-TFIIIC-110.1	S25A	AACATGACTGTGGTAGAC**GCT**CCTGGACAA GAGGTGC
pGST-TFIIIC-110.1	T55A	CCGTAGAGATGTCATTACCT**GCC**CCTTTGC CTGGATTTGAG
pGST-TFIIIC-110.1	S136A	GATCGGCCAGAATCTCAA**GCT**CCAAAGAGG CCCCCTG
pGST-TFIIIC-110.1	T137A	TCAATCCAACCCTCTGTCC**GCC**CCCATGCC TAAGAAACGAG
pGST-TFIIIC-110.2	S871A	ATTTTGTCCGTGGACTCGCC**GCC**CCACTGG GCCACCGTATG

3. Cell culture

3.1. Cell lines

The mammalian cell lines used in this work are as follows:

- HEK-293T: epithelial cell line derived from human embryonic kidney transformed with the SV40 virus large T antigen.
- HeLa: epithelial cell line derived from human cervical adenocarcinoma.
- IMR90: fibroblastic cell line derived from human lung.
- T47D: epithelial cell line derived from human breast ductal carcinoma.
- T98G: fibroblastic cell line derived from human glioblastoma.
- U2OS: epithelial cell line derived from human osteosarcoma.

The cell lines were supplied by the American Type Culture Collection (atcc.org). All cell lines, except for T47D and IMR90, were cultured in Dulbecco's Modified Eagle's Medium (DMEM, Invitrogen) containing 10% foetal bovine serum (FBS, Invitrogen) and supplemented with antibiotics (100 U/ml penicillin and 100 μg/ml streptomycin, Invitrogen) at 37ºC and in a 5% CO_2 atmosphere. The T47D and IMR90 cells were grown in the presence of RPMI supplemented with 10% FBS. The T47D cells and the IMR90 cells were a kind gift from Miguel Beato's group (CRG) and Fatima Gebauer's group (CRG), respectively.

For T98G serum starvation, cells were plated at 40% confluency. One day after, cells were washed twice with phosphate-buffered saline (PBS) to remove residual FBS and incubated in serum-free media for 48 h. Treatment of T98G cells with harmine (Sigma-Aldrich, final concentration 10 μM), or dimethyl sulfoxide (DMSO) as vehicle, was carried out for 16 h.

For depletion of protein expression, small interfering RNAs (siRNAs) or short hairpin RNAs (shRNAs) were used. They were delivered by lipofectamine transfection (MM3.2) and lentiviral infection (MM3.3), respectively. Experiments only proceeded when the knock-down efficiency was at least 50% or higher. The expression levels were assessed by Western blot (MM4.2).

3.2. Cell transfection

For siRNAs delivery, Lipofectamine® 3000 transfection kit (Thermo Fisher Scientific) was used according to the manufacturer's instructions. Briefly, 30 nM siRNA was added to HeLa cells incubated in DMEM without antibiotics. Sixteen hours after transfection, cells were washed with PBS and fresh complete DMEM was added. After 24 h, the cells were processed according to the purpose of the experiment. siRNAs were obtained from GE Healthcare Dharmacon Inc.

- siControl: ON-TARGETplus Non-Targeting Pool (D-0018110-10) with the target sequences UGGUUUACAUGUCGACUAA, UGGUUUACAUGUUGUGUGA, UGGUUUACAUGUUUUCUGA, and UGGUUUACAUGUUUUCCUA.
- siDYRK1A: ON-TARGETplus human DYRK1A (1859) siRNA SMARTpool (L-004805-00) with the target sequences GGGAAUGCCUUAUGACCUU, AAAAGUGGAUGGAUCGUUA, UAAG GAGCUUGAUUAUGA, and GAAUUCAACCUUAUUAUGC.
- siBDP1: ON-TARGETplus human BDP1 siRNA SMARTpool (L-020228-00) with the target sequences UCAGACAGAUACCG AAUAU, GAAGAGCAAUAUCUCAAUA, CCAAACUGCUCGACAAGUA, GGUCAAGCCUGUAGGUAAA.

3.3. Preparation of lentiviral stocks and infection

The CRG has all the permits to work with lentivirus in a biological contention level 2 (A/ES/05/I-13 and A/ES/05/14), and the activity of the group has been positively evaluated by the CRG Biological Safety Committee. To generate a viral stock, HEK-293T cells were seeded at a density of 2.5 x 10^6 cells in 100-mm plates and transfected with 3.4 μg of pCMV-VSV-G envelope plasmid, 6.3 μg of pCMV-dR8.91 packaging construct and 9.8 μg of the pLKO-based plasmids using the calcium phosphate precipitation method (Graham and van der Eb, 1973). Fresh DMEM was added 24 h after transfection, and the lentivirus containing supernatant was harvested at 48 h and 72 h after transfection. After harvesting, the supernatant was spun at 1,000 x *g* for 10 min and filtered through a 0.45 μm filter (Millipore). The supernatants were pooled together and concentrated by centrifugation (20,200 rpm for 2 h at 4ºC using a SW32Ti rotor in a Beckman Coulter centrifuge) followed by re-suspension of the viral pellet in PBS, aliquoted and stored at -80ºC.

For infection, cells were seeded at a density of 4 x 10^5 cells in 100-mm plates. The virus was added to the medium with the cells in suspension. Positive selection was performed the day after by adding 1.25 μg/ml of puromycin and incubated for another 48 h. After that time, another round of selection with puromycin was performed before processing the day after.

4. Techniques for protein analysis

4.1. Preparation of cell lysates

Total cell lysates were prepared by lysing cells in SDS lysis buffer (25 mM Tris-HCl pH 7.5, 1% [w/v] sodium dodecyl sulphate [SDS], 1 mM ethylendiamine tetracetic acid [EDTA], 10 mM $Na_4P_2O_7$ [NaPPi], 20 mM β-glycerolphosphate), vortexed for 10 sec and heated for 10 min at 98ºC (the process was repeated until the lysate got fluid).

Soluble cell lysates were prepared by lysing the cells in HEPES lysis buffer (50 mM 4-[2-hydroxyethyl]-1-piperazineethanesulfonic acid [HEPES] pH 7.4, 150 mM sodium chloride [NaCl], 2 mM EDTA, 1% [v/v] Nonidet P-40 [NP-40, Sigma]), supplemented with a protease inhibitor cocktail (complete Mini; Roche Diagnostic) and phosphatase inhibitors (2 mM Na_3VO_4, 30 mM NaPPi, and 25 mM NaF); the cell suspension was incubated for 20 min at 4ºC, followed by centrifugation at 13,200 rpm (Eppendorf 5424 Microcentrifuge) for 30 min at 4ºC to separate the lysate from insoluble cellular components. Protein quantification was done with the BCA Protein Assay Kit (Pierce – Thermo Scientific) according to the manufacturer's instructions.

4.2. Western blot (WB) analysis

Protein extracts were denatured by adding 6x loading buffer (350 mM Tris-HCl pH 6.8, 30% [v/v] glycerol, 10% SDS, 600 mM dithiothreitol [DTT], 0.012% [w/v] bromophenol blue) and incubated at 98ºC for 10 min. The proteins were resolved on SDS-polyacrylamide gels (SDS-PAGE) of various acrylamide percentages (depending on the molecular weight of the proteins of interest) at 130 V in 1x electrophoresis running buffer (25 mM Tris-base, 200 mM glycine, 0.1% SDS). Proteins were transferred onto Hybond-ECL nitrocellulose membranes (Amersham Biosciences) at 0.4 A for 1 h at 4ºC in 1x transfer buffer (25 mM Tris-HCl pH 8.3, 200 mM glycine, 20% [v/v] methanol). The presence of proteins in the membrane was checked by Ponceau S (Sigma) staining.

Transferred membranes were blocked with either 10% (w/v) non-fat milk (PanReac AppliChem ITW reagents) or 5% (w/v) bovine serum albumin (BSA) diluted in TBS-T (10 mM Tris-HCl pH 7.5, 100 mM NaCl, 0.1% [v/v] Tween-20 [Sigma]) for 1 h at room temperature. The membranes were incubated with the primary antibody diluted in either 5% non-fat milk or 3% BSA in TBS-T for 16 h at 4ºC (see Table MM.7). Removal of the non-bound primary antibody was done by performing three 10 min washes of the membranes with TBS-T, followed by the addition of the secondary

antibody (horseradish peroxidase (HRP)-conjugated, see Table MM.8), diluted in either 5% non-fat milk or 3% BSA in TBS-T. The incubation proceeded at room temperature for 1 h. After three 10 min washes with TBS-T, the signal on the membranes was revealed by chemiluminescence with Western Lightning Plus ECL (Perkin Elmer) and exposed in a LAS-3000 image analyser (Fuji PhotoFilm) with the LAS3000-pro software. Band intensities were quantified with the ImageStudio™ Acquisition software (LI-COR Biosciences). Relative protein levels were calculated using either α-Tubulin or vinculin as loading control.

Table MM.7: Properties and working dilution of the primary antibodies used for WB.

Primary antibody	Host	Dilution	Commercial brand
BDP1	Rabbit	1:1000	M. Teichmann's lab (crude and AP)
BDP1	Goat	1:1000	Santa Cruz (N-20, sc-15945)
BRF1	Rabbit	1:1000	Bethyl (A301-227A)
DYRK1A	Mouse	1:1000	Santa Cruz (RR.7, sc-100376)
DYRK1A	Mouse	1:1000	A gift from Dr. Stephanie Simon (iBiTec-S, France).
DYRK1A p-S520	Rabbit	1:250	(Alvarez et al., 2007)
GST	Mouse	1:500	Santa Cruz (B-14, sc-138)
TFIIIC-220	Rabbit	1:1000	Bethyl (A301-293A)
GTF3C3	Rabbit	1:1000	Bethyl (A301-238A)
P70S6K (total)	Rabbit	1:1000	Cell Signaling (#9202)
P70S6K (pT389)	Rabbit	1:1000	Cell Signaling (#9234)
POLR3A	Rabbit	1:1000	Abcam (ab96328)
RPBI NTD (POL II)	Rabbit	1:1000	Cell Signaling (D8L4Y, #14958)
TBP	Rabbit	1:1000	Abcam (ab63766)
TFIIIC-110	Mouse	1:1000	Santa Cruz (23952C2a, sc-81406)
α-Tubulin	Mouse	1:5000	Sigma (T6199)
Vinculin	Mouse	1:10000	Sigma (V9131)

Table MM.8: Properties and working dilution of the secondary (HRP-conjugated) antibodies used for WB.

Secondary antibody	Host	Dilution	Commercial brand
Anti-mouse	Rabbit	1:2000-10000	Dako (P0260)
Anti-rabbit	Goat	1:1000-2000	Dako (P0448)
Anti-goat	Rabbit	1:2000	Abcam (ab6741)

4.3. Testing BDP1 antibodies for WB analysis

To be able to study the interaction between DYRK1A and BDP1, three different antibodies (one commercial and two from the lab of M. Teichmann, listed in Table MM.7) were tested in WB analysis. Each antibody recognized a complex and different pattern of bands (Figure MM.1C). To distinguish bands that are specific to BDP1, HeLa cells were transfected with siRNAs specific either to BDP1, DYRK1A as a positive control, or a negative control, and cell extracts were subjected to SDS-page followed by WB analysis (Figure MM.1B).

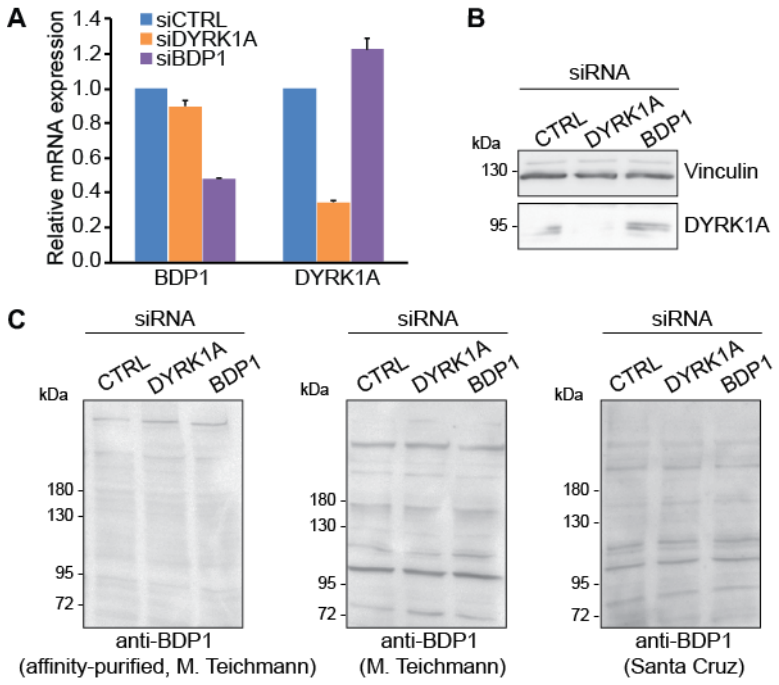

Figure MM.1: Testing of BDP1 antibodies by Western blot analysis. (A) RT-qPCR results showing the reduced RNA expression of BDP1 and DYRK1A following transfection of HeLa cells with respective siRNAs. Data are represented as RNA levels relative to the siControl (siCTRL) condition set as 1 (mean±SD of n=3 technical triplicates). **(B)** DYRK1A and BDP1 knock-down was performed in HeLa cells with siRNA transfection. Total extracts were analysed by WB with DYRK1A antibody. Vinculin is used as a loading control. **(C)** HeLa were transfected with the indicated siRNAs, and total cell extracts were analysed by WB using three different antibodies targeting BDP1, as indicated. The position of molecular weight markers is indicated.

The downregulation efficiency of BDP1-siRNA was confirmed by reverse transcription followed by quantitative PCR (RT-qPCR) analysis (MM6.3). Although there was a 50% knockdown of BDP1 at the RNA level (Figure MM.1A), all the bands recognized by the three antibodies were insensitive to the siRNA treatment (see Figure MM.1C). These results raise a concern about the specificity of the antibodies, and, therefore, BDP1 was no longer considered in this study.

4.4. Immunoprecipitation (IP) assay

Immunoprecipitation (IP) assays were performed using either soluble cell extracts or commercial HeLa nuclear extracts (CIL Biotech). The assays were carried out using Protein G or Protein A coupled to magnetic beads (Invitrogen), depending on the host of the antibody used (Protein G for mouse antibodies and Protein A for rabbit antibodies). The beads were incubated with the specific antibody or control immunoglobulins G (IgGs) (see Table MM.9) for 1 h at room temperature. In the case of the HeLa nuclear extracts, pre-clearing was carried out by incubating the extract with beads for 1 h at 4ºC. Afterwards, the antibody-bound beads and the extracts were incubated for 2 h at 4ºC. The beads were washed three times with washing buffer (50 mM HEPES pH 7.4, 150 mM NaCl, 2 mM EDTA) containing 0.1% NP-40 followed by one additional wash in washing buffer without detergent. Finally, the immunoprecipitated proteins were eluted in 2x loading buffer (100 mM Tris-HCl pH 6.8, 200 mM DTT, 4% SDS, 20% glycerol, 0.2% bromophenol blue) and boiled at 98ºC for WB analysis (MM4.2).

Table MM.9: Properties and amount of the antibodies used for IP.

Antibody	Host	Amount	Commercial brand
BRF1	Rabbit	3 μg	Bethyl (A301-227A)
DYRK1A	Mouse	1.5 μg	Santa Cruz (RR.7, sc-100376)
DYRK1A	Mouse	3 μg	A gift from Dr. Stephanie Simon (iBiTec-S, France).
DYRK1A	Rabbit	3 μg	Abcam (ab69811)
DYRK1A	Rabbit	3 μg	Sigma (D1694)

TFIIIC-220	Rabbit	3 μg	Bethyl (A301-291A)
TFIIIC-110	Mouse	3 μg	Santa Cruz (23952C2a, sc-81406)
Normal IgGs	Mouse	3 μg	Santa Cruz (sc-2025)
Normal IgGs	Rabbit	3 μg	Santa Cruz (sc-2027)/Cell Signaling (2729)

4.5. Purification of GST-fusion proteins

For the production of GST-fusion proteins, one fresh colony of *E. coli* BL21 (DE3) pLysS B F' (Agilent Technologies) containing the plasmid of interest was inoculated in 5 ml LB medium supplemented with 100 μg/ml ampicillin. The culture grew over night (O/N) at 37ºC shaking with 220 rpm. Then, it was re-inoculated (1:50 - 1:100 dilution) in 100 - 200 ml LB medium with 100 μg/ml ampicillin. The bacterial culture grew at 37ºC with 220 rpm agitation until an absorbance at 600 nm (A_{600}) of 0.6 -0.8 was reached.

Conditions for protein production with 0.1 mM IPTG induction were assessed using growth temperature and induction time as variables. Thus, inductions for 8 h at 20ºC were used for GST-DYRK1A, GST-TFIIIC-220.1, GST-TFIIIC-220.2, GST-TFIIIC-220.5, GST-TFIIIC-110.1, GST-TFIIIC-102.1 and GST-TFIIIC-90 (and their corresponding non-phosphorylatable derivatives); whereas inductions for 4 h at 37ºC were used for unfused GST, GST-TFIIIC-110.2, GST-TFIIIC-102.2, GST-TFIIIC-63 and GST-TFIIIC-35 (and their corresponding non-phosphorylatable derivatives). Bacteria were then centrifuged at 6,000 x *g* for 15 min at 4ºC and pellets were re-suspended in 10 ml of GST lysis buffer (10 mM Tris-HCl pH 8, 100 mM NaCl, 0.5% NP-40 and 1 mM EDTA) supplemented with protease inhibitor cocktail (Complete Mini, Roche Diagnostic). The lysates were sonicated with a Branson Sonifier-250 (3 pulses of 15 sec, 10% amplitude) followed by centrifugation at 10,000 x *g* for 15 min at 4ºC.

For the purification of the fusion proteins, the bacterial soluble supernatant was incubated for 1.5 h at room temperature with 100 μl of glutathione-

Sepharose beads (Amersham Biosciences) and washed three times in GST lysis buffer. When required, fusion proteins were eluted by incubation in 100 μl of elution buffer (10 mM L-glutathione reduced [Sigma], 50 mM Tris-HCl pH 8) three times for 10 min rotation at room temperature to a final volume of 300 μl. Unfused GST was used as a control in some experiments, and in this case elution was performed with 300 μl of elution buffer in one single step. To remove the free glutathione, proteins were dialysed against dialysis buffer (50 mM HEPES pH 7.4, 150 mM NaCl, 2 mM EDTA) O/N at 4ºC using dialysis tubing (MWCO 12-14,000, Spectra/Por).

Finally, protein concentration and quality was assessed by resolving the samples by SDS-PAGE and gel staining with Coomassie (0.25% [w/v] Coomassie brilliant blue [Sigma] in 90% methanol and 10% [v/v] acetic acid), using known amounts of BSA as a standard.

4.6. Attempts of purification of the GST-TFIIIC-220.3 fragment

A different approach was necessary to purify the GST-TFIIIC-220.3 fragment, as the fusion protein did not solubilise using the standard approach described in MM4.5 (data not shown). Thus, 1% sarcosyl (N-Lauroyl sarcosine sodium salt, Sigma) was added to the GST lysis buffer before sonication. Following sonication, Triton X-100 (Roche) was added to a 1% final concentration before centrifugation at 11,000 rpm at 4ºC for 20 min. Thereafter, Triton-X was added to the supernatant to a final concentration of 3%, before incubating the supernatant with 100 μl of glutathione-Sepharose beads for 1.5 h at room temperature. When assessing the quality by resolving the sample by SDS-PAGE and WB analysis using an antibody recognizing the GST tag, it was discovered that a fusion protein of the expected molecular weight was induced by the IPTG treatment (compared "pre-" with "post-IPTG" in Figure MM.2) and it was solubilised in the conditions used (compared "post-IPTG" with "soluble" in Figure MM.2A). However, the fusion protein did not bind to the

beads (compared "beads" with "post-beads" in Figure MM.2). Therefore, due to fact that the GST-TFIIIC-220.3 fusion protein could not be purified, no further analysis was possible with this fragment.

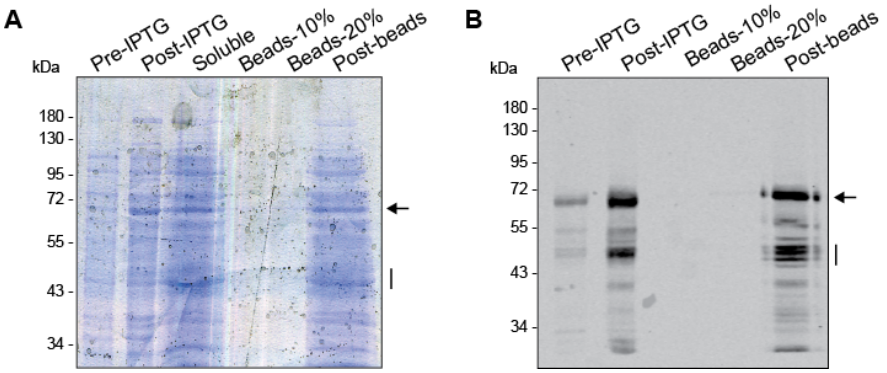

Figure MM.2: Attempt of purification of GST-TFIIIC-220.3. Equivalent samples for the purification procedure of the GST-TFIIIC-220.3 fusion protein was analysed by SDS PAGE and Coomassie staining **(A)** or WB analysis with an antibody against GST **(B)**, as follows: bacterial lysates before IPTG induction (pre-IPTG), after IPTG induction (post-IPTG), soluble extracts (soluble), beads after incubation with the soluble extracts (beads), and the unbound fraction (post-beads). The arrow indicates the band corresponding to GST-TFIIIC-220.3, and the vertical lane a group of C-terminal truncated proteins.

4.7. *In vitro* kinase assay

For the *in vitro* kinase assays (IVK), the source of enzyme was GST-DYRK1A expressed in bacteria and purified through glutathione-affinity chromatography (CRG Biomolecular Screening and Protein Technologies Unit). The enzyme was incubated with 50 μM ATP in the presence of 2.5 μCi [γ^{32}P]-ATP (3000 Ci/mmol, Perkin Elmer) and the specific substrate, bacterially expressed and purified, for 20 min at 30ºC in 20 μl of kinase buffer (25 mM HEPES, pH 7.4, 5 mM $MgCl_2$, 5 mM $MnCl_2$, 0.5 mM DTT). ^{32}P incorporation was determined by eluting the samples from the beads in 2x loading buffer and resolving them by SDS-PAGE. The gel was stained with Coomassie, dried for 1 h at 80ºC and exposed to a film or a Phosphoimager screen (revealed using the GE Typhoon Trio imager). The signal was normalised to the substrate amounts evaluated by WB or Coomassie staining.

The identification of DYRK1A-dependent TFIIIC phosphosites was performed by incubating bacterially expressed and purified GST-TFIIIC fragments with GST-DYRK1A in kinase buffer with 1 mM ATP for 1 h at 30ºC.

4.8. Mass spectrometry analysis

Mass spectrometry (MS) analysis was used to identify DYRK1A-dependent TFIIIC phosphorylation sites. Samples phosphorylated *in vitro* (MM4.7) were washed three times with 100 mM ammonium bicarbonate (ABC) buffer, re-suspended in 100 μl of 6 M Urea diluted in 100 mM ABC buffer and incubated for 1 h at 37ºC in the presence of 0.3 mM DTT. Alkylation was carried out with 0.6 mM iodoacetamide (Sigma) for 30 min at room temperature in the dark. Then, proteins were digested in additional 194 μl of 100 mM ABC buffer with 1 μg endoprotease Lys-C (Wako) O/N at 37ºC. Further digestion was performed with 295.8 μl of 100 mM ABC buffer plus 1 μg sequence-grade trypsin (Promega) over day at 37ºC. Finally, digestion was stopped by adding 60.5 μl of formic acid. Peptides were desalted using Ultra Micro Spin Columns C18 (The Nest Group INC).

Samples were analysed using an LTQ-Orbitrap Fusion Lumos mass spectrometer (MS, Thermo Scientific) coupled to an EasyLC (Thermo Scientific, Proxeon) at the CRG/UPF Proteomics Unit. Peptides were loaded onto the analytical column at a flow rate of 1.5-2 μl/min using a wash-volume of 4 times the injection volume, and were separated by reversed-phase chromatography using a 50-cm column with an inner diameter of μm, packed with 2 μm C18 particles spectrometer (Thermo Scientific). Chromatographic gradients started at 95% buffer A (0.1% [v/v] formic acid in H_2O) and 5% buffer B (0.1% formic acid in acetonitrile) with a flow rate of 300 nl/min and gradually increased to 22% buffer B in 52 min and then to 35% buffer B in 8 min. The column was washed for 10 min with 5% buffer A and 95% buffer B after each sample. The MS was

operated in Automated Data Dependent Acquisition (DDA) mode and full MS scans with 1 micro scans at resolution of 120,000 were used over a mass range of m/z 350-1,500 with detection in the Orbitrap. Auto gain control was set to 2e5 and dynamic exclusion to 60 sec. In each DDA analysis cycle, following each survey scan Top Speed, ions with charged 2 to 5 above a threshold ion count of 1e4 were selected for fragmentation. Each precursor ion was fragmented both with high-energy collision dissociation (HCD) and electron transfer dissociation (ETD) with collision-induced dissociation supplemental activation at 35%. The quadruple isolation window was set to 1.6 m/z. Fragment ion spectra produced via HCD were acquired at a normalised collision energy of 28% and both HCD and ETD spectra were acquired in the Orbitrap at 30K. Data were acquired with Xcalibur software (v3.0.63, Thermo Fisher Scientific).

Acquired data were analysed using the Proteome Discoverer software suite (v2, Thermo Fisher Scientific), and data were searched with Mascot search engine (v2.6, Matrix Science) against SwissProt *H. sapiens*, where the most common contaminants were added. The phosphoRS node was used for phosphor-site probability determination. The identified peptides were filtered using a false discovery rate (FDR) <5%.

5. Chromatin immunoprecipitation (ChIP) associated procedures

5.1. ChIP assay

ChIP assays were performed in collaboration with Chiara Di Vona. The assays were performed with 5 x 10^6 T98G cells per IP. Briefly, formaldehyde was added to the cell culture medium, at the time of processing, to a final concentration of 1% (v/v) and incubated for 10 min at room temperature with gentle shaking. Crosslinking was quenched with 0.125 M glycine for 5 min. Crosslinked cells were washed twice with cold PBS, re-suspended in Lysis buffer I (5 mM PIPES pH 8.0, 85 mM KCl, 0.5% NP-40) supplemented with the protease inhibitor cocktail, and

incubated on ice for 10 min. Cells were collected by centrifugation (2,000 rpm for 5 min at 4ºC) and the cell pellet was re-suspended in Lysis buffer II (1% SDS, 10 mM EDTA, 50 mM Tris-HCl pH 8.0) supplemented with protease inhibitor cocktail, and incubated for an additional 10 min on ice. The chromatin was sonicated to an average size of 0.2 - 0.5 kb using the Bioruptor (Diagenode). Finally, 20 μl of chromatin was reverse-crosslinked at 65ºC O/N and DNA was purified using phenol-chloroform to quantify concentration using Qubit ® dsDNA BR Assay Kit (Thermo Fisher Scientific), and to check the size and quality of the DNA fragments by fractionation in 1% agarose gel.

For each IP, the chromatin amount corresponding to 150 μg of the non-purified cross-linked DNA was diluted in 1 ml of IP buffer (300 mM NaCl, 200 mM Tris-HCl pH 8.0, 10 mM EDTA, 1% SDS and 5% Triton X-100). Samples were incubated with rotation O/N at 4ºC with specific antibodies or control IgGs (see Table MM.10). The immunocomplexes were recovered by adding 30 μl of protein A sepharose beads (GE Healthcare), and incubated for an additional 3 h at 4ºC with rotation. Beads were washed with three successive 1 ml washes of Low Salt buffer (140 mM NaCl, 50 mM HEPES pH 7.4, 1% Triton-X 100), one wash with High Salt buffer (500 mM NaCl, 50 mM HEPES pH 7.4, 1% Triton-X 100), one wash with LiCl buffer (10 mM Tris-HCl pH 8.0, 250 mM LiCl, 1% NP-40, 1% [v/v] deoxycholic acid and 1 mM EDTA), and a final wash in TE buffer (10 mM Tris-HCl pH 7.6, 1 mM EDTA) (all buffers contained the protease inhibitor cocktail). Elution of DNA from beads was achieved by incubating the samples in 250 μl of Elution buffer (1% SDS, 100 mM $NaHCO_3$) for 30 min twice at 65ºC with constant agitation (1,000 rpm in a Thermomixer [Eppendorf]); the supernatant was recovered by centrifugation at 3,600 rpm for 5 min at room temperature in a Microfuge. The crosslinking was reverted by an additional incubation of the samples in 200 mM NaCl at 65ºC O/N with agitation at 1,000 rpm. Chromatin-associated proteins were further degraded by adding 1.6 U of protease K (New England Biolabs) for

2 h at 45ºC with 1,000 rpm agitation. The ChIP-DNA was purified by phenol/chloroform extraction followed by ethanol precipitation. Finally, the DNA was re-suspended in 10 μl of nuclease-free water and quantified using the Qubit ® dsDNA HS Assay Kit (Thermo Fisher Scientific) for the ChIP-DNA and the Qubit ® dsDNA BR Assay Kit for the input-DNA.

Table MM.10: Properties and amount of the antibodies used for ChIP.

Antibody	Host	Amount	Commercial brand
DYRK1A	Rabbit	6 μg	Abcam (ab69811)
RPBI NTD	Rabbit	6 μg	Cell Signaling (D8L4Y, #14958)
POLR3A	Rabbit	6 μg	Abcam (ab96328)
TFIIIC-110	Rabbit	6 μg	M. Teichmann lab (#3420)
Normal IgGs	Rabbit	6 μg	Santa Cruz (sc-2027)/Cell Signaling (2729)

5.2. DNA library preparation for ChIP-seq analysis

Libraries were prepared after checking the quality of the ChIP by evaluating several positive and negative control targets by qPCR. The libraries were generated using the Ovation® Ultralow Library System V2 (NuGEN) following the manufacturer's instructions. Before sequencing, a quality control was carried out by qPCR analysis of control targets. Libraries were sequenced on an Illumina GAIIx sequencer (HiSeq sequencing v4 chemistry) with a read length of 50 base pair (bp) single end at the CRG Genomics Unit according to established protocols at the Unit.

5.3. Bioinformatics analysis of ChIP-seq data

The bioinformatics analysis including read mapping and peak identification was done by Chiara Di Vona. The analysis was performed basically as described in (Ferrari et al., 2012), with few modifications. Briefly, reads were mapped to the unmasked human (hg38) genome assembly using Bowtie software (Langmead et al., 2009), and the Poisson distribution was used to estimate the probability of observing the ChIP counts within a window given the expected counts un the input sample window. All windows with *p*-values less than 1×10^{-8} were considered to

have significant peaks. The algorithm produced several files that were subsequently used for analysis: BED files contain the coordinates of the significant windows of enrichment and Wiggle (wig) files (chromosome tiling, fixed step) with normalised read counts for the significant windows. When different biological replicates were obtained, the reads coming from them were combined and used for peak calling to improve the coverage of the analysis and reduce possible false positives. This was the case for DYRK1A in normal growing conditions.

For peak annotation, an in-house gene and promoter annotation pipeline developed by Sarah Bonnin (CRG Bioinformatics Unit) was used.

The Integrated Genomics Browser v9.0.0 (Nicol et al., 2009) and the UCSC Genome Browser were used for visualisation of ChIP-seq data sets. Downstream analysis of the ChIP-seq data was carried out with C. Di Vona. Cis-regulatory Elements Annotation System (CEAS) (Ji et al., 2006) was used to create overlaps of significant peaks with genomic annotated regions. Sitepro, as part of the Cistrome Analysis pipeline (cistrome.dfci.harvard.edu/ap), was used to profile average binding (density plot) for defined genomic intervals: plotted values are the –log10 of Poisson *p*-values. Heat maps were generated using computeMatrix and plotHeatmap tools from deepTools v3.0.0 (Ramirez et al., 2016), and increasing shades of colour in the colour bar scales in the plots stand for higher enrichment and refer to the -log10 of Poisson *p*-values. When indicated, clusters were computed using the k-means algorithm. In some cases, the heat maps were classified according to Pol III promoter type (Canella et al., 2010), and it is indicated in the Figure legend. Correlation analysis of selected ChIP datasets were generated using multiBigwigSummary and plotCorrelation tools from deepTools (Ramirez et al., 2016). Correlation coefficients were computed according to the Spearman method v3.0.0 (Spearman, 1987).

For *de novo* detection of motifs associated to the peak regions, the HOMER suite (v4.9, 2-20-2017) was used (Heinz et al., 2010).

6. RNA analysis

6.1. RNA purification and reverse transcription (RT)

Total RNA was isolated with the RNeasy extraction kit (Qiagen) or with Trizol (Ambion) following the corresponding manufacturer's instructions. In some cases, samples were treated with DNase I (Ambion, 2 U/μl) for 30 min at 37ºC to eliminate the remaining genomic DNA. The RNA was quantified NanoDrop. For reverse transcription, 0.5-1 μg RNA was subjected to cDNA synthesis using Superscript II Reverse Transcriptase (RT) (Invitrogen) and random primers recommended by the manufacturer's instructions.

6.2. Quantitative Polymerase Chain Reaction (qPCR)

PCR reactions (10 μl) were performed using 1/10 dilution of cDNA as template in triplicate with SYBR Green (Roche) and 10 pmol of specific primers (see Table MM.11) in 384 well plates using the Roche LC-480 equipment (Roche Applied Science), and the PCR programme specified in Table MM.12. The crossing point (Cp) was calculated for each sample using the second derivative maximum method with the Lightcycler 480 1.2 software (Roche), and data analysed for relative quantification. The expression of the housekeeping gene *GAPDH* or *PPIA* was assessed as a control. No PCR products were observed in the absence of template. All primer sets gave narrow single melting point curves that were checked at the end of each run.

Table MM.11: Sequences of oligonucleotides used for RT-qPCR experiments.

Gene	Forward primer	Reverse primer
BDP1	GGCCACCAGATCGTTCAAAA	CTGGAGTCGATGGCTTTTCAG
DYRK1A	CCTTGATAGGCAAAGGTTCC	CGCACTTCTATCTGTGCTTG
GAPDH	ACCCAGAAGACTGTGGATGG	TTCAGCTCAGGGATGACCTT
PPIA	GCCGACCAAAACCGTGTACT	GTCTTTGGGACCTTGTCTGC

tRNA-Ser-GCT-3-1	GGTAAGGCGATGGACTGCT	GAACCCACGCGTGCAAAG
tRNA-Pro-TGG-2-1	GGCTCGTTGGTCTAGGGG	GGACCCAAACCGAGAATCAT
tRNA-iMET-CAT	CTGGGCCCATAACCCAGAG	CTGGGCCCATAACCCAGAG
tRNA-MET-CAT	CTCGTTAGCGCAGTAGGTAGC	GGTCGAACTCACGACCTTC

Table MM.12: PCR conditions for the qPCR reaction.

	T	Time
Denaturation	95ºC	5 min
45 cycles	95ºC	15 sec
	60ºC	20 sec
	72ºC	20 sec

7. Databases and other computational tools

Protein and DNA sequences were searched and analysed by using public databases of the National Centre for Biotechnology Information (NCBI, www.ncbi.nlm.nih.gov) and Ensembl (ensembl.org). The tRNA genome in *H. sapiens* were searched and analysed using the public Genomic tRNA database (GtRNAdb, gtrnadb.ucsc.edu/genomes/eukaryota/hsapi38).

Bibliography references were queried with the database Pubmed from NCBI.

The BioVenn free software (www.biovenn.nl) was used to overlap gene targets from different datasets (Hulsen et al., 2008).

Conservation analysis of the TFIIIC fragments was performed using COBALT (Constraint-based Multiple Alignment Tool) from NCBI (Papadopoulos and Agarwala, 2007). For the comparison, the proteins in *H. sapiens* were compared to *Bos taurus*, *Mus musculus*, *Gallus gallus* and *X. tropicalis* (see Table MM.13).

Table MM.13: The accession numbers for the TFIIIC subunits, in the indicated species, used in the conservation analysis.

Protein	*H. sapiens*	*B. taurus*	*M. musculus*	*G. gallus*	*X. tropicalis*
TFIIIC-220	NP_001511	NP_001180170	NP_997122	XP_004945401	XP_002938335
TFIIIC-110	NP_001512	XP_003586709	NP_082177	XP_428530	XP_002943430

8. Statistical tools

Bar graphs for RT-qPCR experiments were generated with Microsoft Excel v15.33. The other bar graphs were generated using R Studio software and the R package ggplot2. Statistical significance was calculated with a two-tailed unpaired Student's t-test (Microsoft Excel v15.33). The data in the graphs represent the mean ± standard deviation (SD) of independent experiments or technical replicates (indicated in each Figure Legend). A *p*-value ≤ 0.05 was considered statistically significant.

Results

1. Characterisation of DYRK1A recruitment to Pol III genes

1.1. Pol III associated DYRK1A regions in the genome lack the DYRK1A palindromic motif

DYRK1A is recruited mostly to proximal promoters of Pol II-transcribed genes that are enriched in a palindromic motif TCTCGCGAGA (Di Vona et al., 2015). However, a subset of DYRK1A-associated peaks (around 30%) overlap with intergenic regions (Di Vona et al., 2015). To better characterize these regions, we performed ChIP-seq experiments using antibodies targeting DYRK1A, Pol II (largest subunit POLR2A), and Pol III (largest subunit POLR3A).

Three specific clusters of genomic regions were identified using an unbiased k-means clustering of DYRK1A-associated regions (Figure R.1A). The largest cluster overlapped with Pol II-associated promoters and is enriched in the DYRK1A palindromic motif TCTCGCGAGA, and corresponds to the previously described one (Di Vona et al., 2015) (Figure R.1A-B). The second cluster is mostly enriched in intergenic regions, in which DYRK1A co-localises with Pol III. Interestingly, this cluster shows no enrichment for the palindromic motif; instead, the most enriched motifs in the cluster belong to the B-box and A-box of the type 2 Pol III-transcribed genes (Figure R.1A-B). Of note, Pol II is not completely absent from these regions (Figure R.1A). In fact, the presence of the two polymerases in a subset of Pol III genes have already been reported (Barski et al., 2010; Canella et al., 2010; Moqtaderi et al., 2010; Oler et al., 2010). The DYRK1A motif was not detected in the common Pol III/Pol II loci, suggesting that even in these cases the recruitment of DYRK1A is very likely independent of its functional association with Pol II. Finally, the DYRK1A-only cluster showed enrichment for the CTCF binding motif as previously observed (Barba, 2018). These results indicate that DYRK1A is recruited to Pol III-associated regions and suggests that the method of

DYRK1A recruitment to these sites could be different to that of the Pol II-transcribed genes.

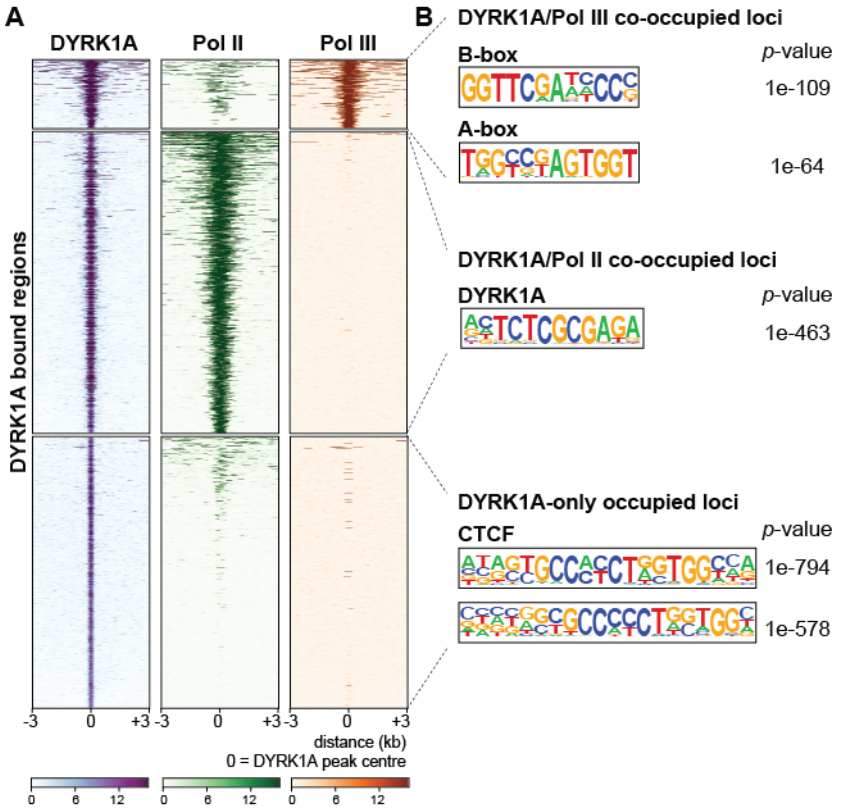

Figure R.1: DYRK1A-associated regions are bound by Pol II and Pol III. (A) Heat maps showing DYRK1A, Pol II and Pol III occupancies at DYRK1A bound regions relative to the DYRK1A peak centre in T98G cells. The colour bar indicates the binding score as calculated in MM.5.4. k-means clustering resulted into three different clusters of DYRK1A-associated regions. **(B)** Motif enrichment analysis of the three different clusters using HOMER. The parameters for the search were -250/+250 base pairs from the DYRK1A peak centre. The corresponding *p*-values are indicated.

To validate the recruitment of DYRK1A to Pol III-bound regions, DYRK1A occupancy was assessed in control cells and in cells where the levels of DYRK1A were depleted by lentiviral delivery of a shRNA to DYRK1A. Although the efficiency of DYRK1A downregulation was not very strong at the protein level (around ~70 %, Figure R.2A), chromatin-associated DYRK1A was reduced at target Pol III-bound genes (Figure R.2B-C).

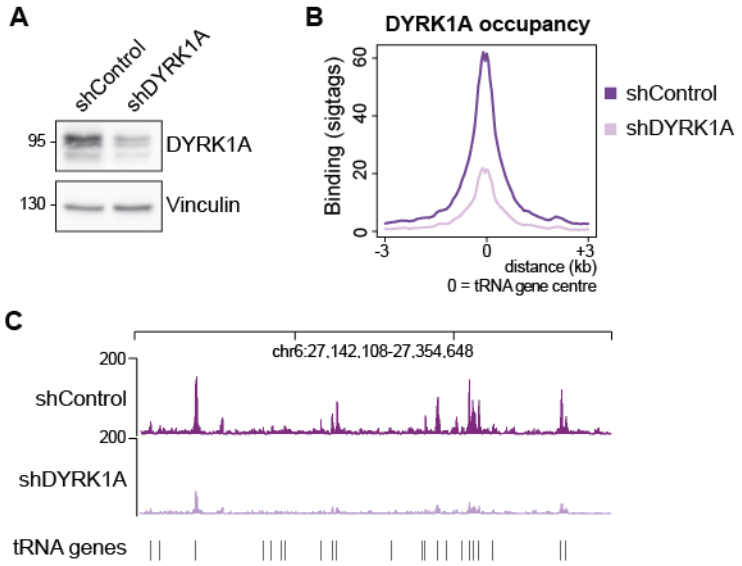

Figure R.2: DYRK1A recruitment to Pol-II transcribed and Pol III-transcribed genes is specific. (A) The reduction in DYRK1A levels in the shDYRK1A-T98G cells used in the ChIP assays was assessed by WB. Vinculin detection was used as a loading control. **(B)** Density plot indicating the average binding of DYRK1A at tRNA genes, from ChIP-seq experiments in shControl (dark purple) and shDYRK1A (light purple) cells using the ChIP-seq significant tags. **(C)** Representative example of DYRK1A ChIP-seq peaks in shControl (dark purple) and shDYRK1A (light purple) cells. Visualisation of wiggle files was performed using the Integrated Genome Browser. A track corresponding to mappable tRNA genes (from GtRNAdb) was uploaded to visualize tRNA genes' positions (depicted in black bars). The y-axis shows the significant reads (sigtags).

1.2. DYRK1A binds mostly to type 2 and type 3 Pol III promoters

As mentioned in the Introduction, Pol III-associated genes are divided into three types based on their promoters that in turn recruit different set of transcription factors (I2.1 and Figure R.3A). To understand whether DYRK1A has specificity for one particular class of Pol III promoters, we performed ChIP-seq experiments using antibodies targeting Pol III, TFIIIC (the TFIIIC-110 subunit), and DYRK1A.

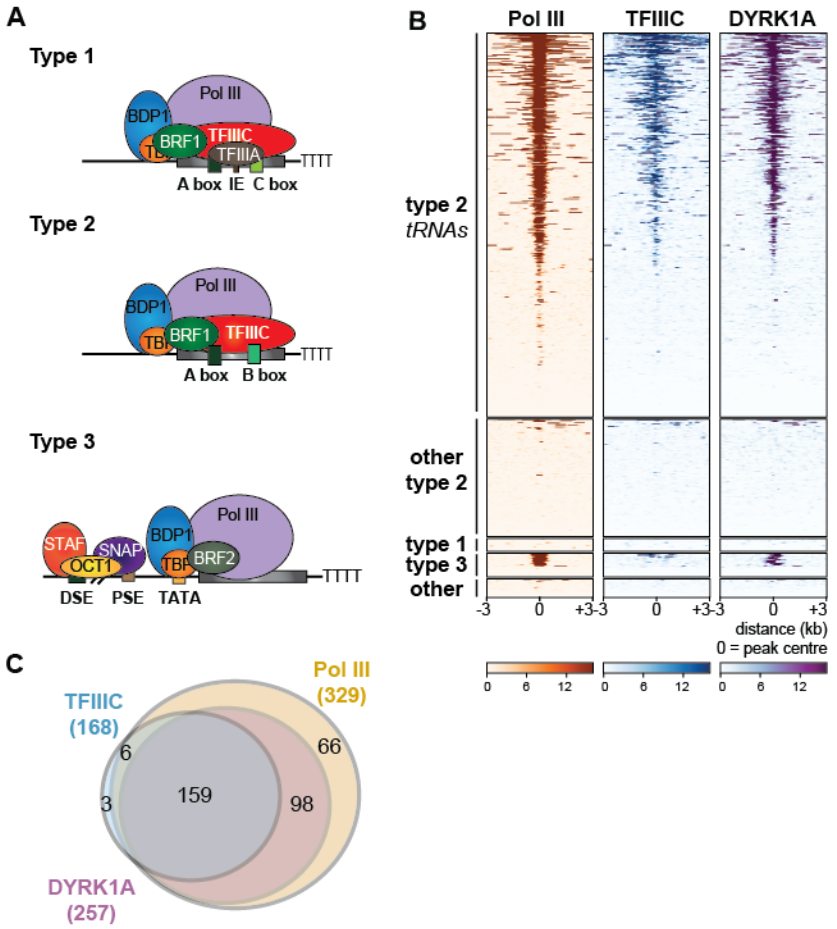

Figure R.3: Characterisation of DYRK1A on Pol III-associated promoters. (A) Scheme depicting the classification of the Pol III-associated promoters (adapted from Oler et al., 2010). **(B)** Heat map showing the genomic occupancy of Pol III, TFIIIC and DYRK1A in T98G cells. Pol III associated genes (based on Canella et al., 2010) have been classified by promoter type and ranked by the average binding of Pol III, TFIIIC and DYRK1A. The colour bar indicates the binding score as calculated in MM.5.4. **(C)** Venn diagram indicating the overlap of binding between Pol III, TFIIIC and DYRK1A at Pol III-associated genes. The number of genes bound is indicated in parenthesis.

Pol III occupied both type 2, which includes tRNA genes, and type 3, which includes U6 and 7SK- promoters, whilst TFIIIC was only found associated with type 2 genes (Figure R.3B and Table R.1). No information could be extracted for type 1 genes because they are not included in the version of the genome used for the mapping. In the case of Pol III, the results are consistent with previous reports that showed that Pol III was found only at around 60% of annotated Pol III genes (Barski et al., 2010;

Canella et al., 2010; Moqtaderi et al., 2010; Oler et al., 2010). Interestingly, the majority of DYRK1A-bound regions were positive for both Pol III and TFIIIC (Figure R.3C). A compilation of gene types and occupancy is provided in Table R.1.

Table R.1: Occupancy of Pol III, TFIIIC and DYRK1A on Pol III genes in T98G cells

Pol III promoter Type	Class of RNA	Number of genes in reference genome	Number of genes occupied by Pol III	Number of genes occupied by TFIIIC	Number of genes occupied by DYRK1A
Type 2	tRNA	605	298	160	236
	Alu	43	2	3	0
	MIR	5	1	0	1
	snaR	14	0	0	0
	HVG or Vault	3	3	0	3
	7SL or SRP	3	2	2	2
Type 3	RNA-Y	4	4	0	3
	U6	5	4	0	4
	U6atac	1	1	1	1
	RNase P	1	1	0	1
	RNase MRP	1	1	0	1
	7SK	1	1	0	1
	tRNASec	2	1	0	1
Other		21	4	0	1

It is assumed that Pol III occupancy implies active transcription (Barski et al., 2010; Canella et al., 2010; Moqtaderi et al., 2010; Oler et al., 2010), so the results suggest that DYRK1A-occupied Pol III genes that are actively transcribed. Indeed, RT-qPCR data show expression of tRNA genes co-occupied by DYRK1A and Pol III (Figure R.4A). Furthermore, the tRNA genes co-occupied by Pol III and DYRK1A encompasses all the isotypes of the tRNAs (Figure R.4B), with no apparent preference for a specific isotype observed. Thus, a possibility could be that DYRK1A acts as a general regulator of Pol III transcription.

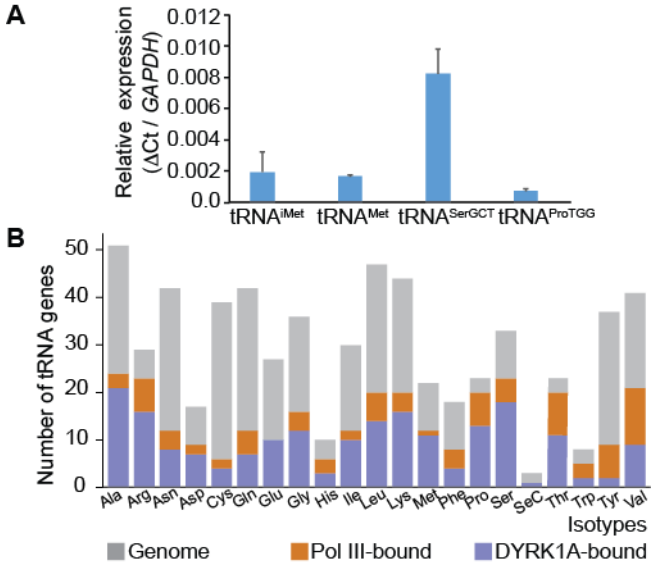

Figure R.4: Overview of DYRK1A on tRNA genes. (A) RT-qPCR results showing the expression of selected tRNAs relative to *GAPDH* in T98G cells (mean±SD of technical triplicates). **(B)** Bar graph illustrating the number of tRNA genes bound by Pol III and DYRK1A classified according to the isotype.

1.3. DYRK1A only associates with TFIIIC in Pol III-bound regions in the genome

TFIIIC is present not only at Pol III-bound regions in the genome, but also at ETC sites (Moqtaderi et al., 2010; Oler et al., 2010). Indeed, the number of identified TFIIIC peaks (1617) outnumbered the Pol III peaks (505) in our experimental system. Due to this observation, and the finding that most DYRK1A-occupied tRNA genes are also occupied by TFIIIC, we wondered whether DYRK1A was present at any other regions bound by TFIIIC. Thus, we analysed how chromatin-bound DYRK1A was distributed along all the TFIIIC-bound regions in the genome.

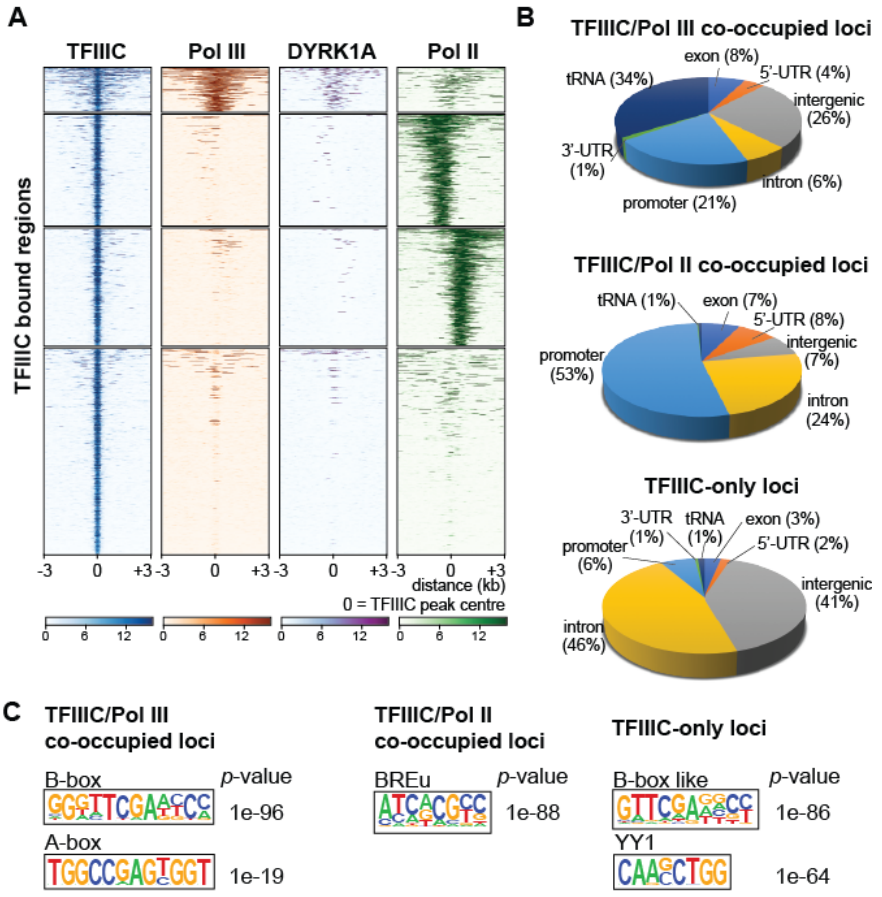

Figure R.5: DYRK1A associates with TFIIIC only at Pol III-bound regions. (A) Heat maps showing TFIIIC, Pol III, DYRK1A and Pol II occupancies at TFIIIC bound regions relative to the TFIIIC peak centre. The colour bar indicates the binding score as calculated in MM.5.4. The ChIP-associated regions have been separated into four clusters to differentiate the Pol II- and Pol III-positive TFIIIC-associated regions. **(B)** Pie charts illustrating the distribution of the TFIIIC loci over some genomic features across the different clusters. **(C)** Motif enrichment analysis for the different clusters using HOMER. The parameters for the search were -250/+250 base pairs from the TFIIIC peak centre. The corresponding *p*-values are indicated.

Based on the co-occupancy with the other factors, the TFIIIC-associated regions were classified into different clusters by using the k-means algorithm, which defined three subsets of loci (Figure R.5A). Around 50% of the TFIIIC-bound sites are associated with Pol II, and are within 1.5 kb of the Pol II peaks. These sites are mostly located close to the promoters of Pol II-bound genes (Figure R.5B), which is in agreement with reports

showing that around 70% of ETC loci are located within 1 kb of the TSSs of Pol II-transcribed genes (Moqtaderi et al., 2010). Furthermore, one of the Pol II core promoter motifs, TFIIB recognition element (BREu), is present in around 50% of the loci, which is in accordance with the number of promoters present in the cluster (Figure R.5B-C). This cluster is mostly devoid of DYRK1A, with only seven loci occupied by DYRK1A and all contain the DYRK1A motif (Figure R.5A).

The TFIIIC-only regions represent around 40% of all the TFIIIC-bound sites found in T98G cells, and are mostly devoid of both Pol II, Pol III and DYRK1A (Figure R.5A). Moreover, unlike the Pol II-associated regions there is no enrichment for promoters, but rather intergenic regions and introns (Figure R.5B). However, around 50% of the loci have a motif that is very similar to the B-box (Figure R.5C). Interestingly, this cluster was enriched in the transcription factor Yin Yang 1 (YY1) motif, with the motif present at nearly 80% of the sites (Figure R.5C). In addition, the CTCF motif was found at 7% of the sites in this cluster (data not shown). Like CTCF, YY1 is involved in mediating the enhancer-promoter interactions and thus regulates gene expression (Weintraub et al., 2017). These results suggest that TFIIIC could be involved in regulating enhancers belonging to this cluster in T98G cells.

Lastly, the regions where TFIIIC co-localises with Pol III represent around 10% of all TFIIIC peaks. Interestingly, DYRK1A only associates with TFIIIC at these Pol III-bound regions, suggesting that any cross-talk at the chromatin level between DYRK1A and TFIIIC should occur at these regions. Most of the co-occupied loci with DYRK1A, Pol III and TFIIIC belong to tRNA genes (Figure R.3C and Table R.1). This observation, in addition to the continually growing evidence showing the role of tRNAs in disease, as discussed in Introduction section 2.4, has made the tRNAs the focus of this study.

1.4. DYRK1A localises to Pol III-bound tRNA genes in a cell-specific manner

Several studies have shown that tRNAs show cell-type specific expression (Dittmar et al., 2006). Thus, we wondered whether DYRK1A was able to bind different subsets of tRNA species. We thus performed ChIP-seq experiments of DYRK1A in other three additional cell lines: breast ductal carcinoma epithelial T47D cells, bone osteosarcoma epithelial U2OS cells, and immortalised lung fibroblasts IMR90. The protein levels of DYRK1A vary in the different cell lines with a higher level in T98G and T47D cells compared to IMR90 and U2OS cells (Figure R.6A).

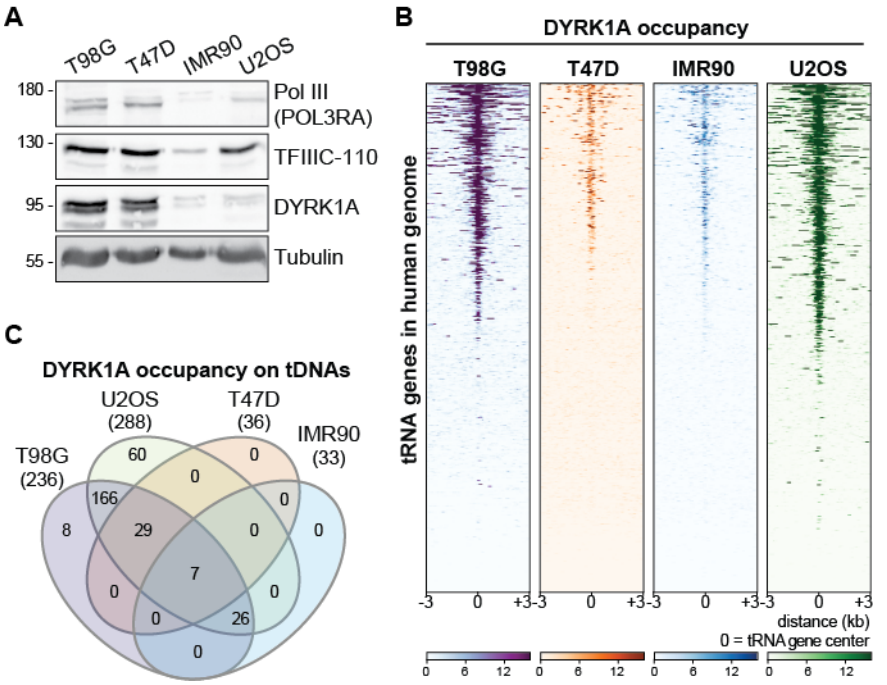

Figure R.6: Differential DYRK1A occupancy on tRNA genes in various cell types. (A) Total cell extracts from the indicated human cell lines were analysed by WB to show the expression of the different proteins. Tubulin was used as a loading control. Note that POLR3A is detected as several bands, which could be the result of post-translational modifications. **(B)** Heat maps showing DYRK1A occupancy on all annotated human tRNA genes in T98G, T47D, IMR90 and U2OS cells. The colour bar indicates the binding score as calculated in MM.5.4. **(C)** Venn diagram indicating the overlap of DYRK1A-bound tRNA genes in the various cell lines. The number of tRNA genes bound is indicated in parenthesis.

As shown in the heat map, DYRK1A binds to tRNA genes in all the cell lines analysed, despite the different protein levels (Figure R.6B). However, the occupancy in the different cell lines was very variable, but it was not a reflection of the DYRK1A protein levels. In fact, the total number of tRNA genes occupied by DYRK1A in T47D and IMR90 cells was much lower (36 and 33 genes, respectively) compared to T98G and U2OS cells (236 and 288 genes, respectively) (Figure R.6C). Interestingly, only seven tRNA genes (tRNA-Leu-CAA-4-1, tRNA-Leu-AAG-2-4, tRNA-Leu-TAG-3-1, tRNA-Leu-CAG-2-2, tRNA-Thr-CGT-4-1, tRNA-Gly-TCC-3-1, tRNA-Pro-CGG-1-3) were occupied by DYRK1A in all cell lines (Figure R.6C). These results suggest that, although there is a considerable overlap among the tRNA genes bound by DYRK1A in different cell lines, there are some tRNA genes that are cell-type specific in terms of DYRK1A binding.

Given that cell-type specificity has been previously demonstrated for Pol III binding on tRNA genes (Oler et al., 2010), we wanted to explore if the differences in DYRK1A binding to tRNA genes correlated with a change in the binding of Pol III. To this end, we performed ChIP-seq experiments of both DYRK1A and Pol III in T47D cells, which showed that not only does DYRK1A bind a smaller pool of tRNA genes compared with T98G cells, so does Pol III, which binds only 147 tRNA genes (Figure R.7A). Interestingly, DYRK1A co-localises with Pol III-bound tRNA genes in T47D cells as in T98G cells based on correlation studies (Figure R.7B). These results indicate that changes in Pol III binding may reflect a change in DYRK1A binding at tRNA genes, or *vice versa*. They further suggest that DYRK1A-recruitment occurs mainly to actively transcribed tRNA genes.

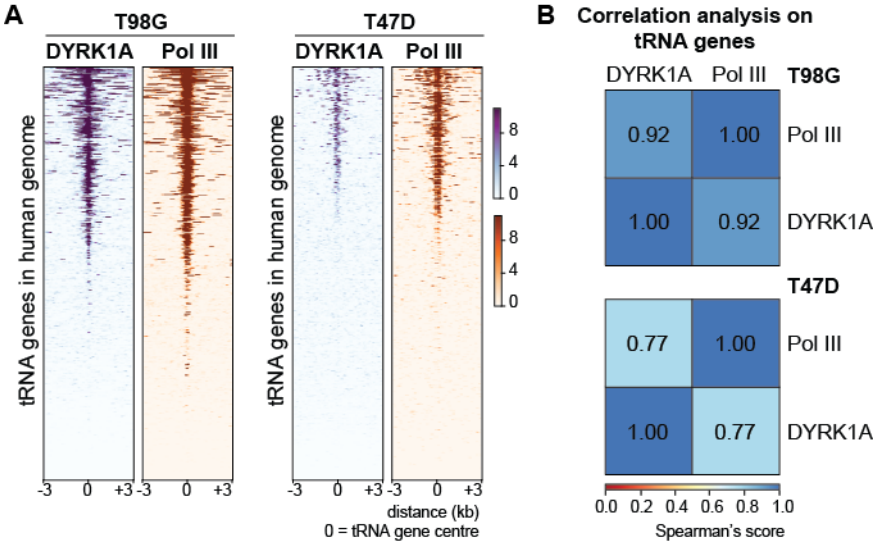

Figure R.7: DYRK1A occupies Pol III-bound tRNA genes in T98G and T47D cells. (A) Heat maps showing DYRK1A and Pol III occupancies on tRNA genes in T98G (left panel) and T47D (right panel) cells. The colour bar indicates the binding score as calculated in MM.5.4. **(B)** The graphs show the Spearman's correlation scores for DYRK1A and Pol III occupancies on tRNA genes in T98G cells (left panel) and T47D cells (right panel). The colour bar indicates Spearman's score. Values corresponding to each comparison are indicated within the squares.

1.5. A differential adaptive response of Pol III machinery to serum starvation

It has been previously described that changes in the proliferative status of the cell can affect Pol III binding to its genomic targets (Alla and Cairns, 2014; Gingold et al., 2014). Indeed, serum depletion in IMR90-tert cells leads to a decreased occupancy of Pol III on tRNA genes (Orioli et al., 2016). We therefore assessed if Pol III chromatin recruitment was sensitive to environmental changes in our model cell line T98G by comparing its occupancy in cells grown in the presence or absence of serum. Upon serum starvation, there was a general reduction in Pol III occupancy at all regions tested, including tRNA genes (Figure R.8A-B), in accordance with what has been observed in IMR90-tert cells (Orioli et al., 2016). This decrease in binding was not due to reduced Pol III protein levels following serum starvation (Figure R.8C).

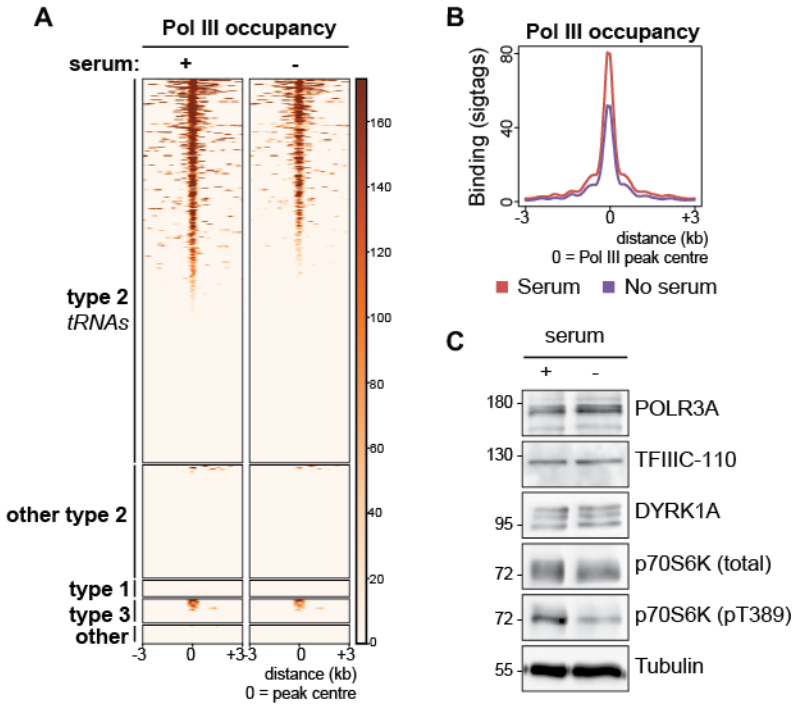

Figure R.8: Pol III occupancy on Pol III loci decreases during serum starvation in T98G cells. (A) Heat maps showing Pol III occupancy in T98G cells grown in the presence (+) or absence of serum (-). The Pol III genes have been classified by promoter type. The colour bar indicates the binding score as calculated in MM.5.4. **(B)** Density plot indicating the average binding using the ChIP-seq significant tags following the same criteria as in panel **A** across all Pol III-occupied genes. **(C)** WB analysis of the expression levels of the indicated proteins in total T98G cell extracts corresponding to panel **A**. Antibodies targeting phosphorylated 70S6K at Thr389 (pT389) were used to show the effect of serum starvation. Tubulin was used as a loading control.

In contrast, only a slight overall decrease is observed in DYRK1A occupancy in response to serum starvation (Figure R.9A). Interestingly, Pol III responds differently to serum starvation depending on the presence or absence of DYRK1A. Notably, Pol III occupancy is in average a lot stronger in the DYRK1A positive cluster (Figure R.9B-C). While in DYRK1A-positive tRNA genes, Pol III occupancy has a small decrease upon serum starvation, on tRNA genes where DYRK1A is absent, Pol III occupancy has a stronger response with over a 50% decrease in binding (Figure R.9C-D). Thus, the presence of DYRK1A could possibly explain the differences observed in the response of Pol III to serum.

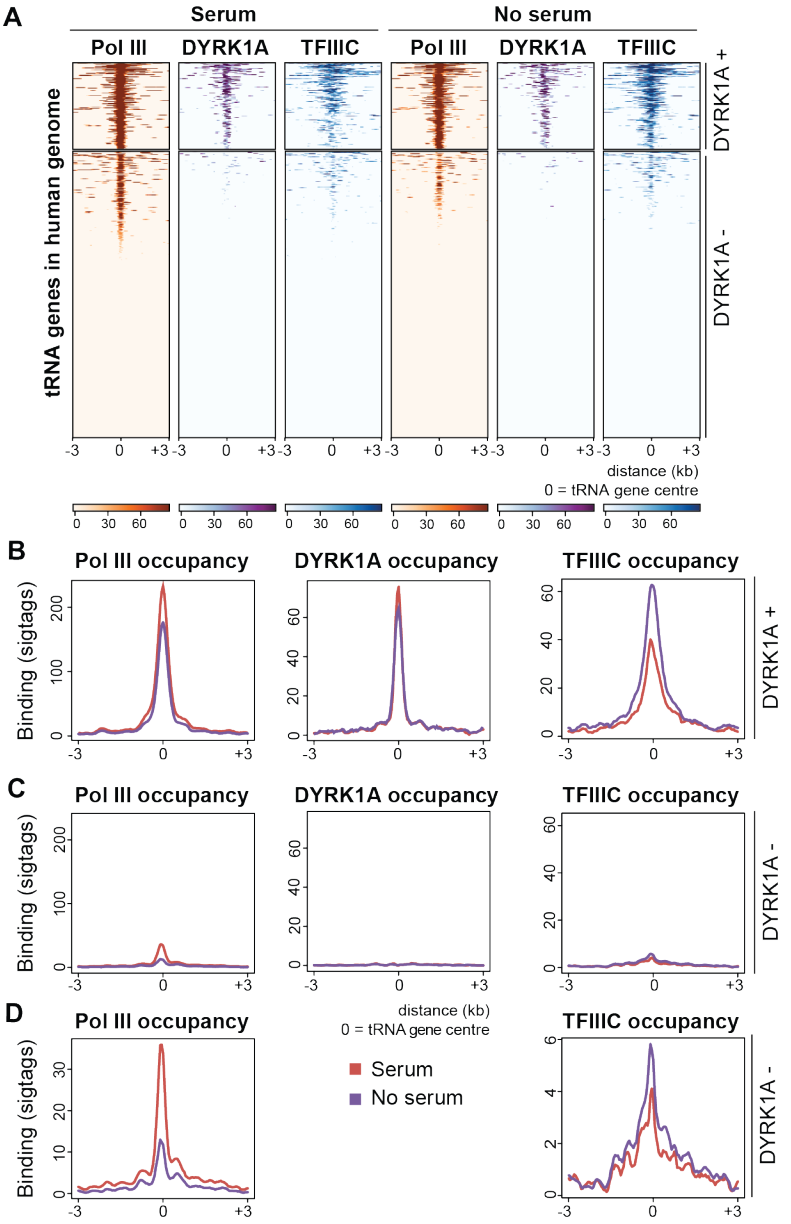

Figure R.9: Differential behaviour of Pol III and TFIIIC occupancy in response to serum starvation. (A) Heat maps showing Pol III, DYRK1A and TFIIIC occupancies on tRNA genes in T98G cells grown in the presence (serum) or absence (No serum) of serum. The colour bar indicates the binding score as calculated in MM.5.4. The ChIP-associated regions have been divided into DYRK1A positive (+) and negative (-) tRNA genes according to the results in the presence of serum. **(B-D)** Density plots indicating the average binding using the ChIP-seq significant tags following the same criteria as in **(A)** for DYRK1A+ **(B)** and DYRK1A- **(C, D)** tRNA genes. In **D**, the y-axis scale has been changed to highlight the differential binding in the serum-starved cells.

In contrast to Pol III occupancy, TFIIIC occupancy increases nearly 30% at tRNA genes occupied following serum starvation (Figure R.9A-D). This result is in accordance with studies in yeast showing an increase in TFIIIC occupancy at tRNA genes following nutrient deprivation (Ciesla et al., 2018; Roberts et al., 2003). Unlike Pol III, the percentage in increase of TFIIIC occupancy is the same in both clusters (Figure R.9B-D). Thus, our results show that during nutrient deprivation Pol III and TFIIIC have a differential adaptive response in occupancy on tRNA genes in T98G cells. As no changes are observed at the protein level (Figure R.8B), the differences observed in chromatin binding are more likely due to a change in recruitment of TFIIIC and Pol III to tRNA genes following serum starvation. However, it is important to note that as with Pol III, TFIIIC occupancy is in average a lot higher in the cluster where DYRK1A is present, compared to the cluster without DYRK1A bound (Figure R.9B-C). Therefore, it appears that DYRK1A binds to the tRNA genes that are more strongly bound by the Pol III machinery.

2. Functional interaction of DYRK1A with the Pol III machinery

2.1. DYRK1A does not physically interact with the TFIIIB complex

Our results have shown that DYRK1A occupies Pol III-bound tRNA genes. Next, we aimed to investigate a potential cross-talk between DYRK1A and the members of the Pol III machinery. As mentioned in Introduction section 2.2, the TFIIIB complex is responsible for recruiting Pol III to tRNA genes through interaction with most factors involved in the regulation of Pol III transcription. Thus, we assessed whether DYRK1A was able to interact with some of the components of TFIIIB (Figure R.10A).

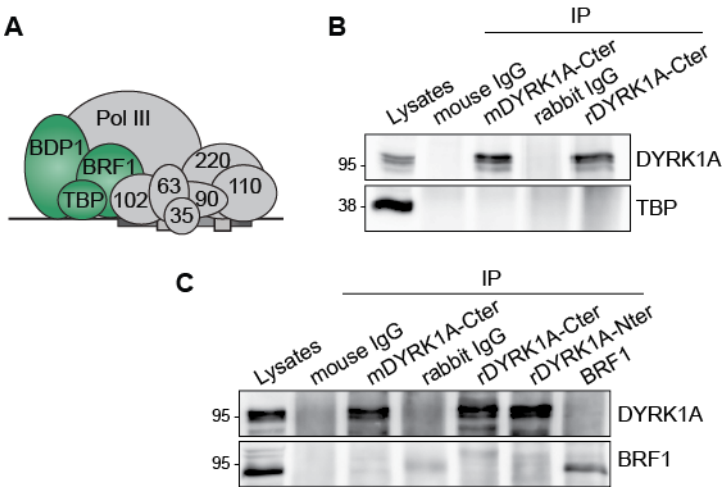

Figure R.10: DYRK1A does not physically interact with the TFIIIB complex within the nucleus. (A) Scheme showing the Pol III machinery on a tRNA gene. The TFIIIB complex is highlighted in green. **(B)** DYRK1A was immunoprecipitated from HeLa nuclear extracts with two antibodies targeting the C-terminal part (mDYRK1A-Cter, Santa Cruz RR7; rDYRK1A-Cter, Abcam ab69811). **(C)** HeLa nuclear extracts were immunoprecipitated with three antibodies to DYRK1A, two targeting the C-terminal part (DYRK1A-Cter) and one targeting the N-terminal part (rDYRK1A-Nter, Sigma D1694), or with an anti-BRF1 antibody. In **B** and **C**, normal IgGs were used as negative controls (r, rabbit; m, mouse). The lysate (10%) and immunocomplexes were analysed by WB with antibodies for the indicated proteins.

First, we explored its potential relationship with TBP, which is a common component of both the Pol III and Pol II machinery, by co-IP assays performed using concentrated commercial HeLa nuclear extracts. The experiment showed that TBP was not found in immunocomplexes using two antibodies against DYRK1A (Figure R.10B). Next, we checked the interaction between DYRK1A and BRF1 using the same strategy. Neither BRF1 was found in DYRK1A-associated immunocomplexes nor DYRK1A was found in BRF1-immunoprecipitates (Figure R.10C). As mentioned in MM.4.3, the interaction between DYRK1A with BDP1 could not be assessed due to no suitable antibodies for BDP1. These results do not exclude that an interaction between DYRK1A and the TFIIIB complex exists, which might be restricted to chromatin.

2.2. DYRK1A and the TFIIIC complex interact in cells

As mentioned in Introduction 2.1, TFIIIC it is a six-subunit complex that recognises the internal promoters of tRNA genes, and in turn recruits the TFIIIB complex (Figure R.11A). To investigate if DYRK1A physically interacts with the TFIIIC complex in the nucleus, IP assays were performed using commercial HeLa nuclear extract.

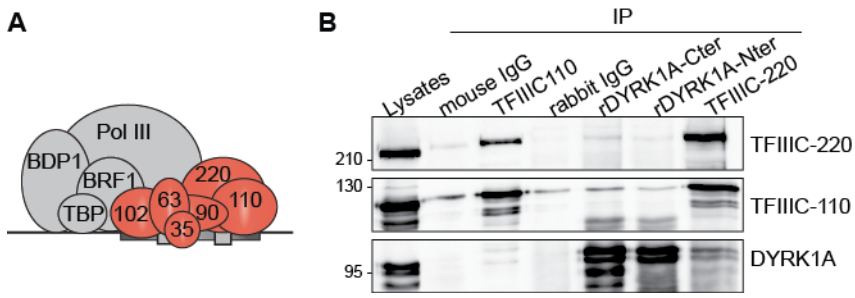

Figure R.11: DYRK1A physically interacts with TFIIIC in the nucleus. (A) Scheme depicting the Pol III machinery on a tRNA gene, highlighting the six subunits of the TFIIIC complex in red. **(B)** HeLa nuclear extracts were immunoprecipitated with antibodies to DYRK1A (as in Figure R.10C), and with antibodies against subunits of the TFIIIC complex, TFIIIC-110 and TFIIIC-220. Normal IgGs were used as negative controls. The lysates (10%) and immunocomplexes were analysed by WB with antibodies for the indicated proteins.

The two subunits TFIIIC-110 and TFIIIC-220 were co-immunoprecipitated using antibodies targeting either protein (Figure R.11B). Notably, DYRK1A was found in immunocomplexes when TFIIIC-220 was immunoprecipitated. In addition, TFIIIC-220 was found to co-immunoprecipitate when using antibodies towards DYRK1A. These results suggest that DYRK1A physically interacts with TFIIIC in the nucleus.

2.3. Analysis of the members of the TFIIIC as putative DYRK1A substrates

Given that DYRK1A interacts with TFIIIC, and since DYRK1A is a kinase, we wondered if some of the components of the TFIIIC complex may be substrates of DYRK1A. To validate this hypothesis, GST-tagged fusion proteins for all the components of the TFIIIC complex were generated

(Figure R.12A), either covering the entire protein or fragments (as detailed in MM.2.3), to use them as substrates in IVK assays (Figure R.12B).

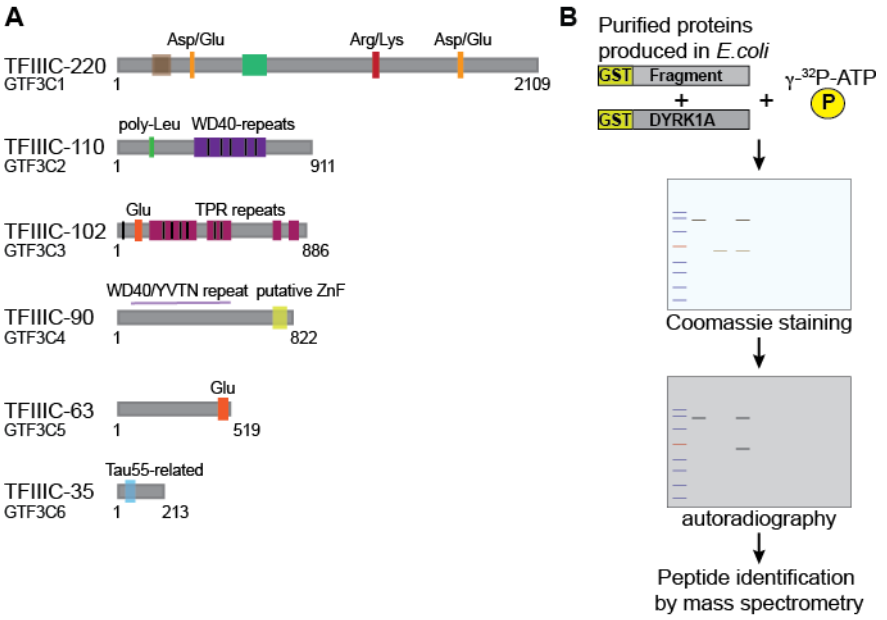

Figure R.12: Schematic view of the DYRK1A phosphorylation screen of the TFIIIC complex. (A) Protein structure of the six members of the TFIIIC complex showing the main domains. The regions enriched in certain amino acids are shown. WD40-repeats: WD or β-transducin repeat; TPR-repeats: tetratricopeptide repeats; ZnF: zinc-finger. The official gene names for each member are also indicated. **(B)** Schematic representation of the DYRK1A phosphorylation screen based on IVK assays.

2.3.1. The TFIIIC subunits 102, 90, 63 and 35 are not substrates of DYRK1A

GST-tagged TFIIIC-35 was expressed in *E. coli* and a radioactive IVK assay was performed using either GST-tagged DYRK1A as the enzyme or a kinase inactive DYRK1A form generated by mutation of the ATP binding site (K179R), as a negative control. No incorporation of the radiolabel ATP could be observed for TFIIIC-35, as the bands appearing around the approximate size of GST-tagged TFIIIC-35 correspond to degraded bands of DYRK1A (Figure R.13B), indicating that TFIIIC-35 is not a substrate of DYRK1A.

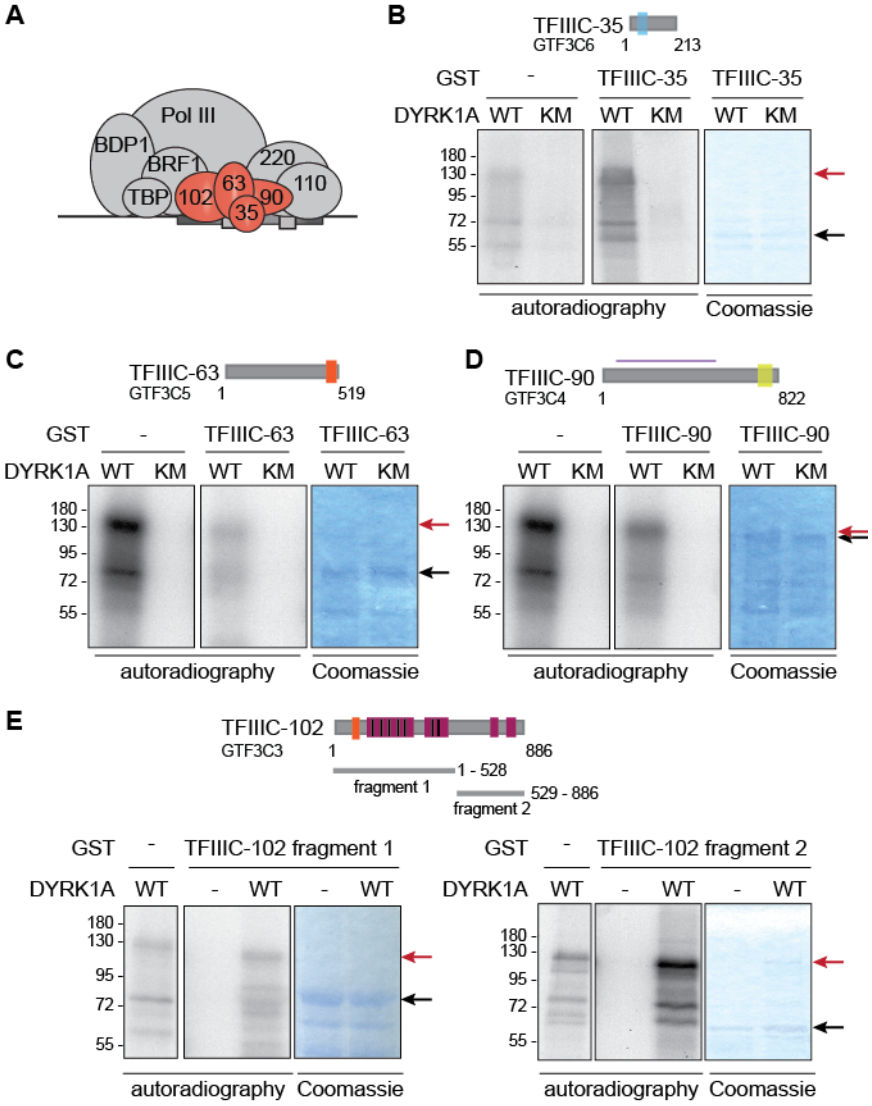

Figure R.13: TFIIIC subunits 102, 90, 63 and 35 are not substrates of DYRK1A. (A) Scheme highlighting the four subunits of the TFIIIC complex shown in this figure. **(B-E)** Bacterially produced GST-TFIIIC-35 **(B)**, GST-TFIIIC-63 **(C)**, GST-TFIIIC-90 **(D)**, or two fragments of GST-TFIIIC-102 **(E)** were subjected to an IVK assay in the presence of either GST-DYRK1A (WT) or a kinase inactive version (KM) and [γ^{32}P]-ATP. Samples were resolved by SDS-PAGE and incorporation of ^{32}P analysed by autoradiography. Unfused GST was used as negative control (-). The expression levels of the putative substrate were assessed by Coomassie staining. The red arrow indicates the auto-phosphorylation of GST-DYRK1A and the black arrow the approximate size of the GST-fusion used as substrate.

The same strategy was applied for GST-TFIIIC-63, GST-TFIIIC-90, and TFIIIC-102, which was assayed in two fragments. Similar results as those for TFIIIC-35 were observed (Figure R.13C-D), with very low levels of phosphorylation in the case of the N-terminal half of TFIIIC-102. The results indicate, therefore, that none of these components of the TFIIIC complex is a substrate of DYRK1A *in vitro*.

2.3.2. DYRK1A phosphorylates TFIIIC-110 and TFIIIC-220 *in vitro*

In the case of TFIIIC-110, GST-tagged fusions of the protein were generated as two fragments (Figure R.14A-B).

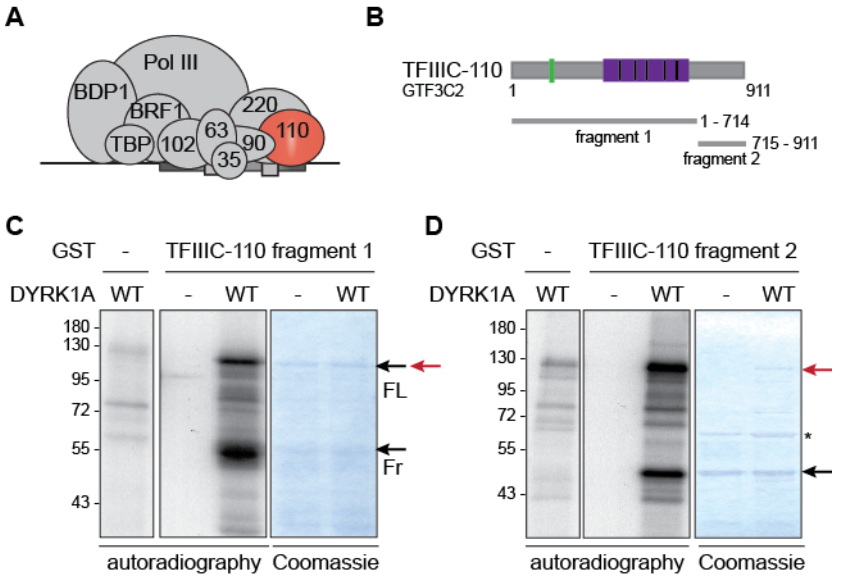

Figure R.14: TFIIIC-110 is phosphorylated by DYRK1A *in vitro*. (A) Scheme highlighting the TFIIIC-110 subunit of the TFIIIC complex. **(B)** Scheme indicating the protein structure of TFIIIC-110 and the two GST-tagged fragments used in the IVK assays. The numbers indicate the length of the fragments. **(C-D)** IVK assay of the N-terminal half **(C)** or the C-terminal half of TFIIIC-110 **(D)** performed as described in Figure R.13. Black arrows point to the GST-fusion protein used as substrates, while red arrows point to auto-phosphorylated GST-DYRK1A. FL refers to the full-length GST-fusion of the fragment, and Fr is a truncated band of the fusion protein. The asterisk indicates a non-specific band, co-purifying with the fragment. GST alone was used as negative control (-).

The N-terminal half fusion protein moves approximately around the same size as GST-DYRK1A, making difficult to determine if the signal observed in the autoradiography is due to incorporation of the radiolabel signal

within the fragment or if it is due to the auto-phosphorylation of DYRK1A (Figure R.14C). However, a truncated band of around 55 kDa showed incorporation of the radiolabel (Figure R.14C, indicated as Fr), thus confirming that the fragment is phosphorylated by DYRK1A. In the case of the C-terminal half, a radioactive signal was observed at the expected size when incubated with DYRK1A (Figure R.14D), indicating that this fragment of TFIIIC-110 is also phosphorylated by DYRK1A.

Due to the size of the largest subunit TFIIIC-220, multiple fragments were generated as GST-tagged fusion proteins (Figure R.15A-B). Suitable conditions for the solubilisation and/or purification of the fusion proteins expressed in bacteria could not be attained for all the fragments (detailed in MM.4.6), and thus, only three of them were screened in the IVK assays. TFIIIC-220 fragment 1 showed no radioactive signal when incubated with DYRK1A indicating that the N-terminus of TFIIIC-220 is not phosphorylated by DYRK1A (Figure R.15C). However, when the fragments 2 or 5 were incubated with DYRK1A, a signal could be observed for the full-length version of the fragments, which was absent when the fragment was incubated with a DYRK1A kinase inactive mutant (Figure R.15D-E). These results indicate that there are putative DYRK1A phosphorylation sites within aa 715-804 and 1596 - 2109 of TFIIIC-220.

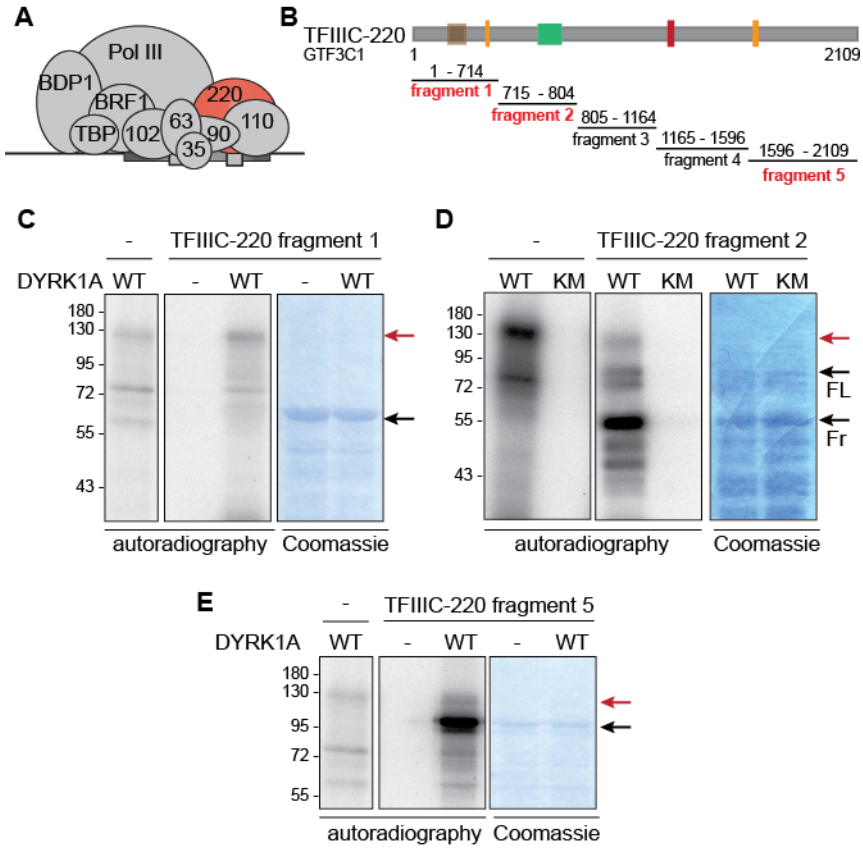

Figure R.15: TFIIIC subunit 220 is phosphorylated by DYRK1A *in vitro*. **(A**) Scheme highlighting the TFIIIC-220 subunit of the TFIIIC complex. **(B)** Scheme showing the primary structure of TFIIIC-220 and the GST-tagged fragments generated, with the fragments screened in the IVK assays highlighted in red. **(C-E)** IVK assay of TFIIIC-220 fragments 1 **(C)**, 2 **(D)** or 5 **(E)** performed as described in Figure R.13 using either GST (-) or a DYRK1A kinase-dead version (KM) as negative controls. Black arrows point to the GST-fusion protein used as substrates, while red arrows point to auto-phosphorylated GST-DYRK1A. In **D**, FL refers to the full-length version of the substrate fragment, and Fr is a truncated band of the corresponding fusion protein. Note that the truncated band shows most of the radioactive signal suggesting that the DYRK1A phosphorylation sites are mostly located there.

2.4. DYRK1A phosphorylates several residues of TFIIIC-110 and TFIIIC-220

To determine which residues of TFIIIC-110 and TFIIIC-220 were phosphorylated by DYRK1A, cold IVK assays were performed with the GST-fusion proteins positive in the IVK screen followed by identification of the phospho-sites by MS. For both TFIIIC components, several phospho-sites were identified and are summarised in Figure R.16.

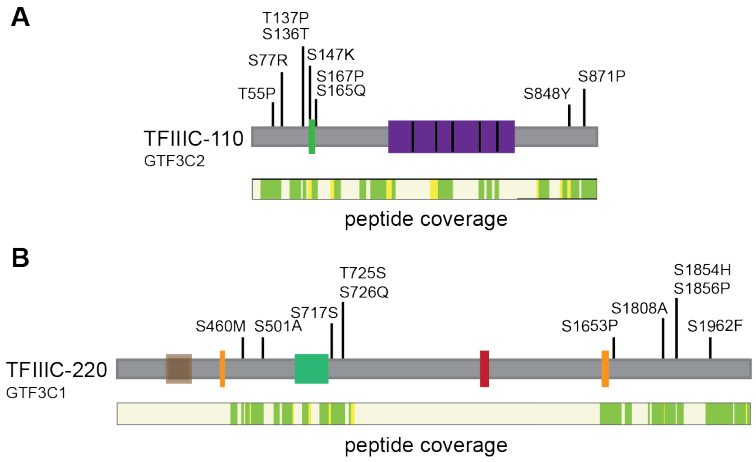

Figure R.16: Identification of DYRK1A-dependent phosphosites in TFIIIC-110 and TFIIIC-220. Cold IVK assays were performed on the GST-fragments positive from the IVK screen on TFIIIC-110 **(A)** or TFIIIC-220 **(B)**, and the phosphorylated peptides identified by MS analysis. The position of the phospho-sites within the primary structure is indicated in black; peptide coverage is also shown (FDR≤1%, green; FDR≤5%, yellow). Note that for TFIIIC-220, protein coverage corresponds to fragments 2 and 5.

To validate the phospho-sites identified in the MS as genuine DYRK1A targets, non-phosphorylatable mutants were generated of the residues of interest by introducing a change to alanine (strategy detailed in MM.2.4). In these initial screenings, the sites chosen to be mutated were those sites that had a proline at the P+1 position, as DYRK1A is proposed to be a proline-directed kinase. Radioactive IVK assays were performed with the mutants, and their phosphorylation was compared to the WT fragment. In some cases, residues not identified in the MS screen, because the tryptic peptide was not captured, were also included in the screen due to the presence of a proline in the P+1 position (depicted in orange in Figure R.17A, R.18A-B).

In the case of TFIIIC-110, the mutant proteins Thr55Ala and Thr137Ala showed a decrease in the phosphorylation signal compared to the WT protein, which was not due to a difference in protein levels as observed in the Coomassie staining (Figure R.17A). No changes in the phosphorylation levels were observed for Ser25Ala or Ser871Ala mutants (Figure R.17A-B), indicating that these sites are not phosphorylated by

DYRK1A. Notably, none of the mutations tested completely abolished the phosphorylation of any of the fragments, suggesting that more sites are phosphorylated by DYRK1A in TFIIIC-110.

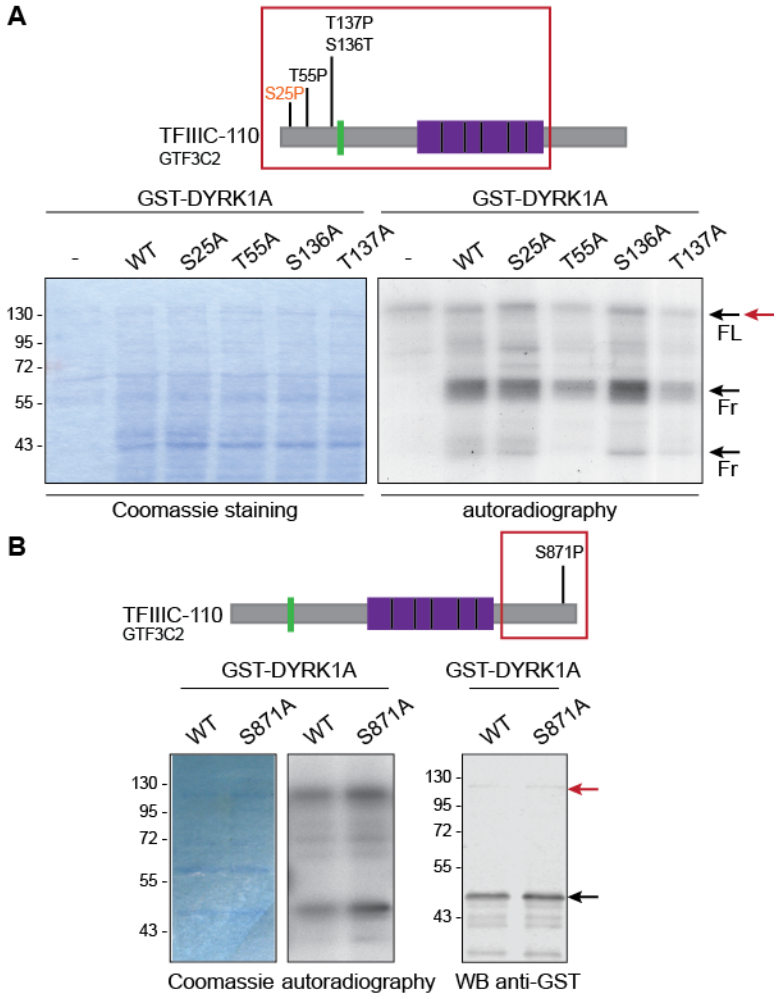

Figure R.17: Residues Thr55 and Thr137 of TFIIIC-110 are phosphorylated by DYRK1A. Hot IVK assays were performed with GST-DYRK1A using either the wild type (WT) version or the non-phosphorylatable mutants of fragment 1 **(A)** or 2 **(B)** of TFIIIC-110 (framed in red in the scheme). The scheme shows the protein structure indicating the residues mutated (black: identified by MS; orange: manually selected). Black arrows: GST-fusion protein used as substrates; red arrows: auto-phosphorylated GST-DYRK1A. FL refers to the full-length version of the fragment, and Fr corresponds to a truncated band. In **B**, WB analysis assessing the protein levels of the fragment using an anti-GST antibody has been included.

In the case of the fragment 2 of TFIIIC-220, multiple sites were identified, but they had a low score (data not shown) and none of them lay within a consensus for DYRK1A (Figure R.16B), nor were conserved among different species (data not shown).

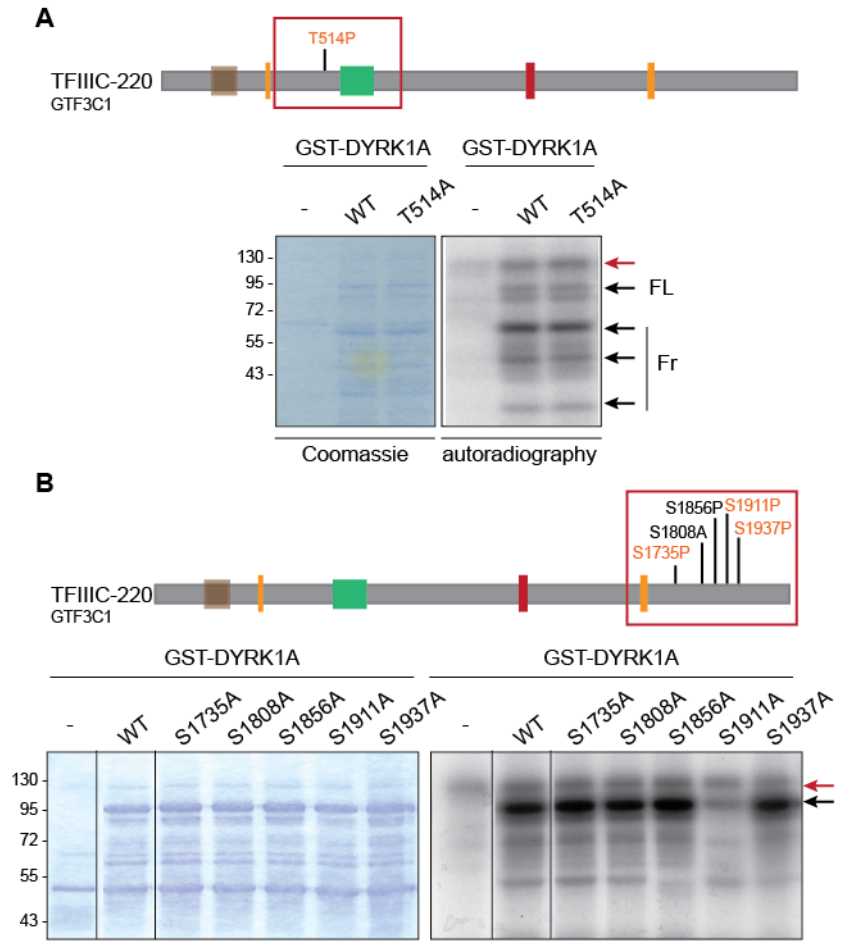

Figure R.18: Residue Ser1911 of TFIIIC-220 is phosphorylated by DYRK1A. Hot IVK assays were performed with GST-DYRK1A using either the wild type (WT) version or the non-phosphorylatable mutants for fragment 2 **(A)** or fragment 5 **(B)** of TFIIIC-220. On top of the gels, the scheme shows the protein structure indicating the residues mutated, including the ones identified by MS (black) and the ones selected manually (orange), with the fragment assayed framed in red. Black arrows point to the GST-fusion protein used as substrates, while red arrows point to auto-phosphorylated GST-DYRK1A. FL refers to the full-length version of the fragment, and Fr corresponds to a truncated band. In **B**, a vertical line indicates where part of the image has been cropped out.

Thus, we manually selected the residue Thr514 from a peptide not captured in the MS as a candidate for validation, based on the following reasons: i) it has a proline at the P+1 position; ii) it has been identified in several studies as phosphorylated (see full details at phosphosite.org); iii) it lies within the first 200 aa from the N-terminus of the fragment, and therefore within the truncated band observed as labelled in the IVK assays (Figure R.15D); and iv) it was highly conserved in vertebrates (data not shown). However, no changes were observed in the phosphorylation signal between the WT and the mutant protein neither for the full-length nor for the degraded band (Figure R.18A). Therefore, further investigation is required to properly identify the DYRK1A-dependent phosphosites within this fragment.

Regarding the most C-terminal fragment of TFCIII-220, only the residue Ser1911, among all the residues tested, was validated as target of DYRK1A phosphorylation as the signal in the non-phosphorylatable mutant protein decreased heavily compared to the non-mutated one (Figure R.18B). The strong reduction in the phosphorylation levels of this mutant suggests that this may be the main DYRK1A-dependent phospho-site, although the residual incorporation of radiolabelled ATP suggests that other possible phosphorylation sites might exist.

2.5. The interaction between TFIIIC and DYRK1A is not dependent on DYRK1A kinase activity

Next, we asked if the kinase activity of DYRK1A was required for its physical interaction with the TFIIIC complex. To this end, co-IP assays were performed in T98G soluble cell extracts from cells that had been treated with harmine, a specific inhibitor of DYRK1A kinase activity (Bain et al., 2007; Gockler et al., 2009). Treatment with harmine efficiently inhibited DYRK1A kinase activity, measured as decreased levels of auto-phosphorylation of serine residue 520 (Figure R.19B; Alvarez et al., 2007). The DYRK1A kinase activity did not appear to be important for its interaction with TFIIIC, as DYRK1A was still co-immunoprecipitating with

TFIIIC (Figure R.19A). Moreover, treatment with harmine did not affect the formation of the TFIIIC complex, as TFIIIC-110 was still able to interact with TFIIIC-220.

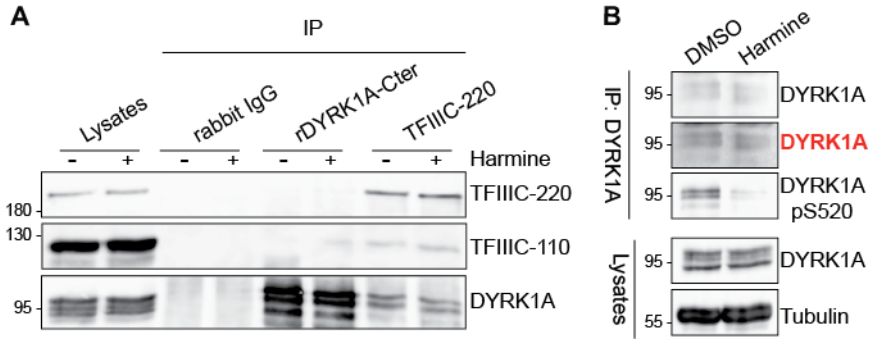

Figure R.19: The kinase activity of DYRK1A is not necessary for its interaction with TFIIIC. (A) Soluble cell extracts from T98G treated with either DMSO (vehicle) or 10 μM harmine for 16 h were immunoprecipitated with anti-DYRK1A or anti-TFIIIC-220 antibodies. Normal IgGs used as negative controls. Lysates (5%) and immunocomplexes were analysed by WB with antibodies for the indicated proteins. **(B)** Cell extracts from **A** were analysed for the inhibitory effect of harmine using the auto-phosphorylation of Ser520 as a proxy. The DYRK1A panel in red corresponds to an image with adjusted brightness in Photoshop.

2.6. Recruitment of TFIIIC and DYRK1A to tRNA genes partially depends on the catalytic activity of DYRK1A

The TFIIIC complex has been shown to be phosphorylated in one or several of its components (Shen et al., 1996); however, no further details on the functional importance of these events are known. Our results show that DYRK1A phosphorylates TFIIIC-220 and TFIIIC-110 *in vitro* at several residues. Since these two subunits are necessary to recognise and bind the B-box within Pol III type 2 promoters, we wondered if DYRK1A phosphorylation could regulate the binding of TFIIIC to tRNA genes. To explore this hypothesis, ChIP-seq experiments were performed for DYRK1A, TFIIIC and Pol III in T98G cells, treated or not with the DYRK1A inhibitor harmine.

The occupancy of DYRK1A to tRNA genes decreased when its kinase activity was inhibited (Figure R.20A), with a reduction in average binding of 40% (Figure R.20B). This result indicates that the catalytic activity of DYRK1A could be required for its recruitment and/or stabilised binding on tRNA genes. The occupancy of Pol III on tRNA genes was hardly affected, with only a 15% decrease in the average binding upon harmine treatment (Figure R.20A-B). In contrast, the binding of TFIIIC on tRNA genes was reduced upon harmine treatment, with a 50% decrease in its average binding (Figure R.20A-B). This finding is in accordance with results from yeast showing that de-phosphorylation of TFIIIC leads to a reduced presence on tRNA genes (Ducrot et al., 2006). There were no changes in the protein levels of TFIIIC or DYRK1A that could explain the decrease in binding observed (Figure R.20C), supporting that the activity of DYRK1A is important for the presence of TFIIIC on tRNA genes.

Altogether, these results indicate that the phosphorylation of TFIIIC by DYRK1A is important for the binding of TFIIIC to tRNA genes, possibly by acting on the recognition of the B-box, since no effect on complex formation in the presence of the DYRK1A inhibitor was observed.

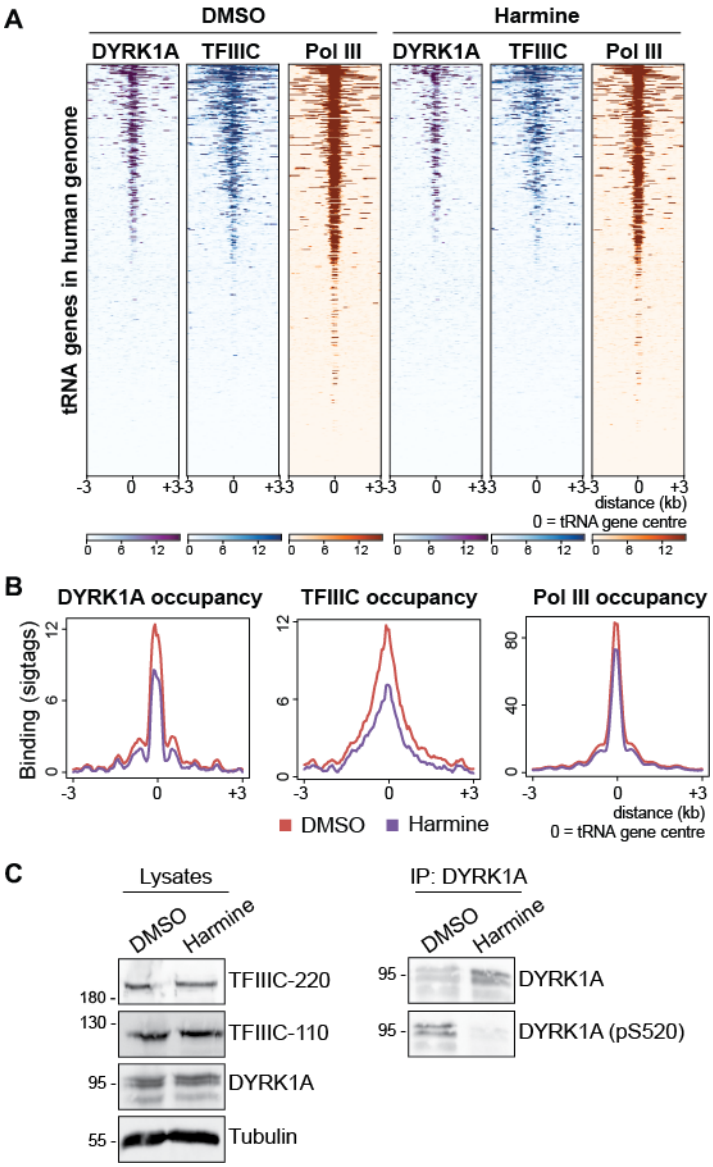

Figure R.20: Harmine affects the recruitment of TFIIIC to tRNA genes. (A) Heat maps showing DYRK1A, TFIIIC and Pol III occupancies on tRNA genes in T98G cells treated with either vehicle (DMSO) or 10 μM harmine for 16 h. The colour bar indicates the binding score as calculated in MM.5.4. **(B)** Density plots indicating the average binding using significant peaks (sigtags) following the same criteria as in **A. (C) Left panel:** Protein expression levels of indicated proteins in T98G soluble extracts as in **A**. Tubulin was used as a loading control. **Right panel:** Assessment of harmine inhibitory effect for experiment in **A**, using auto-phosphorylation of DYRK1A Ser520 as a proxy. Extracts from **C** were immunoprecipitated with an anti-DYRK1A antibody and analysed by WB with antibodies for DYRK1A and phospho-Ser520 (pS520).

2.7. DYRK1A activity affects differentially the recruitment of TFIIIC to distinct genomic loci

We have observed that TFIIIC is recruited to multiple loci aside from tRNA genes in our model cell line (Figure R.5), and that TFIIIC occupancy on tRNA genes partially depends on the catalytic activity of DYRK1A (Figure R.20). Therefore, we wondered if the kinase activity of DYRK1A is important to the recruitment of TFIIIC all across the genome, or if it is specific to where TFIIIC co-localise with DYRK1A on the chromatin. Thus, we compared the average binding of TFIIIC to chromatin across the three clusters identified in Figure R.5 in T98G cells treated or not with the DYRK1A inhibitor harmine.

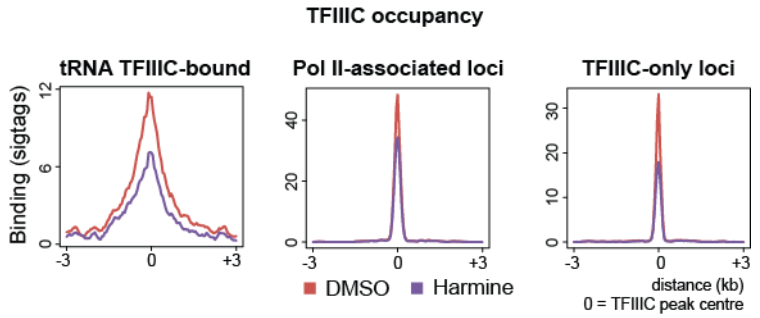

Figure R.21: Harmine affects the recruitment of TFIIIC to tRNA genes as well as to TFIIIC only loci. Density plots indicating the average binding of TFIIIC using significant tags following the same criteria as in Figure R.19A across the three different clusters identified in Figure R.5.

As previously observed, the binding of TFIIIC on tRNA genes decreases nearly 50% following harmine treatment (Figure R.21). However, TFIIIC occupancy on the Pol II-associated loci was not as strongly affected (Figure R.21). Interestingly, TFIIIC binding on the TFIIIC-specific loci decreased about 50% (Figure R21), despite the absence of DYRK1A at these loci. These results suggest that DYRK1A might be involved in regulating TFIIIC at these loci, and not only at tRNA genes; furthermore, the lack of co-localisation with DYRK1A points to the effect occurring outside chromatin.

Discussion

1. DYRK1A binds to both Pol II and Pol III associated regions

This thesis work aimed to determine the putative role of DYRK1A in Pol III transcription. The results show that the DYRK1A-bound chromatin regions can be classified into three specific groups based on the co-localisation of DYRK1A with either Pol II or Pol III (Figure R.1). The largest cluster consists of the Pol II associated regions, which are enriched in the DYRK1A-motif, TCTCGCGAGA, in accordance with previous work from our group (Di Vona et al., 2015). Indeed, recent work in the laboratory has shown that DYRK1A is capable of directly binding *in vitro* to a single-stranded oligonucleotide harbouring the DYRK1A-motif sequence, suggesting that the motif could confer specificity in binding and/or enhance the binding affinity of DYRK1A to these regions (Barba, 2018).

The cluster of loci co-occupied by Pol III and DYRK1A shows no enrichment of the DYRK1A-motif (Figure R.1B), suggesting an alternative method of recruitment for DYRK1A to these specific loci. DYRK1A occupies Pol III-associated genes transcribed by type 2 promoters as well as by type 3 promoters (Figure R.3 and Table R.1). In fact, aside from the internal type 2 promoters' specific sequences, the A-box and B-box, there was no significant enrichment of any other DNA motifs in the Pol III-associated regions. This observation would suggest that DYRK1A recruitment to the Pol III-associated regions is not influenced by a specific DNA motif in the vicinity of Pol III genes, and that DYRK1A could be thereby recruited through interactions with members of the Pol III machinery itself.

Lastly, the DYRK1A-only regions show enrichment for CTCF-associated motifs (Figure R.1B), in accordance with previous results from the laboratory (Barba, 2018). This study showed that a subset of DYRK1A occupied loci, enriched for the DYRK1A-motif, is co-occupied by co-repressor ZBTB33/KAISO and the tumour suppressor BRCA1. However, DYRK1A-associated regions depleted of both KAISO and BRCA1 were

enriched for the CTCF motif (Barba, 2018), which is agreement with the observation that DYRK1A-specifc loci are enriched in the CTCF motif. CTCF is a known insulator that is associated with cohesin, and is located close to the borders of TADs regulating long-distance DNA interactions (reviewed in Rowley and Corces, 2018). Interestingly, some human tRNA genes have been shown to act as insulators capable of long-range interactions (Raab et al., 2012). Furthermore, it has been observed that CTCF is associated to a small subset of tRNA genes in HeLa cells (Oler et al., 2010). Given these results, DYRK1A may be involved in long-range interactions and act as a chromatin barrier, not only at the DYRK1A-specific regions, but possibly also at the tRNA genes. However, to further explore the potential role of DYRK1A in chromatin organisation, experimental approaches providing information on higher order chromatin interactions, such as chromosome conformation capture methods, would be required. For instance, Hi-C experiments in control cells and in cells in which the levels of DYRK1A have been depleted would allow to generate contact maps all across the genome and to determine the potential impact of DYRK1A on long-range interactions.

2. DYRK1A is recruited to Pol III-bound tRNA genes

Further characterisation of the association of DYRK1A with Pol III at Pol III-associated genes revealed that DYRK1A occupies both type 2 (tRNAs) and type 3 (7SL and U6) genes (Figure R.3 and Table R.1). Unfortunately, no conclusion can be drawn for type 1 genes from the data. This is a consequence of the mapping strategy used in this Thesis work, as the type 1 genes (5S rRNAs) are not included in the hg38 version of the human genome. Nevertheless, these results indicate that DYRK1A occupancy at Pol III-associated loci is not restricted to a specific promoter type, as type 2 and type 3 genes have internal and external promoters, respectively. These data further suggest that the recruitment of DYRK1A to Pol III-associated genes may be mediated by interactions with components of the Pol III machinery and raise the possibility of different methods of recruitment of DYRK1A to the Pol III-associated genes

depending on their promoter; alternatively, DYRK1A recruitment could be mediated by components of the machinery common to both types of genes as BDP1, TBP or subunits of the Pol III holoenzyme. As this Thesis work has focused on type 2 promoters, and on the transcription factor TFIIIC, further investigations with members associated with type 3 promoters will be required to fully determine the method of recruitment of DYRK1A to these loci.

Regarding type 2 genes, the analysis shows that approximately 50% of all human tRNA genes are bound by Pol III in the cell system used in this work (Table R.1). Thus, the results are in agreement with other studies that have shown that Pol III occupies around 60% of all tRNA genes in various cell lines in humans and mice (Barski et al., 2010; Canella et al., 2010; Moqtaderi et al., 2010; Oler et al., 2010). DYRK1A occupies around 40% of all the tRNA genes (Table R.1). Notably, almost all DYRK1A-bound tRNA genes are positive for the presence of Pol III and TFIIIC. (Figure R.3B-C). Finally, the Pol III and DYRK1A co-occupied tRNA genes show, globally, a higher occupancy of both Pol III and TFIIC compared to tRNA genes not occupied by DYRK1A (Figure R.9B-C).

Recent published data showed that Pol III occupancy correlates with the pre-tRNA levels in IMR90-htert cells (Orioli et al., 2016). Considering these facts, the results in T98G may suggest that the DYRK1A-occupied tRNA genes are actively transcribed, which is supported by our preliminary data (Figure R.4A). Interestingly, the tRNA genes co-occupied by Pol III and DYRK1A encompass all the tRNA isotypes, with no apparent preference for a specific isotype or isoacceptor observed (Figure R.4B). Therefore, the results suggest that DYRK1A could be a general regulator of tRNA transcription. Indeed, previous results from our laboratory have shown the reduced expression of some tRNAs upon the depletion of DYRK1A (Di Vona, 2013). However, to fully understand the role of DYRK1A in the transcription of tRNAs, a global-wide assessment of tRNA levels will be required (see Discussion section 6).

Finally, the results show that DYRK1A occupies tRNAs in a cell-type specific manner (Figure R.6), while maintaining a good correlation with Pol III co-occupancy (Figure R.7). This correlation might be especially relevant in cellular contexts in which both proteins play a crucial role. The fact that mutations in either DYRK1A or in components of the Pol III machinery are linked to neurodevelopmental disorders (reviewed in Introduction 1.3 and 2.4) points to neural differentiation as such a physiological context.

3. A differential adaptive response of Pol III to serum starvation

Data in the present work show that Pol III occupancy globally decreases following serum starvation in T98G cells (Figure R.8A-B). However, this response was not uniform across the tRNA genes. Indeed, DYRK1A-positive tRNA genes seemed to be less responsive to serum starvation as Pol III occupancy hardly decreased, in comparison to tRNA genes not occupied by DYRK1A in which Pol III occupancy decreased around 50% (Figure R.9B-D). In addition, we observed an increase of nearly 30% in TFIIIC binding to tRNA genes following serum starvation independent of the presence of DYRK1A (Figure R.9B-D). These changes occur with DYRK1A occupancy hardly affected (Figure R.9B). Moreover, none of the observed changes can be explained by differences in protein levels (R.8C), thus they are likely due to changes in recruitment capabilities or in reinitiation potential of the Pol III machinery. The behaviour of Pol III and TFIIIC in response to serum withdrawal could be the consequence of alterations in signalling cascades, such as the mTOR pathway (Orioli et al., 2016), or be cell cycle-related via p53 or pRb (Crighton et al., 2003; Sutcliffe et al., 1999) since serum withdrawal induces a change in the cell cycle profile of T98G cells, with cells mostly found in the G1 phase (Di Vona, 2013).

This heterogeneous adaptive response of Pol III occupancy has already been observed in serum-starved human fibroblast cells (Orioli et al., 2016). In this experimental system, Pol III occupied genes were classified

into two groups, unstable and stable, according to their response to serum starvation. The majority of the genes (unstable) had a reduced occupancy of Pol III following serum starvation, and subsequently reduced RNA expression. On the contrary, a small group of genes (stable), containing a subset of tRNA genes from all isotypes, was strongly bound by Pol III and had an unchanged Pol III occupancy in both conditions, which was reflected in their expression levels (Orioli et al., 2016). Our data suggest that the DYRK1A-bound tRNA genes could belong to the more stable class of tRNA genes, although in T98G this class represents the largest group. Orioli and colleagues, however, did not assess the occupancy of any other Pol III machinery component, so it is not known how TFIIIC occupancy was affected. In this regard, reports from yeast show that nutrient deprivation results in increased TFIIIC occupancy (Ciesla et al., 2018; Roberts et al., 2003), in agreement with the results in T98G, but TFIIIC occupancy decreases on tRNA genes following serum starvation in T47D cells (Ferrari et al., 2019). These data suggest that a differential and cell type-dependent response of TFIIIC recruitment to chromatin in response to serum depletion could exist, although an explanation to this phenomenon is not available at the present moment.

Orioli and colleagues proposed the general Pol III negative repressor MAF1 as responsible for the adaptive response of Pol III to serum starvation (Orioli et al., 2016), based on: i) the dependence on mTORC1 as rapamycin, a specific inhibitor of mTORC1, prevented recovery of Pol III occupancy following insulin stimulation after serum starvation; ii) the increase of MAF1 binding on Pol III-occupied tRNA genes in serum-starved cells; and iii) the higher enrichment of Pol III occupancy on targets following serum starvation in MAF1 knocked-down cells. In this scenario, the presence of DYRK1A would assure the expression of a subset of tRNAs to maintain cellular homeostasis, possibly by preventing Pol III eviction exerted by MAF1. However, this effect would be independent of the catalytic activity of DYRK1A as harmine, a DYRK1A inhibitor, does not affect the occupancy of Pol III, TFIIIC and DYRK1A on tRNA genes during

serum starvation in T98G cells (data not shown). Thus, DYRK1A itself could stabilise Pol III binding on tRNA genes during serum starvation. Considering that the majority of the tRNA genes are occupied by DYRK1A in T98G cells and are less responsive to serum starvation regarding Pol III loss (Figure R.9B), it could also be possible that the association of MAF1 to tRNA genes is not enhanced upon serum starvation in these cells, thus no eviction of Pol III occurs. This possibility could be evaluated by analysing the recruitment of MAF1 to tRNA genes, which is not known yet in T98G cells.

4. Characterisation of TFIIIC-bound loci in T98G cells

In the present work, TFIIIC-bound regions can be classified into three clusters based on the co-occupancy with Pol III and Pol II in T98G cells, as it has been shown in mESCs (Yuen et al., 2017) (Figure R.5). The smallest cluster is enriched in Pol III, and it comprises mostly tRNA genes. Notably, DYRK1A co-localised with TFIIIC only at these regions, suggesting that any cross-talk at the chromatin level between these two factors should be restricted to the Pol III-positive loci.

The two other clusters, enclosing around 90% of the peaks, are outside of Pol III regions and they represent ETC sites, in agreement with published observations (Barski et al., 2010; Moqtaderi et al., 2010; Oler et al., 2010). One of the clusters contains about half of the TFIIIC peaks and includes loci that are associated with a Pol II peak in close proximity (within 1.5 kb), and correspond mostly to Pol II-dependent promoter regions (Figure R.5A-B), suggesting a potential involvement of TFIIIC in regulating Pol II transcription at these regions. In fact, TFIIIC has been shown to be present at promoters of NMYC target genes, where it facilitates Pol II escape and pause release (Buchel et al., 2017).

Finally, the third cluster of TFIIIC-specific loci shows no enrichment in Pol II promoter regions, in accordance with another recent study (Yuen et al., 2017). Indeed, this cluster is enriched in intergenic regions and introns

(Figure R.5B). Around 80% of these loci are positive for the DNA binding motif of YY1 (Figure R.5C), a transcription factor recently described to be involved in mediating enhancer-promoter interactions (Weintraub et al., 2017). TFIIIC participates in long-range interactions that affect the transcription of Pol II genes in various physiological contexts (Crepaldi et al., 2013; Ferrari et al., 2019; Van Bortle et al., 2017). Thus, a possibility could be that TFIIIC is involved in mediating the regulation of enhancers via interactions with YY1.

TFIIIC has been implicated in chromatin organisation not only at ETC sites, but also at Pol III regions (detailed in Introduction 2.5) through association with chromatin organisation factors such as cohesin and condensin II (Carriere et al., 2012; Yuen et al., 2017). In addition, ETC sites are often located close to CTCF binding sites (Carriere et al., 2012; Moqtaderi et al., 2010). However, the vast majority of the TFIIIC-bound regions are devoid of the CTCF motif in our system. Taken into account that DYRK1A-associated loci in intergenic regions are enriched for the CTCF binding motif (Figure R.1B) and that DYRK1A interacts with TFIIIC (Figure R.11), we could speculate on the participation of the three factors, via protein-protein interactions, in long-range chromatin interactions for those loci in which none of the RNA polymerases are present. This would represent an extra layer of transcriptional regulation for the functional interaction between DYRK1A and TFIIIC, which deserves to be further investigated.

5. DYRK1A: a novel kinase of the TFIIIC complex

This work shows that DYRK1A physically interacts with TFIIIC (Figure R.11), although which TFIIIC component is responsible of the recruitment of DYRK1A to the complex has not been identified yet. Unlike TFIIIB, not much is known about the regulation of TFIIIC (detailed in Introduction 2.3). Five of the six human TFIIIC subunits are phosphorylated (Shen et al., 1996), and de-phosphorylation of the TFIIIC complex inhibits Pol III transcription (Clark and Dasgupta, 1990). However, no kinase has been

identified to directly phosphorylate TFIIIC so far. This Thesis work demonstrates that two TFIIIC subunits, TFIIIC-220 and TFIIIIC-110, are phosphorylated *in vitro* by DYRK1A at multiple sites (Figures R.14-16). Among the residues identified by MS, the residue Ser1911 of TFIIIC-220 and the residues Thr55 and Thr137 of TFIIIC-110 have been experimentally validated (Figure R.17 and R.18). Both Ser1911 and Thr137 have already been identified as phospho-sites in high-throughput MS analysis (data from Phosphosite; Dephoure et al., 2008; Kettenbach et al., 2011), which support that the phospho-sites exist *in vivo*. However, the identification in this work is based on *in vitro* studies, and further investigation, based on phospho-specific antibodies, is required to confirm if these phosphorylation sites are dependent on DYRK1A *in vivo*.

TFIIIC-220 Ser1911 is located in the C-terminal portion of the protein and shows no conservation when comparing orthologues (Figure D.1A), suggesting that the requirement for this phosphorylation event has arisen recently in evolution, and its function could be specific for TFIIIC-220 in humans. Although the site is not located within a specific domain of the protein, it has been demonstrated that the C-terminus of TFIIIC-220 is responsible for the interaction with the TFIIIC-102 and TFIIIC-63 subunits of the complex (Shen et al., 1996). In yeast, the interaction between the corresponding homologues of TFIIIC-220 and TFIIIC-102 plays an important role in the conformational changes of the TFIIIC complex during transcription (Male et al., 2015). Moreover, the PKA-dependent phosphorylation of the homologue of TFIIIC-220 is important for its interaction with TFIIIC-102 in yeast (Ciesla et al., 2018). Thus, a possible role for Ser1911 phosphorylation could be to facilitate the interaction between TFIIIC-220 and TFIIIC-102.

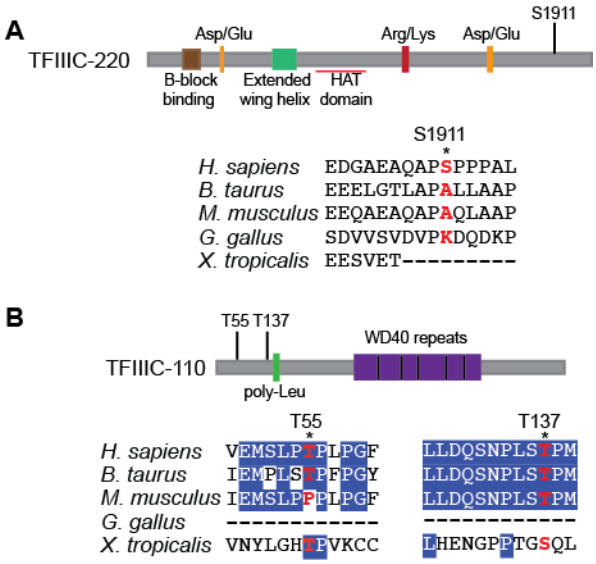

Figure D.1: Location and conservation of validated DYRK1A-dependent phosphosites in TFIIIC-220 and TFIIIC-110. Schematic diagram of full-length TFIIIC-220 **(A) a**nd TFIIIC-110 **(B)** indicating the location of the DYRK1A phospho-sites validated in this work. The alignment of the sequence surrounding the sites is shown for *H. sapiens*, *B. taurus*, *M. musculus*, *G. gallus* and *X. tropicalis* using COBALT is also shown.

Unlike TFIIIC-220, the two sites identified in TFIIIC-110 show a higher level of conservation, at least among the orthologues in mammals (Figure D.1B), implying that the phosphorylation event may be conserved at these sites. Yet, none of the sites are located within any specific domains of the protein. TFIIIC-110 interacts with the N-terminus portion of TFIIIC-220, and these two subunits together recognise and bind the B-box at the tRNA genes' promoter (Shen et al., 1996). However, as of yet it is not known which part of TFIIIC-110 is important for this function. Thus, it is possible that the phosphorylation of the TFIIIC-110 residues by DYRK1A could be involved in mediating this function.

However, the results show that the interaction between TFIIIC-220 and TFIIIC-110 is independent of the kinase activity of DYRK1A (Figure R.19), excluding the hypothesis of a DYRK1A-depending effect on the interaction between these two TFIIIC subunits; nevertheless, it should be noticed that, since the interaction has been assayed in soluble cell extracts, it

cannot be ruled out that the phosphorylation affects the formation of the complex on chromatin. It has also been reported that whilst the N-terminus of TFIIIC-220 is required for interacting with TFIIIC-110, the C-terminus is important for the interaction with the remaining subunits (Shen et al., 1996), so the possibility that the interaction of TFIIIC-220 with the other subunits may be dependent on DYRK1A phosphorylation still exist. Finally, mTOR interacts with TFIIIC-110 and TFIIIC-63 to regulate Pol III transcription through the repressor MAF1 (Kantidakis et al., 2010). Therefore, another possibility could be that the DYRK1A-dependent phosphorylation is important for the interaction between TFIIIC-110 and mTOR.

Despite the lack of effect on the TFIIIC-subunits interaction, treatment of T98G cells with the DYRK1A inhibitor harmine results in a non-uniform reduction of TFIIIC binding to chromatin (Figure R.20 and R.21; Figure D.2). The binding of TFIIIC to tRNA genes with DYRK1A-associated decreases nearly 50% (Figure R.20A-B). Interestingly, this response is not restricted to loci where TFIIIC co-localise with DYRK1A as the reduction is also observed at the TFIIIC-specific loci but not at Pol II-associated loci (Figure R.21). Taking these results into account, two possible scenarios can be envisioned: in one, DYRK1A-dependent phosphorylation of TFIIIC occurs both on chromatin and outside chromatin, while in the other, it occurs only outside chromatin, and the differential response in binding is the result of other components of the chromatin environment (Figure D.2). Currently, the data does not allow to choose any of them. In humans, TFIIIC-220 and TFIIIC-110 are the two subunits responsible for recognising and binding the B-box promoter on tRNA genes (Shen et al., 1996). Thus, a possible explanation for the decrease in TFIIIC binding to tRNA genes could be that DYRK1A-dependent phosphorylation of TFIIIC regulates its affinity for the conserved B-box element within the tRNA genes and the ETC-sites not associated to Pol II. To further investigate this possibility, electrophoretic mobility shift assays could be performed to compare the affinity in binding to the B-box when using TFIIIC fractionated

from nuclear extracts prepared from either unperturbed cells or cells treated with harmine. Additionally, harmine induces a decrease in binding of DYRK1A to tRNA genes concomitantly to the decrease of TFIIIC (around 40%, Figure R.20), raising the possibility that DYRK1A interaction with TFIIIC is important for its recruitment to tRNA genes. To explore this hypothesis, ChIP-seq experiments comparing the occupancy of DYRK1A at tRNA genes in control cells to cells where TFIIIC has been depleted would be needed.

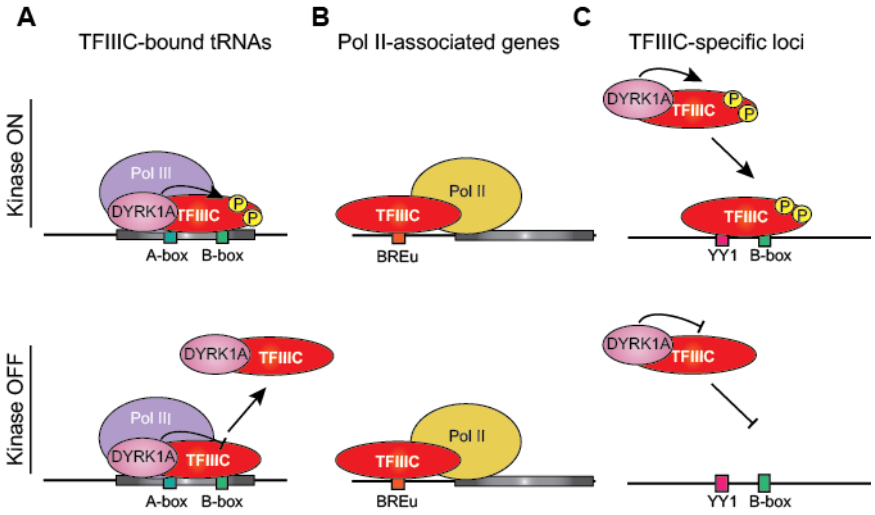

Figure D.2: Schematic representation of the effect of DYRK1A phosphorylation-dependent recruitment on TFIIIC recruitment to chromatin. Proposed model of DYRK1A regulation of TFIIIC recruitment to chromatin on **(A)** TFIIIC-bound tRNA genes, **(B)** Pol II-associated genes and **(C)** TFIIIC-only loci. See text for further details.

In any case, the results point to a role for DYRK1A in regulating tRNA transcription via TFIIIC phosphorylation, and also other TFIIIC-related activities such as TFIIIC-mediated long-range interactions or chromatin remodelling. In this context, it has been shown that TFIIIC-220, TFIIIC-110 and TFIIIC-90 possess HAT activity (Hsieh et al., 1999; Kundu et al., 1999). Whereas no domain has been identified for TFIIIC-110 that could be responsible for the HAT activity, a catalytic domain has been proposed for TFIIIC-220 in the mid-region of the protein (Basu et al., 2019) (Figure D.1A). Unfortunately, we have not been able to test whether DYRK1A

phosphorylates TFIIIC-220 at this region due to problems with its purification (detailed in Materials and Methods 4.6), and thereby its possible involvement in the regulation of the TFIIIC-220 associated HAT activity still remains to be investigated. Since TFIIIC-220 acetylates specifically H3K18, the assessment of H3K18ac levels in cells depleted of DYRK1A or treated with harmine could provide clues on this effect. However, both TFIIIC and DYRK1A have been reported to interact with the histone acetyltransferase p300 (Li et al., 2018; Mertens and Roeder, 2008). Thus, it will be important to distinguish if the effect is due to p300 or TFIIIC. Conversely, analysis of available data of p300 occupancy in T98G cells (Ramos et al., 2010), revealed that p300 did not bind tRNA genes in our model cell line (data not shown), therefore indicating that p300 would not be responsible for the H3K18ac at tRNA genes.

Finally, phosphorylation by DYRK1A regulates different functional aspects of its substrates, including their half-life (Jung et al., 2011; Liang et al., 2008). However, DYRK1A does not appear to regulate the protein stability of TFIIIC-220 and TFIIIC-110, as inhibiting the catalytic activity of DYRK1A does not affect the levels of these two proteins (Figure R.19-20).

6. The potential role of DYRK1A on Pol III transcription

This Thesis work shows that DYRK1A occupies Pol III-bound tRNA genes in multiple cell lines (Figure R.7). Whilst this suggests that the tRNA genes occupied by DYRK1A are being actively transcribed, it does not necessarily imply that DYRK1A is required for this process. However, preliminary data from our laboratory have shown that the expression levels of some target tRNAs is reduced when assessed by RT-qPCR upon DYRK1A depletion (Di Vona, 2013). These results would indicate that DYRK1A could be involved in the regulation of tRNA genes transcription. Furthermore, this work shows that DYRK1A and TFIIIC occupancy decreases on tRNA genes upon harmine treatment (Figure R.20A-B). Concordantly, treatment of HeLa cells with the DYRK1A inhibitor EGCG reduces Pol III activity (Jacob et al., 2007). Together these

data suggest that the kinase activity of DYRK1A may play a role in regulating tRNA levels. However, to fully establish the role of DYRK1A in tRNA transcription it would be essential to assess its impact on global scale. Unfortunately, by the time of writing this report, data on the impact of DYRK1A on global tRNA levels have not been generated and no answers can be provided. The next step will be to assess the role of the DYRK1A activity on tRNA expression by comparing the expression profiles of unperturbed cells and cells treated with harmine or cells in which the levels of DYRK1A has been reduced by the delivery of a shRNA. Both pre-tRNA and mature tRNA levels will be measured. These comparisons should provide information on the effect on transcription (pre-tRNAs) and of alterations in post-transcriptional modifications of tRNAs (mature tRNAs).

At this point in the Discussion, I would like to speculate on the possible involvement of DYRK1A in tRNA transcription (see model in Figure D.3). However, until the impact on global tRNA expression has been assessed, any proposed model of DYRK1A as a regulator of Pol III transcription, based on our current results, is highly speculative.

During the assembly of the Pol III complex on tRNA genes, there is a sequential recruitment of the of the complexes (detailed in Introduction 2.2). Binding of TFIIIC to tRNA genes is critical for the recruitment of TFIIIB. Subsequently, TFIIIB recruits the Pol III holoenzyme to the pre-initiation complex. This work shows that Pol III occupancy was hardly affected by the harmine treatment, with only a 15% decrease observed in binding (Figure R.20A-B). This could indicate that TFIIIB recruitment and its ability to recruit Pol III are not dependent on DYRK1A kinase activity. The results further imply that the disappearance of TFIIIC and DYRK1A during harmine treatment (Figure R.20A-B) may occur after the assembly of the pre-initiation complex, and suggest that DYRK1A might be involved in mediating Pol III-associated functions after initiation. Displacement of TFIIIC during elongation has been proposed to be necessary for allowing

Pol III to proceed with transcription (Bardeleben et al., 1994; Roberts et al., 2003; Soragni and Kassavetis, 2008). Supporting this model, *in vitro* studies have shown that TFIIIB and Pol III alone can sustain transcription once bound on tRNA genes (Ferrari et al., 2004). In this scenario, one may speculate that DYRK1A acts as a repressor of Pol III-dependent transcription by keeping TFIIIC in place, and thus blocking Pol III procession during elongation. Therefore, inhibition of DYRK1A kinase activity would release TFIIIC from its bound loci, allowing transcription to proceed. Recently the novel method neusRNA-seq (newly-synthesised EU labelled small RNA-seq), in combination with Pol III ChIP-seq experiments, was used to track the transcriptional activity of gene-bound Pol III (Orioli et al., 2016). Therefore, it would be interesting to monitor actively transcribed tRNAs using neusRNA-seq in unperturbed cells and in cells where the kinase activity of DYRK1A has been inhibited to assess the direct effect DYRK1A has on transcriptional activity. Combining the experiment with ChIP-seq experiments of Pol III, TFIIIC and DYRK1A in the same conditions would provide clues on the effect of the presence TFIIIC at the transcribed genes.

However, the current data indicate that DYRK1A would act as a positive regulator of tRNA transcription (Di Vona, 2013). In this context, several possibilities are envisaged that are not mutually exclusive. First, DYRK1A could be important for the reinitiation step of Pol III transcription, as it has been suggested for TFIIIC. Indeed, *in vitro* studies suggest that co-factors such as DNA topoisomerase I, PC4/SUB1 and NF1 promote multiple rounds of transcription through interactions with TFIIIC at the termination region of tRNA genes (Wang et al., 2000; Wang and Roeder, 1998). Similarly, DYRK1A-dependent phosphorylation of TFIIIC could be involved in mediating these interactions and thus, inhibiting DYRK1A kinase activity would repress tRNA transcription by preventing reinitiation (Figure D.3A). Second, TFIIIC has been shown to be important in relieving chromatin repression to activate tRNA transcription once the pre-initiation complex has been formed, possibly by interacting with p300 (Mertens and

Roeder, 2008). Thus, DYRK1A could be involved in mediating this function of TFIIIC (Figure D.3B). Finally, TFIIIC may bring DYRK1A to the tRNA genes, where it can subsequently functionally interact with other factors on the chromatin such as TFIIIB (Figure D.3C). Preliminary data suggests that DYRK1A phosphorylates the TFIIIB component BDP1 (data not shown). Thus, DYRK1A could promote Pol III dependent transcription by regulating components of the TFIIIB complex. Therefore, further investigations will be required to determine if DYRK1A functionally interacts with other factors involved in regulating the transcription.

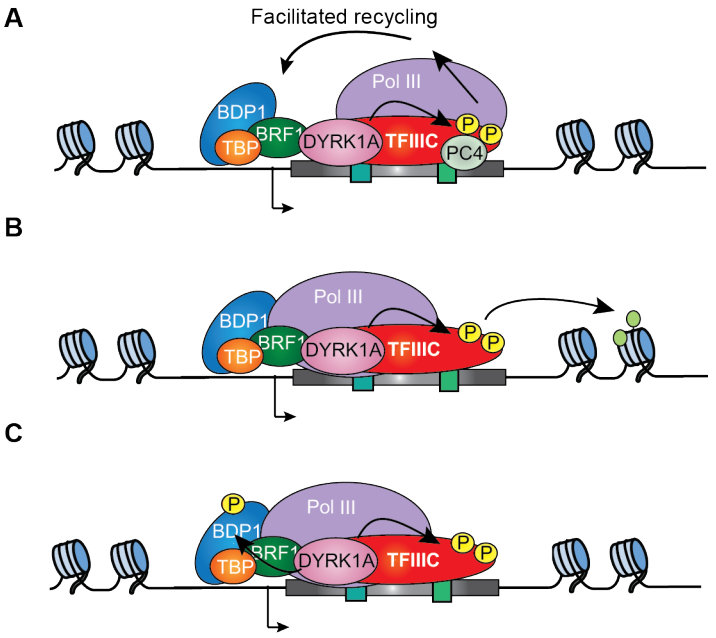

Figure D.3: Schematic representation of the proposed models on how DYRK1A regulates tRNA transcription. (A-C) Proposed mechanisms on how DYRK1A could regulate Pol III transcription via TFIIIC through regulating **(A)** reinitiation, **(B)** chromatin repression and/ or **(C)** TFIIIB functions. See text for further details.

7. Final Remarks: the role of DYRK1A in regulating cell growth

I would like to finish this Discussion by emphasising the role of DYRK1A in regulating cell growth, a process that could be exerted at multiple

regulatory levels, including the regulation of Pol III and Pol II genes related with translation.

In higher eukaryotes, size control is influenced by both intrinsic and extrinsic factors, and protein synthesis is tightly linked to the increase in mass associated with cell growth (reviewed in Amodeo and Skotheim, 2016; Lloyd, 2013). Interestingly, DYRK1A-depleted T98G cells present a reduction in cell volume (Di Vona, 2013), thus indicating that DYRK1A may contribute to cell growth. Moreover, a reduction in translational capacity has also been observed in DYRK1A-depleted T98G cells (Barba, 2018). The impact of DYRK1A in regulating cell growth could be relevant in cell types where reaching the optimal size is important to perform their functions correctly. In this regard, DYRK1A is essential for the development of the CNS by affecting the process of differentiation (see recent review in Arbones et al., 2019). Moreover, alterations observed in the CNS of *Dyrk1a* heterozygous mice have been related to defects in both cell number and cell size (Fotaki et al., 2002). Additionally, the ability of DYRK1A to stimulate myogenic transcription has been recently shown (Yu et al., 2019). Of note, neurons and myocytes are two examples of non-dividing cells that change dramatically in size for proper functionality (Lloyd, 2013).

As previously mentioned, work from our laboratory indicates that DYRK1A could be involved in translation, as depletion of DYRK1A leads to a reduction in translation rate (Barba, 2018). Aside from the potential regulatory role on tRNA transcription, as shown in this Thesis work, DYRK1A has been shown to regulate additional processes related to the control of translation as it is the case of the transcription of ribosomal protein genes, RNA binding proteins involved in the maturation of rRNA (NOL11, UTP6) and factors involved in translation (DENR) (Barba, 2018; Di Vona, 2013). Thus, DYRK1A may affect protein synthesis and thereby cell growth by regulating the transcription of essential components involved in translation (Figure D.4). This capability is in resemblance to

the master regulator of cell growth, mTOR whose contribution is exerted at multiple regulatory levels, including the modulation of Pol I, Pol II and Pol III transcription when bound to chromatin (recent reviews in Kim and Guan, 2019; Tee, 2018). Future investigations will help to unveil the role of DYRK1A activities in the cell, and uncover the links between the role in cytoplasm and nucleus, and how this is united in DYRK1A controlling cell growth.

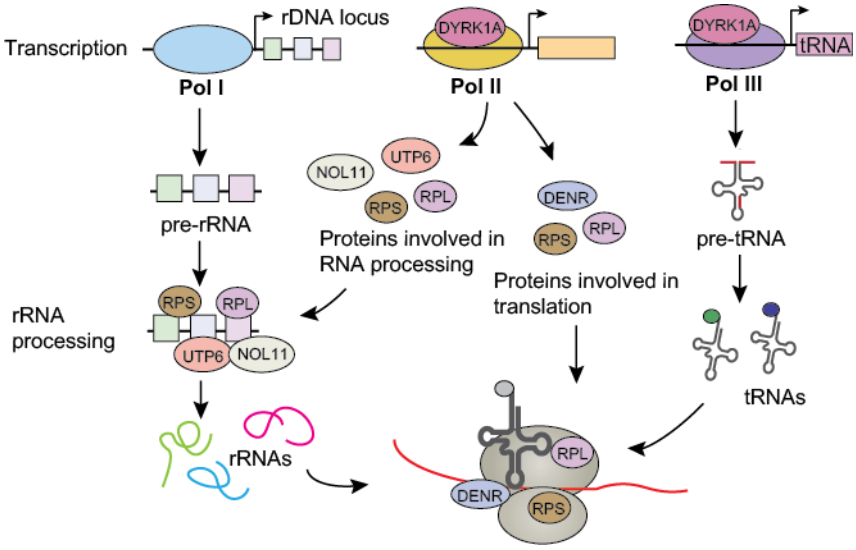

Figure D.4: A schematic representation of DYRK1A regulating protein synthesis. A model illustrating the various process regulated by DYRK1A, thereby affecting translation and protein synthesis. Figure adapted from (Barba, 2018). See text for further details.

Conclusions

1. DYRK1A is recruited to both Pol II- and Pol III-bound regions in the human genome.

2. DYRK1A-associated Pol III-occupied loci lack the DYRK1A palindromic motif TCTCGCGAGA.

3. DYRK1A occupies both type 2 and type 3 Pol III-transcribed genes, including tRNA genes.

4. DYRK1A is recruited to Pol III-bound tRNA genes in a cell-specific manner and depending on its catalytic activity.

5. DYRK1A-occupied tRNA genes have a higher Pol III occupancy than those tRNA genes without DYRK1A and are less responsive to Pol III loss upon serum starvation in T98G cells.

6. DYRK1A associates with TFIIIC only at Pol III-bound regions, including tRNA genes.

7. TFIIIC occupancy increases at tRNA genes during serum starvation in T98G cells, independently of the presence of DYRK1A.

8. DYRK1A does not physically interact with the TFIIIB complex within the nucleus.

9. DYRK1A physically interacts with the TFIIIC complex independently of its catalytic activity.

10. DYRK1A phosphorylates TFIIIC subunits -220 and -110 at several sites *in vitro*.

11. TFIIIC recruitment to tRNA genes is partially dependent on the catalytic activity of DYRK1A.

12. TFIIIC recruitment to TFIIIC-only loci, enriched in the motif for the YY1 transcription factor, is partially dependent on the catalytic activity of DYRK1A.

Abbreviations

Abbreviations

aa: Amino acid
ABC: Ammonium bicarbonate
APP: Amyloid precursor protein
ARIP4: Androgen Receptor-Interacting Protein 4
ASD: Autism spectrum disorders
ATP: Adenosine triphosphate
BDP1: B double prime 1
BRCA1: Breast cancer type 1 susceptibility protein
BRF: TFIIB-related factor
C-terminal: Carboxyl-terminal
CBP: CREB binding protein
CDKL5: Cyclin-dependent kinase-like 5
CDKLs: CDK-like kinases
CDKs: Cyclin-dependent kinases
cDNA: Complementary DNA
CEAS: Cis-regulatory elements annotation system
ChIP-seq: Chromatin immunoprecipitation coupled with high-throughput sequencing
ChIP: Chromatin immunoprecipitation
CK2: Casein kinase 2
CLKs: Cdc2-like kinases
CLP1: Cleavage and polyadenylation factor I subunit 1
CNS: Central nervous system
COBALT: Constraint-based multiple alignment tool
Cp: Crossing point
CREB1: cAMP responsive element binding protein 1
CRY2: Cryptochrome circadian regulator 2
CTCF: CCCTF-binding factor
CTD: Carboxy-terminal domain of the RNA polymerase II
DCAF7: DDB1 and CUL4 associated factor 7
DDA: Data dependent acquisition
DENR: Density-regulated protein
DH-box: DYRK homology box
DMEM: Dulbecco's modified Eagle's medium
DMSO: Dimethyl sulfoxide
DNA: Deoxyribonucleic acid
Dr1: Down-regulator of transcription of 1
DREAM: Dimerization partner, retinoblastoma (Rb)-like, E2F and multi-vulval class B
DS: Down syndrome

dsDNA: Double-stranded DNA
DSE(s): Distal sequence element(s)
DTT: Dithiothreitol
DYRK: Dual-specificity tyrosine-regulated kinase
DYRK1A: Dual-specificity tyrosine-regulated kinase 1A
E2F1: E2F transcription factor 1
EDTA: Ethylendiamine tetracetic acid
EGCG: Epigallocatechin gallate
EMSA: Electrophoretic mobility shift assay
ENCODE: Encyclopaedia of DNA elements
ERK(s): Extracellular signal-regulated kinase(s)
ETC(s): Extra TFIIIC site(s)
ETD: Electron transfer dissociation
FBS: Foetal bovine serum
FL: Full-length
FOXO1: Forkhead box O1
Fr: Truncated band
FUS: FUS RNA binding protein
GAPDH: Glyceraldehyde-3-phosphate dehydrogenase
GLI1: Glioma-associated oncogene 1
GSK3: Glycogen synthase kinase-3
GST: Glutathione S-transferase
GTex: Genotype-tissue expression
GTF(s): General transcription factor(s)
GtRNAdb: Genomic tRNA database
h: Hour/s
H3: Histone 3
HAT(s): Histone acetyltransferase(s)
HCD: High-energy collision dissociation
HeLa: Henrietta Lacks
HEPES: 4-[2-hydroxyethyl]-1-piperazineethanesulfonic acid
HIP1: Huntingtin interacting protein 1
HIPKs: Homeodomain-interacting kinases
HPV16E7: Human papilloma virus type 16
HRD: Histidine rich domain
HRP: Horseradish peroxidase
ID2: Inhibitor of DNA binding 2
IE: Intermediate element
IgG(s): immunoglobulin(s) G
IP: Immunoprecipitation
IPTG: Isopropyl β-D-1-thiogalactopyranoside
IVK: *in vitro* kinase assay

JNK(s): c-Jun N-terminal kinase(s)
KM: Kinase mutant
LATS2: Large tumour suppressor kinase 2
LB: Lysogeny broth
MAF1: Repressor of RNA polymerase III transcription MAF1 homolog
MAP1B: Microtubule-associated protein 1B
MAPKs: Mitogen-activated protein kinases
MDM2: Mouse double minute 2 homolog
mESC(s): Mouse embryonic stem cell(s)
min: Minute/s
MIR(s): Mammalian-wide interspersed repeat(s)
miRNAs: Micro RNAs
mnb: minibrain
MRD7: Mental retardation, autosomal dominant 7
mRNA: Messenger RNA
MS: Mass spectrometry
mTOR: Mammalian target of rapamycin
mTORC1: Mammalian target of rapamycin complex 1
N-terminal: Amino-terminal
N-WASP: Neural Wiskott-Aldrich syndrome protein
NAPA: N-terminal auto-phosphorylation accessory
NaPPi: Na_4P_2O7
NC2β: Negative cofactor 2β
NCBI: National Centre for Biotechnology Information
NF1: Neurofibromatosis type 1
NFAT: Nuclear factor of activated T-cells
NLK: Nemo-like kinase
NLS(s): Nuclear localisation signal(s)
NMDA2A: glutamate ionotropic receptor NMDA type subunit 2A
NOL11: Nucleolar protein 11
NP-40: Nonidet P-40
O/N: Over night
OCT1: Organic cation transporter 1
OMIM: Online Mendelian Inheritance in Man
ORPHA: Orphanet
P-TEFb: Positive transcription elongation factor b
p27/Kip1: Cyclin-dependent kinase inhibitor 1B
p300: EP300; E1A-associated protein p300
p53: tumor protein p53
p70S6K: Ribosomal protein S6 kinase beta-1
PAGE: Polyacrylamide gel electrophoresis
PAHX-AP1: Phytanoyl-CoA alpha-hydroxylase-associated protein 1

PBS: Phosphate-buffered saline
PC4: Positive cofactor 4
PCR: Polymerase chain reaction
PEST: Region rich in proline, glutamic acid, serine and threonine residues
PKA: Protein kinase A
PLK1: Polo-like kinase 1
Pol II: RNA polymerase II
Pol III: RNA polymerase III
Pol(s): RNA polymerase(s)
PPIA: Peptidyl-prolyl-isomerase A
PR: Progesterone receptor
pRb: Retinoblastoma protein
PRC2: Polycomb repression complex 2
PRP4Ks: Pre-messenger RNA processing protein 4 kinases
PS1: Presenilin 1
PSE(s): Proximal sequence element(s)
qPCR: Quantitative polymerase chain reaction
RCAN1: Regulator of calcineurin 1
REST: RE1 silencing transcription factor
RNA: Ribonucleic acid
RNase: Ribonuclease
RNF: Ring finger protein
RPL: Ribosomal proteins of the large subunit
RPMI: Roswell Park Memorial Institute Medium
RPS: Ribosomal proteins of the small subunit
rRNA(s): Ribosomal RNA(s)
RT-qPCR: Reverse transcription followed by quantitative PCR
RT: Reverse transcriptase
Sarcosyl: N-Lauroyl sarcosine sodium salt
SCF: Skp, Cullin, F-box containing complex
SD: Standard deviation
SDS: Sodium dodecyl sulphate
SF3B1: Splicing factor 3B
shRNA(s): Short hairpin RNA(s)
Sigtags: Significant reads
SINE(s): Short interspersed element(s)
siRNA(s): Small interfering RNA(s)
$SNAP_c$: SnRNA activating protein complex
snRNAs: Small nuclear RNA(s)
SPRED1/2: Sprouty-related-EVH1 domain-containing protein 1/2
SRPKs: Serine-arginine-rich protein kinases
SRSF: Serine/arginine-rich splicing factor
STAT3: Signal transducer and activator of transcription-3

TAD(s): Topological associated domain(s)
TBE: Tris/Borate/EDTA
TBP: TATA-binding protein
TBS-T: TBS-tween
TBX5: T-box transcription factor 5
TE: Tris-EDTA
TFIIIA: Transcription factor IIIA
TFIIIB: Transcription factor IIIB
TFIIIC: Transcription factor IIIC
Topo I: Topoisomerase I
TPR: Tetratricopeptide repeat
tRNA(s): Transfer RNA(s)
TRRAP: Transformation/transcription domain associated protein
TSS(s): Transcription start site(s)
UTP6: U3 small nucleolar RNA-associated protein 6 homolog
UTR: Untranslated region
WB: Western blot
Wig: Wiggle
WT: Wild-type
YY1: Yin Yang 1
ZnF: Zinc finger

References

Abascal-Palacios, G., Ramsay, E.P., Beuron, F., Morris, E., and Vannini, A. (2018). Structural basis of RNA polymerase III transcription initiation. Nature *553*, 301-306.

Adayev, T., Chen-Hwang, M.C., Murakami, N., Lee, E., Bolton, D.C., and Hwang, Y.W. (2007). Dual-specificity tyrosine phosphorylation-regulated kinase 1A does not require tyrosine phosphorylation for activity in vitro. Biochemistry *46*, 7614-7624.

Ahn, K.J., Jeong, H.K., Choi, H.S., Ryoo, S.R., Kim, Y.J., Goo, J.S., Choi, S.Y., Han, J.S., Ha, I., and Song, W.J. (2006). DYRK1A BAC transgenic mice show altered synaptic plasticity with learning and memory defects. Neurobiol Dis *22*, 463-472.

Alla, R.K., and Cairns, B.R. (2014). RNA polymerase III transcriptomes in human embryonic stem cells and induced pluripotent stem cells, and relationships with pluripotency transcription factors. PLoS One *9*, e85648.

Altafaj, X., Dierssen, M., Baamonde, C., Marti, E., Visa, J., Guimera, J., Oset, M., Gonzalez, J.R., Florez, J., Fillat, C*., et al.* (2001). Neurodevelopmental delay, motor abnormalities and cognitive deficits in transgenic mice overexpressing Dyrk1A (minibrain), a murine model of Down's syndrome. Hum Mol Genet *10*, 1915-1923.

Alvarez, M. (2004). Localización subcelular de la proteína quinasa DYRK1A: compartimentos señales y regulación (PhD Thesis, Universitat de Barcelona, Spain).

Alvarez, M., Altafaj, X., Aranda, S., and de la Luna, S. (2007). DYRK1A autophosphorylation on serine residue 520 modulates its kinase activity via 14-3-3 binding. Mol Biol Cell *18*, 1167-1178.

Alvarez, M., Estivill, X., and de la Luna, S. (2003). DYRK1A accumulates in splicing speckles through a novel targeting signal and induces speckle disassembly. J Cell Sci *116*, 3099-3107.

Amodeo, A.A., and Skotheim, J.M. (2016). Cell-size control. Cold Spring Harb Perspect Biol *8*, a019083.

Aranda, S., Alvarez, M., Turro, S., Laguna, A., and de la Luna, S. (2008). Sprouty2-mediated inhibition of fibroblast growth factor signaling is modulated by the protein kinase DYRK1A. Mol Cell Biol *28*, 5899-5911.

Aranda, S., Laguna, A., and de la Luna, S. (2011). DYRK family of protein kinases: evolutionary relationships, biochemical properties, and functional roles. FASEB J *25*, 449-462.

Arato, K. (2010). Regulation of the stability of the protein kinase DYRK1A: establishing connections with the Wnt signaling pathway (PhD Thesis, Universitat Pompeu Fabra, Spain).

Arbones, M.L., Thomazeau, A., Nakano-Kobayashi, A., Hagiwara, M., and Delabar, J.M. (2019). DYRK1A and cognition: A lifelong relationship. Pharmacol Ther *194*, 199-221.

Arimbasseri, A.G., Rijal, K., and Maraia, R.J. (2014). Comparative overview of RNA polymerase II and III transcription cycles, with focus on RNA polymerase III termination and reinitiation. Transcription *5*, e27639.

Arimbasseri, A.G., and Maraia, R.J. (2015). Mechanism of transcription termination by RNA polymerase III utilizes a non-template strand sequence-specific signal element. Mol Cell *58*, 1124-1132.

Arranz, J., Balducci, E., Arato, K., Sanchez-Elexpuru, G., Najas, S., Parras, A., Rebollo, E., Pijuan, I., Erb, I., Verde, G*., et al.* (2019). Impaired development of neocortical circuits contributes to the neurological alterations in DYRK1A haploinsufficiency syndrome. Neurobiol Dis *127*, 210-222.

Arron, J.R., Winslow, M.M., Polleri, A., Chang, C.P., Wu, H., Gao, X., Neilson, J.R., Chen, L., Heit, J.J., Kim, S.K*., et al.* (2006). NFAT dysregulation by increased dosage of DSCR1 and DYRK1A on chromosome 21. Nature *441*, 595-600.

Bain, J., Plater, L., Elliott, M., Shpiro, N., Hastie, C.J., McLauchlan, H., Klevernic, I., Arthur, J.S., Alessi, D.R., and Cohen, P. (2007). The selectivity of protein kinase inhibitors: a further update. Biochem J *408*, 297-315.

Barba, L. (2018). Chromatin-bound DYRK1A: promoter occupancy and implications in the regulation of ribosomal protein gene expression (PhD Thesis, Universitat Pompeu Fabra, Spain).

Bardeleben, C., Kassavetis, G.A., and Geiduschek, E.P. (1994). Encounters of Saccharomyces cerevisiae RNA polymerase III with its transcription factors during RNA chain elongation. J Mol Biol *235*, 1193-1205.

Barski, A., Chepelev, I., Liko, D., Cuddapah, S., Fleming, A.B., Birch, J., Cui, K., White, R.J., and Zhao, K. (2010). Pol II and its associated epigenetic marks are present at Pol III-transcribed noncoding RNA genes. Nat Struct Mol Biol *17*, 629-634.

Basu, M., Boopathi, R., Das, S., and Kundu, T.K. (2019). The largest subunit of human TFIIIC complex, TFIIIC220, a lysine acetyltransferase targets histone H3K18. BioRxiv, doi.org/10.1101/513127.

Becker, W., and Joost, H.G. (1999). Structural and functional characteristics of Dyrk, a novel subfamily of protein kinases with dual specificity. Prog Nucleic Acid Res Mol Biol *62*, 1-17.

Becker, W., and Sippl, W. (2011). Activation, regulation, and inhibition of DYRK1A. FEBS J *278*, 246-256.

Becker, W., Weber, Y., Wetzel, K., Eirmbter, K., Tejedor, F.J., and Joost, H.G. (1998). Sequence characteristics, subcellular localization, and substrate specificity of DYRK-related kinases, a novel family of dual specificity protein kinases. J Biol Chem *273*, 25893-25902.

Belgardt, B.F., and Lammert, E. (2016). DYRK1A: A promising drug target for Islet transplant-based diabetes therapies. Diabetes *65*, 1496-1498.

Bellmaine, S.F., Ovchinnikov, D.A., Manallack, D.T., Cuddy, C.E., Elefanty, A.G., Stanley, E.G., Wolvetang, E.J., Williams, S.J., and Pera, M. (2017). Inhibition of DYRK1A disrupts neural lineage specificationin human pluripotent stem cells. Elife *6*.

Bernard, G., Chouery, E., Putorti, M.L., Tetreault, M., Takanohashi, A., Carosso, G., Clement, I., Boespflug-Tanguy, O., Rodriguez, D., Delague, V.*, et al.* (2011). Mutations of POLR3A encoding a catalytic subunit of RNA polymerase Pol III cause a recessive hypomyelinating leukodystrophy. Am J Hum Genet *89*, 415-423.

Birch, J., Clarke, C.J., Campbell, A.D., Campbell, K., Mitchell, L., Liko, D., Kalna, G., Strathdee, D., Sansom, O.J., Neilson, M.*, et al.* (2016). The initiator methionine tRNA drives cell migration and invasion leading to increased metastatic potential in melanoma. Biol Open *5*, 1371-1379.

Blazek, J.D., Abeysekera, I., Li, J., and Roper, R.J. (2015). Rescue of the abnormal skeletal phenotype in Ts65Dn Down syndrome mice using genetic and therapeutic modulation of trisomic Dyrk1a. Hum Mol Genet *24*, 5687-5696.

Bogenhagen, D.F., and Brown, D.D. (1981). Nucleotide sequences in Xenopus 5S DNA required for transcription termination. Cell *24*, 261-270.

Bogenhagen, D.F., Sakonju, S., and Brown, D.D. (1980). A control region in the center of the 5S RNA gene directs specific initiation of transcription: II. The 3' border of the region. Cell *19*, 27-35.

Boguta, M. (2013). Maf1, a general negative regulator of RNA polymerase III in yeast. Biochim Biophys Acta *1829*, 376-384.

Boni, J. (2019). DYRK1A in cancer: good or evil? Defining properties of DYRK1A kinase as a novel tumor driver (PhD Thesis, Universitat Pompeu Fabra, Spain).

Borck, G., Hog, F., Dentici, M.L., Tan, P.L., Sowada, N., Medeira, A., Gueneau, L., Holger, T., Kousi, M., Lepri, F.*, et al.* (2015). BRF1 mutations alter RNA polymerase III-dependent transcription and cause neurodevelopmental anomalies. Genome Res *25*, 609.

Buchel, G., Carstensen, A., Mak, K.Y., Roeschert, I., Leen, E., Sumara, O., Hofstetter, J., Herold, S., Kalb, J., Baluapuri, A.*, et al.* (2017). Association with Aurora-A controls N-

MYC-dependent promoter escape and pause release of RNA polymerase II during the Cell Cycle. Cell Rep *21*, 3483-3497.

Cabart, P., Lee, J., and Willis, I.M. (2008). Facilitated recycling protects human RNA polymerase III from repression by Maf1 in vitro. J Biol Chem *283*, 36108-36117.

Campbell, J., Ryan, C.J., Brough, R., Bajrami, I., Pemberton, H.N., Chong, I.Y., Costa-Cabral, S., Frankum, J., Gulati, A., Holme, H.*, et al.* (2016). Large-scale profiling of kinase dependencies in cancer cell lines. Cell Rep *14*, 2490-2501.

Campbell, K.J., and White, R.J. (2014). MYC regulation of cell growth through control of transcription by RNA polymerases I and III. Cold Spring Harb Perspect Med *4*.

Canella, D., Praz, V., Reina, J.H., Cousin, P., and Hernandez, N. (2010). Defining the RNA polymerase III transcriptome: Genome-wide localization of the RNA polymerase III transcription machinery in human cells. Genome Res *20*, 710-721.

Carriere, L., Graziani, S., Alibert, O., Ghavi-Helm, Y., Boussouar, F., Humbertclaude, H., Jounier, S., Aude, J.C., Keime, C., Murvai, J.*, et al.* (2012). Genomic binding of Pol III transcription machinery and relationship with TFIIS transcription factor distribution in mouse embryonic stem cells. Nucleic Acids Res *40*, 270-283.

Chan, P.P., and Lowe, T.M. (2016). GtRNAdb 2.0: an expanded database of transfer RNA genes identified in complete and draft genomes. Nucleic Acids Res *44*, D184-189.

Chaveroux, C., Eichner, L.J., Dufour, C.R., Shatnawi, A., Khoutorsky, A., Bourque, G., Sonenberg, N., and Giguere, V. (2013). Molecular and genetic crosstalks between mTOR and ERRalpha are key determinants of rapamycin-induced nonalcoholic fatty liver. Cell Metab *17*, 586-598.

Chen, C.Y., Lanz, R.B., Walkey, C.J., Chang, W.H., Lu, W., and Johnson, D.L. (2018). Maf1 and repression of RNA polymerase III-mediated transcription drive adipocyte differentiation. Cell Rep *24*, 1852-1864.

Ciesla, M., Skowronek, E., and Boguta, M. (2018). Function of TFIIIC, RNA polymerase III initiation factor, in activation and repression of tRNA gene transcription. Nucleic Acids Res *46*, 9444-9455.

Clark, M.E., and Dasgupta, A. (1990). A transcriptionally active form of TFIIIC is modified in poliovirus-infected HeLa cells. Mol Cell Biol *10*, 5106-5113.

Clarke, C.J., Berg, T.J., Birch, J., Ennis, D., Mitchell, L., Cloix, C., Campbell, A., Sumpton, D., Nixon, C., Campbell, K.*, et al.* (2016). The initiator methionine tRNA drives secretion of type II collagen from stromal fibroblasts to promote tumor growth and angiogenesis. Curr Biol *26*, 755-765.

Crepaldi, L., Policarpi, C., Coatti, A., Sherlock, W.T., Jongbloets, B.C., Down, T.A., and Riccio, A. (2013). Binding of TFIIIC to sine elements controls the relocation of activity-dependent neuronal genes to transcription factories. PLoS Genet *9*, e1003699.

Crighton, D., Woiwode, A., Zhang, C., Mandavia, N., Morton, J.P., Warnock, L.J., Milner, J., White, R.J., and Johnson, D.L. (2003). p53 represses RNA polymerase III transcription by targeting TBP and inhibiting promoter occupancy by TFIIIB. EMBO J *22*, 2810-2820.

da Costa Martins, P.A., Salic, K., Gladka, M.M., Armand, A.S., Leptidis, S., el Azzouzi, H., Hansen, A., Coenen-de Roo, C.J., Bierhuizen, M.F., van der Nagel, R.*, et al.* (2010). MicroRNA-199b targets the nuclear kinase Dyrk1a in an auto-amplification loop promoting calcineurin/NFAT signalling. Nat Cell Biol *12*, 1220-1227.

de la Torre, R., de Sola, S., Hernandez, G., Farre, M., Pujol, J., Rodriguez, J., Espadaler, J.M., Langohr, K., Cuenca-Royo, A., Principe, A.*, et al.* (2016). Safety and efficacy of cognitive training plus epigallocatechin-3-gallate in young adults with Down's syndrome (TESDAD): a double-blind, randomised, placebo-controlled, phase 2 trial. Lancet Neurol *15*, 801-810.

De la Torre, R., De Sola, S., Pons, M., Duchon, A., de Lagran, M.M., Farre, M., Fito, M., Benejam, B., Langohr, K., Rodriguez, J.*, et al.* (2014). Epigallocatechin-3-gallate, a DYRK1A inhibitor, rescues cognitive deficits in Down syndrome mouse models and in humans. Mol Nutr Food Res *58*, 278-288.

Dephoure, N., Zhou, C., Villen, J., Beausoleil, S.A., Bakalarski, C.E., Elledge, S.J., and Gygi, S.P. (2008). A quantitative atlas of mitotic phosphorylation. Proc Natl Acad Sci U S A *105*, 10762-10767.

Di Vona, C. (2013). Nuclear DYRK1A: new insights into its role within the nucleus (PhD Thesis, Universitat Pompeu Fabra, Spain).

Di Vona, C., Bezdan, D., Islam, A.B., Salichs, E., Lopez-Bigas, N., Ossowski, S., and de la Luna, S. (2015). Chromatin-wide profiling of DYRK1A reveals a role as a gene-specific RNA polymerase II CTD kinase. Mol Cell *57*, 506-520.

Dieci, G., Fiorino, G., Castelnuovo, M., Teichmann, M., and Pagano, A. (2007). The expanding RNA polymerase III transcriptome. Trends Genet *23*, 614-622.

Dieci, G., and Sentenac, A. (1996). Facilitated recycling pathway for RNA polymerase III. Cell *84*, 245-252.

Dittmar, K.A., Goodenbour, J.M., and Pan, T. (2006). Tissue-specific differences in human transfer RNA expression. PLoS Genet *2*, e221.

Dowjat, W.K., Adayev, T., Kuchna, I., Nowicki, K., Palminiello, S., Hwang, Y.W., and Wegiel, J. (2007). Trisomy-driven overexpression of DYRK1A kinase in the brain of subjects with Down syndrome. Neurosci Lett *413*, 77-81.

Ducrot, C., Lefebvre, O., Landrieux, E., Guirouilh-Barbat, J., Sentenac, A., and Acker, J. (2006). Reconstitution of the yeast RNA polymerase III transcription system with all recombinant factors. J Biol Chem *281*, 11685-11692.

Dumay-Odelot, H., Marck, C., Durrieu-Gaillard, S., Lefebvre, O., Jourdain, S., Prochazkova, M., Pflieger, A., and Teichmann, M. (2007). Identification, molecular cloning, and characterization of the sixth subunit of human transcription factor TFIIIC. J Biol Chem *282*, 17179-17189.

Ebersole, T., Kim, J.H., Samoshkin, A., Kouprina, N., Pavlicek, A., White, R.J., and Larionov, V. (2011). tRNA genes protect a reporter gene from epigenetic silencing in mouse cells. Cell Cycle *10*, 2779-2791.

Ehe, B.K., Lamson, D.R., Tarpley, M., Onyenwoke, R.U., Graves, L.M., and Williams, K.P. (2017). Identification of a DYRK1A-mediated phosphorylation site within the nuclear localization sequence of the hedgehog transcription factor GLI1. Biochem Biophys Res Commun *491*, 767-772.

Ernens, I., Goodfellow, S.J., Innes, F., Kenneth, N.S., Derblay, L.E., White, R.J., and Scott, P.H. (2006). Hypoxic stress suppresses RNA polymerase III recruitment and tRNA gene transcription in cardiomyocytes. Nucleic Acids Res *34*, 286-294.

Fairley, Jennifer A., Mitchell, Louise E., Berg, T., Kenneth, Niall S., von Schubert, C., Silljé, Herman H.W., Medema, René H., Nigg, Erich A., and White, Robert J. (2012). Direct regulation of tRNA and 5S rRNA gene transcription by Polo-like kinase 1. Mol Cell *45*, 541-552.

Felton-Edkins, Z.A., Fairley, J.A., Graham, E.L., Johnston, I.M., White, R.J., and Scott, P.H. (2003). The mitogen-activated protein (MAP) kinase ERK induces tRNA synthesis by phosphorylating TFIIIB. EMBO J *22*, 2422-2432.

Ferrari, R., de Llobet Cucalon, L.I., Di Vona, C., Le Dilly, F., Vidal, E., Lioutas, A., Oliete, J.Q., Jochem, L., Cutts, E., Dieci, G*., et al.* (2019). TFIIIC binding to Alu elements controls gene expression via chromatin looping and histone acetylation. BioRxiv, doi.org/10.1101/455733.

Ferrari, R., Rivetti, C., Acker, J., and Dieci, G. (2004). Distinct roles of transcription factors TFIIIB and TFIIIC in RNA polymerase III transcription reinitiation. Proc Natl Acad Sci U S A *101*, 13442-13447.

Ferrari, R., Su, T., Li, B., Bonora, G., Oberai, A., Chan, Y., Sasidharan, R., Berk, A.J., Pellegrini, M., and Kurdistani, S.K. (2012). Reorganization of the host epigenome by a viral oncogene. Genome Res *22*, 1212-1221.

Finlay-Schultz, J., Gillen, A.E., Brechbuhl, H.M., Ivie, J.J., Matthews, S.B., Jacobsen, B.M., Bentley, D.L., Kabos, P., and Sartorius, C.A. (2017). Breast cancer suppression by

progesterone receptors is mediated by their modulation of estrogen receptors and RNA polymerase III. Cancer Res *77*, 4934-4946.

Fotaki, V., Dierssen, M., Alcantara, S., Martinez, S., Marti, E., Casas, C., Visa, J., Soriano, E., Estivill, X., and Arbones, M.L. (2002). Dyrk1A haploinsufficiency affects viability and causes developmental delay and abnormal brain morphology in mice. Mol Cell Biol *22*, 6636-6647.

Garcia-Cerro, S., Martinez, P., Vidal, V., Corrales, A., Florez, J., Vidal, R., Rueda, N., Arbones, M.L., and Martinez-Cue, C. (2014). Overexpression of Dyrk1A is implicated in several cognitive, electrophysiological and neuromorphological alterations found in a mouse model of Down syndrome. PLoS One *9*, e106572.

Garcia-Cerro, S., Rueda, N., Vidal, V., Lantigua, S., and Martinez-Cue, C. (2017). Normalizing the gene dosage of Dyrk1A in a mouse model of Down syndrome rescues several Alzheimer's disease phenotypes. Neurobiol Dis *106*, 76-88.

Gibson, D.G., Young, L., Chuang, R.Y., Venter, J.C., Hutchison, C.A., 3rd, and Smith, H.O. (2009). Enzymatic assembly of DNA molecules up to several hundred kilobases. Nat Methods *6*, 343-345.

Gingold, H., Tehler, D., Christoffersen, N.R., Nielsen, M.M., Asmar, F., Kooistra, S.M., Christophersen, N.S., Christensen, L.L., Borre, M., Sorensen, K.D*., et al.* (2014). A dual program for translation regulation in cellular proliferation and differentiation. Cell *158*, 1281-1292.

Girotto, G., Abdulhadi, K., Buniello, A., Vozzi, D., Licastro, D., d'Eustacchio, A., Vuckovic, D., Alkowari, M.K., Steel, K.P., Badii, R*., et al.* (2013). Linkage study and exome sequencing identify a BDP1 mutation associated with hereditary hearing loss. PLoS One *8*, e80323.

Glenewinkel, F., Cohen, M.J., King, C.R., Kaspar, S., Bamberg-Lemper, S., Mymryk, J.S., and Becker, W. (2016). The adaptor protein DCAF7 mediates the interaction of the adenovirus E1A oncoprotein with the protein kinases DYRK1A and HIPK2. Sci Rep *6*, 28241.

Gockler, N., Jofre, G., Papadopoulos, C., Soppa, U., Tejedor, F.J., and Becker, W. (2009). Harmine specifically inhibits protein kinase DYRK1A and interferes with neurite formation. FEBS J *276*, 6324-6337.

Goodarzi, H., Nguyen, H.C.B., Zhang, S., Dill, B.D., Molina, H., and Tavazoie, S.F. (2016). Modulated expression of specific tRNAs drives gene expression and cancer progression. Cell *165*, 1416-1427.

Goodfellow, S.J., Innes, F., Derblay, L.E., MacLellan, W.R., Scott, P.H., and White, R.J. (2006). Regulation of RNA polymerase III transcription during hypertrophic growth. EMBO J *25*, 1522-1533.

Graczyk, D., Ciesla, M., and Boguta, M. (2018). Regulation of tRNA synthesis by the general transcription factors of RNA polymerase III - TFIIIB and TFIIIC, and by the MAF1 protein. Biochim Biophys Acta - Gene Regul Mech *1861*, 320-329.

Graczyk, D., White, R.J., and Ryan, K.M. (2015). Involvement of RNA polymerase III in immune responses. Mol Cell Biol *35*, 1848-1859.

Graham, F.L., and van der Eb, A.J. (1973). A new technique for the assay of infectivity of human adenovirus 5 DNA. Virology *52*, 456-467.

Guard, S.E., Poss, Z.C., Ebmeier, C.C., Pagratis, M., Simpson, H., Taatjes, D.J., and Old, W.M. (2019). The nuclear interactome of DYRK1A reveals a functional role in DNA damage repair. Sci Rep *9*, 6539.

Guedj, F., Sebrie, C., Rivals, I., Ledru, A., Paly, E., Bizot, J.C., Smith, D., Rubin, E., Gillet, B., Arbones, M*., et al.* (2009). Green tea polyphenols rescue of brain defects induced by overexpression of DYRK1A. PLoS One *4*, e4606.

Guimera, J., Casas, C., Estivill, X., and Pritchard, M. (1999). Human minibrain homologue (MNBH/DYRK1): characterization, alternative splicing, differential tissue expression, and overexpression in Down syndrome. Genomics *57*, 407-418.

Guimera, J., Casas, C., Pucharcos, C., Solans, A., Domenech, A., Planas, A.M., Ashley, J., Lovett, M., Estivill, X., and Pritchard, M.A. (1996). A human homologue of Drosophila minibrain (MNB) is expressed in the neuronal regions affected in Down syndrome and maps to the critical region. Hum Mol Genet *5*, 1305-1310.

Hamdani, O., Dhillon, N., Hsieh, T.S., Fujita, T., Ocampo, J., Kirkland, J.G., Lawrimore, J., Kobayashi, T.J., Friedman, B., Fulton, D.*, et al.* (2019). tRNA genes affect chromosome structure and function via local effects. Mol Cell Biol *39*.

Hammerle, B., Carnicero, A., Elizalde, C., Ceron, J., Martinez, S., and Tejedor, F.J. (2003). Expression patterns and subcellular localization of the Down syndrome candidate protein MNB/DYRK1A suggest a role in late neuronal differentiation. Eur J Neurosci *17*, 2277-2286.

Heinz, S., Benner, C., Spann, N., Bertolino, E., Lin, Y.C., Laslo, P., Cheng, J.X., Murre, C., Singh, H., and Glass, C.K. (2010). Simple combinations of lineage-determining transcription factors prime cis-regulatory elements required for macrophage and B cell identities. Mol Cell *38*, 576-589.

Hendriks, I.A., Lyon, D., Young, C., Jensen, L.J., Vertegaal, A.C., and Nielsen, M.L. (2017). Site-specific mapping of the human SUMO proteome reveals co-modification with phosphorylation. Nat Struct Mol Biol *24*, 325-336.

Hille, S., Dierck, F., Kuhl, C., Sosna, J., Adam-Klages, S., Adam, D., Lullmann-Rauch, R., Frey, N., and Kuhn, C. (2016). Dyrk1a regulates the cardiomyocyte cell cycle via D-cyclin-dependent Rb/E2f-signalling. Cardiovasc Res *110*, 381-394.

Himpel, S., Panzer, P., Eirmbter, K., Czajkowska, H., Sayed, M., Packman, L.C., Blundell, T., Kentrup, H., Grotzinger, J., Joost, H.G.*, et al.* (2001). Identification of the autophosphorylation sites and characterization of their effects in the protein kinase DYRK1A. Biochem J *359*, 497-505.

Himpel, S., Tegge, W., Frank, R., Leder, S., Joost, H.G., and Becker, W. (2000). Specificity determinants of substrate recognition by the protein kinase DYRK1A. J Biol Chem *275*, 2431-2438.

Hsieh, Y.J., Kundu, T.K., Wang, Z., Kovelman, R., and Roeder, R.G. (1999a). The TFIIIC90 subunit of TFIIIC interacts with multiple components of the RNA polymerase III machinery and contains a histone-specific acetyltransferase activity. Mol Cell Biol *19*, 7697-7704.

Hsieh, Y.J., Wang, Z., Kovelman, R., and Roeder, R.G. (1999b). Cloning and characterization of two evolutionarily conserved subunits (TFIIIC102 and TFIIIC63) of human TFIIIC and their involvement in functional interactions with TFIIIB and RNA polymerase III. Mol Cell Biol *19*, 4944-4952.

Hu, P., Samudre, K., Wu, S., Sun, Y., and Hernandez, N. (2004). CK2 phosphorylation of Bdp1 executes cell cycle-specific RNA polymerase III transcription repression. Mol Cell *16*, 81-92.

Hulsen, T., de Vlieg, J., and Alkema, W. (2008). BioVenn - a web application for the comparison and visualization of biological lists using area-proportional Venn diagrams. BMC Genomics *9*, 488.

Jacob, J., Cabarcas, S., Veras, I., Zaveri, N., and Schramm, L. (2007). The green tea component EGCG inhibits RNA polymerase III transcription. Biochem Biophys Res Commun *360*, 778-783.

Jang, S.M., Azebi, S., Soubigou, G., and Muchardt, C. (2014). DYRK1A phoshorylates histone H3 to differentially regulate the binding of HP1 isoforms and antagonize HP1-mediated transcriptional repression. EMBO Rep *15*, 686-694.

Jarhad, D.B., Mashelkar, K.K., Kim, H.R., Noh, M., and Jeong, L.S. (2018). Dual-specificity tyrosine phosphorylation-regulated kinase 1A (DYRK1A) inhibitors as potential therapeutics. J Med Chem *61*, 9791-9810.

Ji, X., Li, W., Song, J., Wei, L., and Liu, X.S. (2006). CEAS: cis-regulatory element annotation system. Nucleic Acids Res *34*, W551-554.

Jin, N., Yin, X., Gu, J., Zhang, X., Shi, J., Qian, W., Ji, Y., Cao, M., Gu, X., Ding, F*., et al.* (2015). Truncation and activation of dual specificity tyrosine phosphorylation-regulated kinase 1A by calpain I: a molecular mechanism linked to Tau pathology in Alzheimer Disease. J Biol Chem *290*, 15219-15237.

Johnson, S.A., Dubeau, L., and Johnson, D.L. (2008). Enhanced RNA polymerase III-dependent transcription is required for oncogenic transformation. J Biol Chem *283*, 19184-19191.

Johnson, S.S., Zhang, C., Fromm, J., Willis, I.M., and Johnson, D.L. (2007). Mammalian Maf1 is a negative regulator of transcription by all three nuclear RNA polymerases. Mol Cell *26*, 367-379.

Johnston, I.M., Allison, S.J., Morton, J.P., Schramm, L., Scott, P.H., and White, R.J. (2002). CK2 forms a stable complex with TFIIIB and activates RNA polymerase III transcription in human cells. Mol Cell Biol *22*, 3757-3768.

Jung, M.S., Park, J.H., Ryu, Y.S., Choi, S.H., Yoon, S.H., Kwen, M.Y., Oh, J.Y., Song, W.J., and Chung, S.H. (2011). Regulation of RCAN1 protein activity by Dyrk1A protein-mediated phosphorylation. J Biol Chem *286*, 40401-40412.

Kaczmarski, W., Barua, M., Mazur-Kolecka, B., Frackowiak, J., Dowjat, W., Mehta, P., Bolton, D., Hwang, Y.W., Rabe, A., Albertini, G*., et al.* (2014). Intracellular distribution of differentially phosphorylated dual-specificity tyrosine phosphorylation-regulated kinase 1A (DYRK1A). J Neurosci Res *92*, 162-173.

Kang, J.E., Choi, S.A., Park, J.B., and Chung, K.C. (2005). Regulation of the proapoptotic activity of huntingtin interacting protein 1 by Dyrk1 and caspase-3 in hippocampal neuroprogenitor cells. J Neurosci Res *81*, 62-72.

Kantidakis, T., Ramsbottom, B.A., Birch, J.L., Dowding, S.N., and White, R.J. (2010). mTOR associates with TFIIIC, is found at tRNA and 5S rRNA genes, and targets their repressor Maf1. Proc Natl Acad Sci U S A *107*, 11823-11828.

Kantidakis, T., and White, R.J. (2010). Dr1 (NC2) is present at tRNA genes and represses their transcription in human cells. Nucleic Acids Res *38*, 1228-1239.

Kenneth, N.S., Marshall, L., and White, R.J. (2008). Recruitment of RNA polymerase III in vivo. Nucleic Acids Res *36*, 3757-3764.

Kentrup, H., Becker, W., Heukelbach, J., Wilmes, A., Schurmann, A., Huppertz, C., Kainulainen, H., and Joost, H.G. (1996). Dyrk, a dual specificity protein kinase with unique structural features whose activity is dependent on tyrosine residues between subdomains VII and VIII. J Biol Chem *271*, 3488-3495.

Kettenbach, A.N., Schweppe, D.K., Faherty, B.K., Pechenick, D., Pletnev, A.A., and Gerber, S.A. (2011). Quantitative phosphoproteomics identifies substrates and functional modules of Aurora and Polo-like kinase activities in mitotic cells. Sci Signal *4*, rs5.

Kida, E., Walus, M., Jarzabek, K., Palminiello, S., Albertini, G., Rabe, A., Hwang, Y.W., and Golabek, A.A. (2011). Form of dual-specificity tyrosine-(Y)-phosphorylation-regulated kinase 1A nonphosphorylated at tyrosine 145 and 147 is enriched in the nuclei of astroglial cells, adult hippocampal progenitors, and some cholinergic axon terminals. Neuroscience *195*, 112-127.

Kii, I., Sumida, Y., Goto, T., Sonamoto, R., Okuno, Y., Yoshida, S., Kato-Sumida, T., Koike, Y., Abe, M., Nonaka, Y*., et al.* (2016). Selective inhibition of the kinase DYRK1A by targeting its folding process. Nat Commun *7*, 11391.

Kim, D., Won, J., Shin, D.W., Kang, J., Kim, Y.J., Choi, S.Y., Hwang, M.K., Jeong, B.W., Kim, G.S., Joe, C.O*., et al.* (2004). Regulation of Dyrk1A kinase activity by 14-3-3. Biochem Biophys Res Commun *323*, 499-504.

Kim, E.J., Sung, J.Y., Lee, H.J., Rhim, H., Hasegawa, M., Iwatsubo, T., Min do, S., Kim, J., Paik, S.R., and Chung, K.C. (2006). Dyrk1A phosphorylates alpha-synuclein and enhances intracellular inclusion formation. J Biol Chem *281*, 33250-33257.

Kim, H., Lee, K.S., Kim, A.K., Choi, M., Choi, K., Kang, M., Chi, S.W., Lee, M.S., Lee, J.S., Lee, S.Y*., et al.* (2016). A chemical with proven clinical safety rescues Down-syndrome-related phenotypes in through DYRK1A inhibition. Dis Model Mech *9*, 839-848.

Kim, J., and Guan, K.L. (2019). mTOR as a central hub of nutrient signalling and cell growth. Nat Cell Biol *21*, 63-71.

Kinstrie, R., Luebbering, N., Miranda-Saavedra, D., Sibbet, G., Han, J., Lochhead, P.A., and Cleghon, V. (2010). Characterization of a domain that transiently converts class 2 DYRKs into intramolecular tyrosine kinases. Sci Signal *3*, ra16.

Kraoua, I., Karkar, A., Drissi, C., Benrhouma, H., Klaa, H., Samaan, S., Renaldo, F., Elmaleh, M., Ben Hamouda, M., Abdelhak, S*., et al.* (2019). Novel POLR1C mutation in RNA polymerase III-related leukodystrophy with severe myoclonus and dystonia. Mol Genet Genomic Med, e914.

Kuhn, C., Frank, D., Will, R., Jaschinski, C., Frauen, R., Katus, H.A., and Frey, N. (2009). DYRK1A is a novel negative regulator of cardiomyocyte hypertrophy. J Biol Chem *284*, 17320-17327.

Kumar, K., Wang, P., Sanchez, R., Swartz, E.A., Stewart, A.F., and DeVita, R.J. (2018). Development of kinase-selective, Harmine-based DYRK1A inhibitors that induce pancreatic human beta-cell proliferation. J Med Chem *61*, 7687-7699.

Kundu, T.K., Wang, Z., and Roeder, R.G. (1999). Human TFIIIC relieves chromatin-mediated repression of RNA polymerase III transcription and contains an intrinsic histone acetyltransferase activity. Mol Cell Biol *19*, 1605-1615.

Kurabayashi, N., Hirota, T., Sakai, M., Sanada, K., and Fukada, Y. (2010). DYRK1A and glycogen synthase kinase 3beta, a dual-kinase mechanism directing proteasomal degradation of CRY2 for circadian timekeeping. Mol Cell Biol *30*, 1757-1768.

Laguna, A., Barallobre, M.J., Marchena, M.A., Mateus, C., Ramirez, E., Martinez-Cue, C., Delabar, J.M., Castelo-Branco, M., de la Villa, P., and Arbones, M.L. (2013). Triplication of DYRK1A causes retinal structural and functional alterations in Down syndrome. Hum Mol Genet *22*, 2775-2784.

Langmead, B., Trapnell, C., Pop, M., and Salzberg, S.L. (2009). Ultrafast and memory-efficient alignment of short DNA sequences to the human genome. Genome Biol *10*, R25.

Lant, J.T., Berg, M.D., Heinemann, I.U., Brandl, C.J., and O'Donoghue, P. (2019). Pathways to disease from natural variations in human cytoplasmic tRNAs. J Biol Chem *294*, 5294-5308.

Lassar, A.B., Martin, P.L., and Roeder, R.G. (1983). Transcription of class III genes: formation of preinitiation complexes. Science *222*, 740-748.

Lee, Y., Ha, J., Kim, H.J., Kim, Y.-S., Chang, E.-J., Song, W.-J., and Kim, H.-H. (2009). Negative feedback inhibition of NFATc1 by DYRK1A regulates bone homeostasis. J Biol Chem *284*, 33343-33351.

Lek, M., Karczewski, K.J., Minikel, E.V., Samocha, K.E., Banks, E., Fennell, T., O'Donnell-Luria, A.H., Ware, J.S., Hill, A.J., Cummings, B.B*., et al.* (2016). Analysis of protein-coding genetic variation in 60,706 humans. Nature *536*, 285-291.

Li, D., Jackson, R.A., Yusoff, P., and Guy, G.R. (2010). Direct association of Sprouty-related protein with an EVH1 domain (SPRED) 1 or SPRED2 with DYRK1A modifies substrate/kinase interactions. J Biol Chem *285*, 35374-35385.

Li, S., Xu, C., Fu, Y., Lei, P.J., Yao, Y., Yang, W., Zhang, Y., Washburn, M.P., Florens, L., Jaiswal, M*., et al.* (2018). DYRK1A interacts with histone acetyl transferase p300 and CBP and localizes to enhancers. Nucleic Acids Res *46*, 11202-11213.

Liang, Y.J., Chang, H.S., Wang, C.Y., and Yu, W.C. (2008). DYRK1A stabilizes HPV16E7 oncoprotein through phosphorylation of the threonine 5 and threonine 7 residues. Int J Biochem Cell Biol *40*, 2431-2441.

Liu, C., Li, S., Dai, X., Ma, J., Wan, J., Jiang, H., Wang, P., Liu, Z., and Zhang, H. (2015). PRC2 regulates RNA polymerase III transcribed non-translated RNA gene transcription

through EZH2 and SUZ12 interaction with TFIIIC complex. Nucleic Acids Res *43*, 6270-6284.

Liu, Q., Liu, N., Zang, S., Liu, H., Wang, P., Ji, C., and Sun, X. (2014). Tumor suppressor DYRK1A effects on proliferation and chemoresistance of AML cells by downregulating c-Myc. PLoS One *9*, e98853.

Liu, Q., Tang, Y., Chen, L., Liu, N., Lang, F., Liu, H., Wang, P., and Sun, X. (2016). E3 ligase SCFbetaTrCP-induced DYRK1A protein degradation is essential for cell cycle progression in HEK293 cells. J Biol Chem *291*, 26399-26409.

Lloyd, A.C. (2013). The regulation of cell size. Cell *154*, 1194-1205.

Lochhead, P.A., Sibbet, G., Morrice, N., and Cleghon, V. (2005). Activation-loop autophosphorylation is mediated by a novel transitional intermediate form of DYRKs. Cell *121*, 925-936.

Lu, H., Yu, D., Hansen, A.S., Ganguly, S., Liu, R., Heckert, A., Darzacq, X., and Zhou, Q. (2018). Phase-separation mechanism for C-terminal hyperphosphorylation of RNA polymerase II. Nature *558*, 318-323.

Lu, M., Zheng, L., Han, B., Wang, L., Wang, P., Liu, H., and Sun, X. (2011). REST regulates DYRK1A transcription in a negative feedback loop. J Biol Chem *286*, 10755-10763.

Luna, J., Boni, J., Cuatrecasas, M., Bofill-De Ros, X., Nunez-Manchon, E., Gironella, M., Vaquero, E.C., Arbones, M.L., de la Luna, S., and Fillat, C. (2019). DYRK1A modulates c-MET in pancreatic ductal adenocarcinoma to drive tumour growth. Gut *68*, 1465-1476.

Maenz, B., Hekerman, P., Vela, E.M., Galceran, J., and Becker, W. (2008). Characterization of the human DYRK1A promoter and its regulation by the transcription factor E2F1. BMC Mol Biol *9*, 30.

Male, G., von Appen, A., Glatt, S., Taylor, N.M., Cristovao, M., Groetsch, H., Beck, M., and Muller, C.W. (2015). Architecture of TFIIIC and its role in RNA polymerase III pre-initiation complex assembly. Nat Commun *6*, 7387.

Malinge, S., Bliss-Moreau, M., Kirsammer, G., Diebold, L., Chlon, T., Gurbuxani, S., and Crispino, J.D. (2012). Increased dosage of the chromosome 21 ortholog Dyrk1a promotes megakaryoblastic leukemia in a murine model of Down syndrome. J Clin Invest *122*, 948-962.

Mange, F., Praz, V., Migliavacca, E., Willis, I.M., Schutz, F., Hernandez, N., and Cycli, X.C. (2017). Diurnal regulation of RNA polymerase III transcription is under the control of both the feeding-fasting response and the circadian clock. Genome Res *27*, 973-984.

Manning, G., Whyte, D.B., Martinez, R., Hunter, T., and Sudarsanam, S. (2002). The protein kinase complement of the human genome. Science *298*, 1912-1934.

Mao, J., Maye, P., Kogerman, P., Tejedor, F.J., Toftgard, R., Xie, W., Wu, G., and Wu, D. (2002). Regulation of Gli1 transcriptional activity in the nucleus by Dyrk1. J Biol Chem *277*, 35156-35161.

Marti, E., Altafaj, X., Dierssen, M., de la Luna, S., Fotaki, V., Alvarez, M., Perez-Riba, M., Ferrer, I., and Estivill, X. (2003). Dyrk1A expression pattern supports specific roles of this kinase in the adult central nervous system. Brain Res *964*, 250-263.

Martinez de Lagran, M., Altafaj, X., Gallego, X., Marti, E., Estivill, X., Sahun, I., Fillat, C., and Dierssen, M. (2004). Motor phenotypic alterations in TgDyrk1a transgenic mice implicate DYRK1A in Down syndrome motor dysfunction. Neurobiol Dis *15*, 132-142.

McElyea, S.D., Starbuck, J.M., Tumbleson-Brink, D.M., Harrington, E., Blazek, J.D., Ghoneima, A., Kula, K., and Roper, R.J. (2016). Influence of prenatal EGCG treatment and Dyrk1a dosage reduction on craniofacial features associated with Down syndrome. Hum Mol Genet *25*, 4856-4869.

McFarlane, R.J., and Whitehall, S.K. (2009). tRNA genes in eukaryotic genome organization and reorganization. Cell Cycle *8*, 3102-3106.

Menon, V.R., Ananthapadmanabhan, V., Swanson, S., Saini, S., Sesay, F., Yakovlev, V., Florens, L., DeCaprio, J.A., Washburn, M.P., Dozmorov, M*., et al.* (2019). DYRK1A

regulates the recruitment of 53BP1 to the sites of DNA damage in part through interaction with RNF169. Cell Cycle *18*, 531-551.

Mertens, C., and Roeder, R.G. (2008). Different functional modes of p300 in activation of RNA polymerase III transcription from chromatin templates. Mol Cell Biol *28*, 5764-5776.

Michels, A.A., Robitaille, A.M., Buczynski-Ruchonnet, D., Hodroj, W., Reina, J.H., Hall, M.N., and Hernandez, N. (2010). mTORC1 directly phosphorylates and regulates human MAF1. Mol Cell Biol *30*, 3749-3757.

Moqtaderi, Z., Wang, J., Raha, D., White, R.J., Snyder, M., Weng, Z., and Struhl, K. (2010). Genomic binding profiles of functionally distinct RNA polymerase III transcription complexes in human cells. Nat Struct Mol Biol *17*, 635-640.

Murakami, N., Bolton, D., and Hwang, Y.W. (2009). Dyrk1A binds to multiple endocytic proteins required for formation of clathrin-coated vesicles. Biochemistry *48*, 9297-9305.

Nguyen, T.L., Fruit, C., Herault, Y., Meijer, L., and Besson, T. (2017). Dual-specificity tyrosine phosphorylation-regulated kinase 1A (DYRK1A) inhibitors: a survey of recent patent literature. Expert Opin Ther Pat *27*, 1183-1199.

Nicol, J.W., Helt, G.A., Blanchard, S.G., Jr., Raja, A., and Loraine, A.E. (2009). The Integrated Genome Browser: free software for distribution and exploration of genome-scale datasets. Bioinformatics *25*, 2730-2731.

Ogawa, Y., Nonaka, Y., Goto, T., Ohnishi, E., Hiramatsu, T., Kii, I., Yoshida, M., Ikura, T., Onogi, H., Shibuya, H.*, et al.* (2010). Development of a novel selective inhibitor of the Down syndrome-related kinase Dyrk1A. Nat Commun *1*, 86.

Oler, A.J., Alla, R.K., Roberts, D.N., Wong, A., Hollenhorst, P.C., Chandler, K.J., Cassiday, P.A., Nelson, C.A., Hagedorn, C.H., Graves, B.J.*, et al.* (2010). Human RNA polymerase III transcriptomes and relationships to Pol II promoter chromatin and enhancer-binding factors. Nat Struct Mol Biol *17*, 620-628.

Orioli, A., Praz, V., Lhote, P., and Hernandez, N. (2016). Human MAF1 targets and represses active RNA polymerase III genes by preventing recruitment rather than inducing long-term transcriptional arrest. Genome Res *26*, 624-635.

Ortiz-Abalia, J., Sahun, I., Altafaj, X., Andreu, N., Estivill, X., Dierssen, M., and Fillat, C. (2008). Targeting Dyrk1A with AAVshRNA attenuates motor alterations in TgDyrk1A, a mouse model of Down syndrome. Am J Hum Genet *83*, 479-488.

Papadopoulos, J.S., and Agarwala, R. (2007). COBALT: constraint-based alignment tool for multiple protein sequences. Bioinformatics *23*, 1073-1079.

Park, J., Oh, Y., Yoo, L., Jung, M.S., Song, W.J., Lee, S.H., Seo, H., and Chung, K.C. (2010). Dyrk1A phosphorylates p53 and inhibits proliferation of embryonic neuronal cells. J Biol Chem *285*, 31895-31906.

Pavon-Eternod, M., Gomes, S., Geslain, R., Dai, Q., Rosner, M.R., and Pan, T. (2009). tRNA over-expression in breast cancer and functional consequences. Nucleic Acids Res *37*, 7268-7280.

Pozo, N., Zahonero, C., Fernandez, P., Linares, J.M., Ayuso, A., Hagiwara, M., Perez, A., Ricoy, J.R., Hernandez-Lain, A., Sepulveda, J.M.*, et al.* (2013). Inhibition of DYRK1A destabilizes EGFR and reduces EGFR-dependent glioblastoma growth. J Clin Invest *123*, 2475-2487.

Raab, J.R., Chiu, J., Zhu, J., Katzman, S., Kurukuti, S., Wade, P.A., Haussler, D., and Kamakaka, R.T. (2012). Human tRNA genes function as chromatin insulators. EMBO J *31*, 330-350.

Raaf, L., Noll, C., Cherifi, M., Benazzoug, Y., Delabar, J.M., and Janel, N. (2010). Hyperhomocysteinemia-induced Dyrk1a downregulation results in cardiomyocyte hypertrophy in rats. Int J Cardiol *145*, 306-307.

Radhakrishnan, A., Nanjappa, V., Raja, R., Sathe, G., Puttamallesh, V.N., Jain, A.P., Pinto, S.M., Balaji, S.A., Chavan, S., Sahasrabuddhe, N.A.*, et al.* (2016). A dual specificity kinase, DYRK1A, as a potential therapeutic target for head and neck squamous cell carcinoma. Sci Rep *6*, 36132.

Rak, R., Dahan, O., and Pilpel, Y. (2018). Repertoires of tRNAs: The couplers of genomics and proteomics. Annu Rev Cell Dev Biol *34*, 239-264.

Ramirez, F., Ryan, D.P., Gruning, B., Bhardwaj, V., Kilpert, F., Richter, A.S., Heyne, S., Dundar, F., and Manke, T. (2016). deepTools2: a next generation web server for deep-sequencing data analysis. Nucleic Acids Res *44*, W160-165.

Ramos, Y.F., Hestand, M.S., Verlaan, M., Krabbendam, E., Ariyurek, Y., van Galen, M., van Dam, H., van Ommen, G.J., den Dunnen, J.T., Zantema, A.*, et al.* (2010). Genome-wide assessment of differential roles for p300 and CBP in transcription regulation. Nucleic Acids Res *38*, 5396-5408.

Ramsay, E.P., and Vannini, A. (2018). Structural rearrangements of the RNA polymerase III machinery during tRNA transcription initiation. Biochim Biophys Acta - Gene Regul Mech *1861*, 285-294.

Raveau, M., Shimohata, A., Amano, K., Miyamoto, H., and Yamakawa, K. (2018). DYRK1A-haploinsufficiency in mice causes autistic-like features and febrile seizures. Neurobiol Dis *110*, 180-191.

Reina, J.H., Azzouz, T.N., and Hernandez, N. (2006). Maf1, a new player in the regulation of human RNA polymerase III transcription. PLoS One *1*, e134.

Rijal, K., and Maraia, R.J. (2016). Active center control of termination by RNA polymerase III and tRNA gene transcription levels in vivo. PLoS Genet *12*, e1006253.

Roberts, D.N., Stewart, A.J., Huff, J.T., and Cairns, B.R. (2003). The RNA polymerase III transcriptome revealed by genome-wide localization and activity-occupancy relationships. Proc Natl Acad Sci U S A *100*, 14695-14700.

Roewenstrunk, J., Di Vona, C., Chen, J., Borras, E., Dong, C., Arato, K., Sabido, E., Huen, M.S.Y., and de la Luna, S. (2019). A comprehensive proteomics-based interaction screen that links DYRK1A to RNF169 and to the DNA damage response. Sci Rep *9*, 6014.

Rogers, S., Wells, R., and Rechsteiner, M. (1986). Amino acid sequences common to rapidly degraded proteins: the PEST hypothesis. Science *234*, 364-368.

Rowley, M.J., and Corces, V.G. (2018). Organizational principles of 3D genome architecture. Nat Rev Genet *19*, 789-800.

Rozen, E.J., Roewenstrunk, J., Barallobre, M.J., Di Vona, C., Jung, C., Figueiredo, A.F., Luna, J., Fillat, C., Arbones, M.L., Graupera, M.*, et al.* (2018). DYRK1A kinase positively regulates angiogenic responses in endothelial cells. Cell Rep *23*, 1867-1878.

Ryoo, S.R., Cho, H.J., Lee, H.W., Jeong, H.K., Radnaabazar, C., Kim, Y.S., Kim, M.J., Son, M.Y., Seo, H., Chung, S.H.*, et al.* (2008). Dual-specificity tyrosine(Y)-phosphorylation regulated kinase 1A-mediated phosphorylation of amyloid precursor protein: evidence for a functional link between Down syndrome and Alzheimer's disease. J Neurochem *104*, 1333-1344.

Ryoo, S.R., Jeong, H.K., Radnaabazar, C., Yoo, J.J., Cho, H.J., Lee, H.W., Kim, I.S., Cheon, Y.H., Ahn, Y.S., Chung, S.H.*, et al.* (2007). DYRK1A-mediated hyperphosphorylation of Tau. A functional link between Down syndrome and Alzheimer disease. J Biol Chem *282*, 34850-34857.

Sakonju, S., Bogenhagen, D.F., and Brown, D.D. (1980). A control region in the center of the 5S RNA gene directs specific initiation of transcription: I. The 5' border of the region. Cell *19*, 13-25.

Salichs, E., Ledda, A., Mularoni, L., Alba, M.M., and de la Luna, S. (2009). Genome-wide analysis of histidine repeats reveals their role in the localization of human proteins to the nuclear speckles compartment. PLoS Genet *5*, e1000397.

Scales, T.M., Lin, S., Kraus, M., Goold, R.G., and Gordon-Weeks, P.R. (2009). Nonprimed and DYRK1A-primed GSK3 beta-phosphorylation sites on MAP1B regulate microtubule dynamics in growing axons. J Cell Sci *122*, 2424-2435.

Schaffer, A.E., Pinkard, O., and Coller, J.M. (2019). tRNA metabolism and neurodevelopmental disorders. Annu Rev Genomics Hum Genet *20*, 359-387.

Schimmel, P. (2018). The emerging complexity of the tRNA world: mammalian tRNAs beyond protein synthesis. Nat Rev Mol Cell Biol *19*, 45-58.

Schramm, L., and Hernandez, N. (2002). Recruitment of RNA polymerase III to its target promoters. Genes Dev *16*, 2593-2620.

Schramm, L., Pendergrast, P.S., Sun, Y., and Hernandez, N. (2000). Different human TFIIIB activities direct RNA polymerase III transcription from TATA-containing and TATA-less promoters. Genes Dev *14*, 2650-2663.

Shen, Y., Igo, M., Yalamanchili, P., Berk, A.J., and Dasgupta, A. (1996). DNA binding domain and subunit interactions of transcription factor IIIC revealed by dissection with poliovirus 3C protease. Mol Cell Biol *16*, 4163-4171.

Shor, B., Wu, J., Shakey, Q., Toral-Barza, L., Shi, C., Follettie, M., and Yu, K. (2010). Requirement of the mTOR kinase for the regulation of Maf1 phosphorylation and control of RNA polymerase III-dependent transcription in cancer cells. J Biol Chem *285*, 15380-15392.

Shukla, A., and Bhargava, P. (2018). Regulation of tRNA gene transcription by the chromatin structure and nucleosome dynamics. Biochim Biophys Acta - Gene Regul Mech *1861*, 295-309.

Sitz, J.H., Tigges, M., Baumgartel, K., Khaspekov, L.G., and Lutz, B. (2004). Dyrk1A potentiates steroid hormone-induced transcription via the chromatin remodeling factor Arip4. Mol Cell Biol *24*, 5821-5834.

Sokolowski, M., Klassen, R., Bruch, A., Schaffrath, R., and Glatt, S. (2018). Cooperativity between different tRNA modifications and their modification pathways. Biochim Biophys Acta - Gene Regul Mech *1861*, 409-418.

Sonamoto, R., Kii, I., Koike, Y., Sumida, Y., Kato-Sumida, T., Okuno, Y., Hosoya, T., and Hagiwara, M. (2015). Identification of a DYRK1A inhibitor that induces degradation of the target kinase using co-chaperone CDC37 fused with luciferase nanoKAZ. Sci Rep *5*, 12728.

Soragni, E., and Kassavetis, G.A. (2008). Absolute gene occupancies by RNA polymerase III, TFIIIB, and TFIIIC in Saccharomyces cerevisiae. J Biol Chem *283*, 26568-26576.

Souchet, B., Audrain, M., Billard, J.M., Dairou, J., Fol, R., Orefice, N.S., Tada, S., Gu, Y., Dufayet-Chaffaud, G., Limanton, E.*, et al.* (2019). Inhibition of DYRK1A proteolysis modifies its kinase specificity and rescues Alzheimer phenotype in APP/PS1 mice. Acta Neuropathol Commun *7*, 46.

Soundararajan, M., Roos, A.K., Savitsky, P., Filippakopoulos, P., Kettenbach, A.N., Olsen, J.V., Gerber, S.A., Eswaran, J., Knapp, S., and Elkins, J.M. (2013). Structures of Down syndrome kinases, DYRKs, reveal mechanisms of kinase activation and substrate recognition. Structure *21*, 986-996.

Spearman, C. (1987). The proof and measurement of association between two things. By C. Spearman, 1904. Am J Psychol *100*, 441-471.

Stewart, S.A., Dykxhoorn, D.M., Palliser, D., Mizuno, H., Yu, E.Y., An, D.S., Sabatini, D.M., Chen, I.S., Hahn, W.C., Sharp, P.A.*, et al.* (2003). Lentivirus-delivered stable gene silencing by RNAi in primary cells. RNA *9*, 493-501.

Sutcliffe, J.E., Cairns, C.A., McLees, A., Allison, S.J., Tosh, K., and White, R.J. (1999). RNA polymerase III transcription factor IIIB is a target for repression by pocket proteins p107 and p130. Mol Cell Biol *19*, 4255-4261.

Tan, A.Y., and Manley, J.L. (2010). TLS inhibits RNA polymerase III transcription. Mol Cell Biol *30*, 186-196.

Tavenet, A., Suleau, A., Dubreuil, G., Ferrari, R., Ducrot, C., Michaut, M., Aude, J.C., Dieci, G., Lefebvre, O., Conesa, C.*, et al.* (2009). Genome-wide location analysis reveals a role for Sub1 in RNA polymerase III transcription. Proc Natl Acad Sci U S A *106*, 14265-14270.

Tee, A.R. (2018). The target of rapamycin and mechanisms of cell growth. Int J Mol Sci *19*.

Teichmann, M., Wang, Z., and Roeder, R.G. (2000). A stable complex of a novel transcription factor IIB- related factor, human TFIIIB50, and associated proteins mediate selective transcription by RNA polymerase III of genes with upstream promoter elements. Proc Natl Acad Sci U S A *97*, 14200-14205.

Tetreault, M., Choquet, K., Orcesi, S., Tonduti, D., Balottin, U., Teichmann, M., Fribourg, S., Schiffmann, R., Brais, B., Vanderver, A.*, et al.* (2011). Recessive mutations in POLR3B, encoding the second largest subunit of Pol III, cause a rare hypomyelinating leukodystrophy. Am J Hum Genet *89*, 652-655.

Thiffault, I., Wolf, N.I., Forget, D., Guerrero, K., Tran, L.T., Choquet, K., Lavallee-Adam, M., Poitras, C., Brais, B., Yoon, G.*, et al.* (2015). Recessive mutations in POLR1C cause a leukodystrophy by impairing biogenesis of RNA polymerase III. Nat Commun *6*, 7623.

Towpik, J., Graczyk, D., Gajda, A., Lefebvre, O., and Boguta, M. (2008). Derepression of RNA polymerase III transcription by phosphorylation and nuclear export of its negative regulator, Maf1. J Biol Chem *283*, 17168-17174.

Tschop, K., and Dyson, N. (2011). Identifying players in the functional network around pRB. Cell Cycle *10*, 3814-3815.

Turowski, T.W., Lesniewska, E., Delan-Forino, C., Sayou, C., Boguta, M., and Tollervey, D. (2016). Global analysis of transcriptionally engaged yeast RNA polymerase III reveals extended tRNA transcripts. Genome Res *26*, 933-944.

van Bon, B.W., Coe, B.P., Bernier, R., Green, C., Gerdts, J., Witherspoon, K., Kleefstra, T., Willemsen, M.H., Kumar, R., Bosco, P.*, et al.* (2016). Disruptive de novo mutations of DYRK1A lead to a syndromic form of autism and ID. Mol Psychiatry *21*, 126-132.

Van Bortle, K., Phanstiel, D.H., and Snyder, M.P. (2017). Topological organization and dynamic regulation of human tRNA genes during macrophage differentiation. Genome Biol *18*, 180.

Vannini, A., Ringel, R., Kusser, A.G., Berninghausen, O., Kassavetis, G.A., and Cramer, P. (2010). Molecular basis of RNA polymerase III transcription repression by Maf1. Cell *143*, 59-70.

Vorlander, M.K., Khatter, H., Wetzel, R., Hagen, W.J.H., and Muller, C.W. (2018). Molecular mechanism of promoter opening by RNA polymerase III. Nature *553*, 295-300.

Walte, A., Ruben, K., Birner-Gruenberger, R., Preisinger, C., Bamberg-Lemper, S., Hilz, N., Bracher, F., and Becker, W. (2013). Mechanism of dual specificity kinase activity of DYRK1A. FEBS J *280*, 4495-4511.

Wang, F., Zhao, K., Yu, S., Xu, A., Han, W., and Mei, Y. (2019a). RNF12 catalyzes BRF1 ubiquitination and regulates RNA polymerase III-dependent transcription. J Biol Chem *294*, 130-141.

Wang, P., Karakose, E., Liu, H., Swartz, E., Ackeifi, C., Zlatanic, V., Wilson, J., Gonzalez, B.J., Bender, A., Takane, K.K.*, et al.* (2019b). Combined inhibition of DYRK1A, SMAD, and Trithorax pathways synergizes to induce robust replication in adult human beta cells. Cell Metab *29*, 638-652 e635.

Wang, Z., Bai, L., Hsieh, Y.J., and Roeder, R.G. (2000). Nuclear factor 1 (NF1) affects accurate termination and multiple-round transcription by human RNA polymerase III. EMBO J *19*, 6823-6832.

Wang, Z., and Roeder, R.G. (1998). DNA topoisomerase I and PC4 can interact with human TFIIIC to promote both accurate termination and transcription reinitiation by RNA polymerase III. Mol Cell *1*, 749-757.

Wegiel, J., Kuchna, I., Nowicki, K., Frackowiak, J., Dowjat, K., Silverman, W.P., Reisberg, B., DeLeon, M., Wisniewski, T., Adayev, T.*, et al.* (2004). Cell type- and brain structure-specific patterns of distribution of minibrain kinase in human brain. Brain Res *1010*, 69-80.

Weintraub, A.S., Li, C.H., Zamudio, A.V., Sigova, A.A., Hannett, N.M., Day, D.S., Abraham, B.J., Cohen, M.A., Nabet, B., Buckley, D.L.*, et al.* (2017). YY1 is a structural regulator of enhancer-promoter loops. Cell *171*, 1573-1588 e1528.

White, R.J., Khoo, B.C., Inostroza, J.A., Reinberg, D., and Jackson, S.P. (1994). Differential regulation of RNA polymerases I, II, and III by the TBP-binding repressor Dr1. Science *266*, 448-450.

White, R.J., Stott, D., and Rigby, P.W. (1989). Regulation of RNA polymerase III transcription in response to F9 embryonal carcinoma stem cell differentiation. Cell *59*, 1081-1092.

Willis, I.M. (2002). A universal nomenclature for subunits of the RNA polymerase III transcription initiation factor TFIIIB. Genes Dev *16*, 1337-1338.

Willis, I.M., and Moir, R.D. (2018). Signaling to and from the RNA polymerase III transcription and processing machinery. Annu Rev Biochem *87*, 75-100.

Winter, A.G., Sourvinos, G., Allison, S.J., Tosh, K., Scott, P.H., Spandidos, D.A., and White, R.J. (2000). RNA polymerase III transcription factor TFIIIC2 is overexpressed in ovarian tumors. Proc Natl Acad Sci U S A *97*, 12619-12624.

Woods, Y.L., Rena, G., Morrice, N., Barthel, A., Becker, W., Guo, S., Unterman, T.G., and Cohen, P. (2001). The kinase DYRK1A phosphorylates the transcription factor FKHR at Ser329 in vitro, a novel in vivo phosphorylation site. Biochem J *355*, 597-607.

Xu, X., Liu, Q., Zhang, C., Ren, S., Xu, L., Zhao, Z., Dou, H., Li, P., Zhang, X., Gong, Y*., et al.* (2019). Inhibition of DYRK1A-EGFR axis by p53-MDM2 cascade mediates the induction of cellular senescence. Cell Death Dis *10*, 282.

Yabut, O., Domogauer, J., and D'Arcangelo, G. (2010). Dyrk1A overexpression inhibits proliferation and induces premature neuronal differentiation of neural progenitor cells. J Neurosci *30*, 4004-4014.

Yang, C.S., Wang, X., Lu, G., and Picinich, S.C. (2009). Cancer prevention by tea: animal studies, molecular mechanisms and human relevance. Nat Rev Cancer *9*, 429-439.

Yousefelahiyeh, M., Xu, J., Alvarado, E., Yu, Y., Salven, D., and Nissen, R.M. (2018). DCAF7/WDR68 is required for normal levels of DYRK1A and DYRK1B. PLoS One *13*, e0207779.

Yu, D., Cattoglio, C., Xue, Y., and Zhou, Q. (2019). A complex between DYRK1A and DCAF7 phosphorylates the C-terminal domain of RNA polymerase II to promote myogenesis. Nucleic Acids Res *47*, 4462-4475.

Yuen, K.C., Slaughter, B.D., and Gerton, J.L. (2017). Condensin II is anchored by TFIIIC and H3K4me3 in the mammalian genome and supports the expression of active dense gene clusters. Sci Adv *3*, e1700191.

Zhang, Y., Liao, J.M., Zeng, S.X., and Lu, H. (2011). p53 downregulates Down syndrome-associated DYRK1A through miR-1246. EMBO Rep *12*, 811-817.

Zhong, S., and Johnson, D.L. (2009). The JNKs differentially regulate RNA polymerase III transcription by coordinately modulating the expression of all TFIIIB subunits. Proc Natl Acad Sci U S A *106*, 12682-12687.

Zhong, S., Zhang, C., and Johnson, D.L. (2004). Epidermal growth factor enhances cellular TATA binding protein levels and induces RNA polymerase I- and III-dependent gene activity. Mol Cell Biol *24*, 5119-5129.

Zhou, Y., Goodenbour, J.M., Godley, L.A., Wickrema, A., and Pan, T. (2009). High levels of tRNA abundance and alteration of tRNA charging by bortezomib in multiple myeloma. Biochem Biophys Res Commun *385*, 160-164.

Zufferey, R., Nagy, D., Mandel, R.J., Naldini, L., and Trono, D. (1997). Multiply attenuated lentiviral vector achieves efficient gene delivery in vivo. Nat Biotechnol *15*, 871-875.

Rianne Angelica Cort was supported by a FPI predoctoral fellowship of the Spanish Ministry of Economy, Industry and Competitiveness (BES-2015-072815) co-financed by the European Social Fund. This work was supported by grants from the Spanish Ministry of Economy and Competitiveness (BFU2013-44513 and BFU2016-76141-P), and the Secretariat of Universities and Research-Generalitat de Catalunya (2014SGR674). The group belongs to the Rare Diseases Networking Biomedical Research Center (CIBERER). The CRG is a 'Centro de Excelencia Severo Ochoa 2013-2017'.